Delft University of Technology

FACULTY MECHANICAL, MARITIME AND MATERIALS ENGINEERING
Department Marine and Transport Technology

Mekelweg 2
2628 CD Delft
the Netherlands
Phone +31 (0)15-2782889
Fax +31 (0)15-2781397
www.mtt.tudelft.nl

Specialization:	Transport Engineering and Logistics
Report number:	2018.TEL.8234
Title:	**Redevelopment of a Bidirectional Sorter to Improve Parcel Behaviour**
Author:	Étienne Teunissen

Title (in Dutch)	Herontwikkeling van een bidirectionele sorteerder voor verbeterd pakketgedrag

Assignment:	Master thesis
Confidential:	no
Initiator (university):	Ir. Wouter van den Bos
Initiator (company):	M. Kauwenberg (VanRiet, Houten)
Supervisor:	Dr. Ir. Dingena Schott Ir. Wouter van den Bos
Date:	November 7, 2018

Delft University of Technology

FACULTY MECHANICAL, MARITIME AND MATERIALS ENGINEERING
Department Marine and Transport Technology

Mekelweg 2
2628 CD Delft
the Netherlands
Phone +31 (0)15-2782889
Fax +31 (0)15-2781397
www.mtt.tudelft.nl

Student:	Étienne Teunissen	Assignment type:	Master thesis
Supervisor (TUD):	Dr. Ir. Dingena Schott Ir. Wouter van den Bos	Creditpoints (EC):	35
Supervisor (Company)	M. Kauwenberg Y. Zethof	Specialization:	TEL
		Report number:	2018.TEL.8234
		Confidential:	No

Summary

E-commerce markets are constantly growing, while customers expect shorter delivery. Consequently, parcel handlers like DHL and UPS have to deliver more parcels in less time while also handling return streams. To accommodate both streams into a single facility, bidirectional systems were introduced which can be reversed between shifts in order to accommodate transport over the same equipment. These systems use a bidirectional sorter capable of sorting and merging parcels based on frictional forces between the sorter and parcels.
Bidirectional sorters have been applied in several systems proving their advantage over unidirectional sorters. Despite several available bidirectional sorters, insight in the working principles is unknown. Commissioning is expensive since each system is programmed manually and based on dynamic controls. Introducing timing issues and systems highly sensitive for disturbances. Furthermore, uncertainty exist on which types of parcels can be reliably sorted and why certain products show better behaviour. Therefore, insight is necessary into; parcel behaviour over bidirectional sorters, impact of different parcel parameters and influence of product design.
To provide objective and substantiated information a quantitative design method was chosen namely, Set-Based Concurrent Engineering. Resulting in a structured approach to eliminate insufficient designs. In order to eliminate concepts a test is required to verify compliance between requirements and concepts. To save time and expenses a simulation model is used to examine and eliminate different layout configurations.
By conducting experiments using a current available bidirectional sorter (grid), the model is validated and information on parameter influence is acquired. Considering parcel characteristics, ratio (width/length) has the largest impact on position and orientation of the parcel, other parameters have considerably less influence. On equipment level, grid velocity has no influence on lateral position and orientation and can therefore, be used to maintain parcel velocity in longitudinal direction in order to maintain gaps between parcels. Furthermore, divert angle settings can be used to influence the position and orientation of parcels to neatly sort parcels into an outfeed.

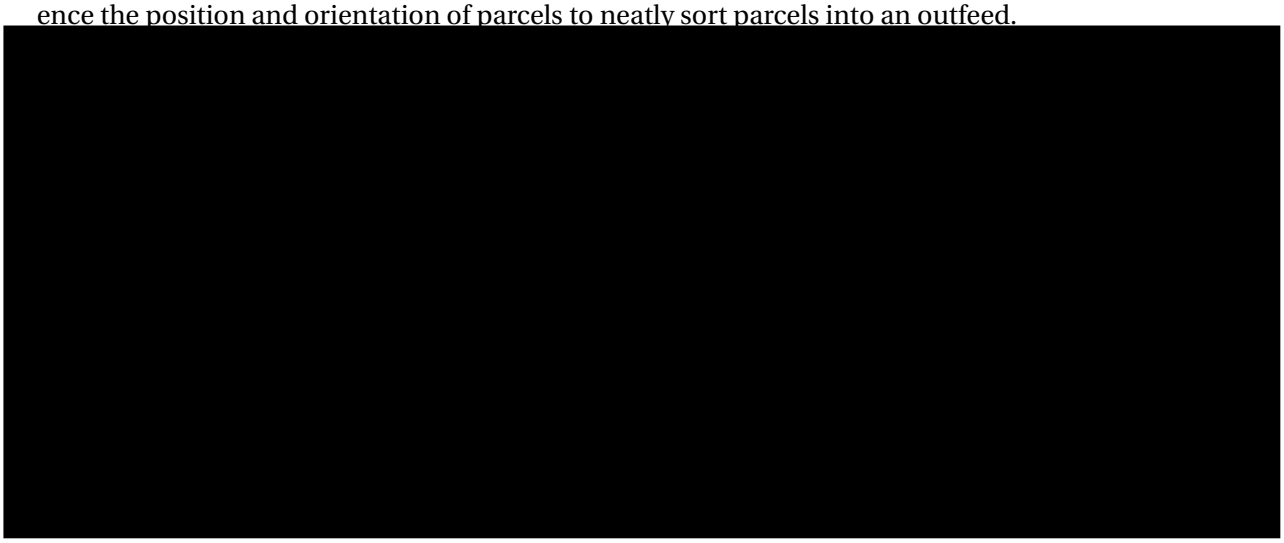

Samenvatting

De E-commerce markt maakt een constante groei door en klanten verwachten dat pakketten steeds sneller worden bezorgd. Hierdoor moeten postbedrijven zoals DHL en UPS meer pakketten bezorgen in minder tijd terwijl ook de stroom van retourzendingen toeneemt. Om zowel heen- als retourzendingen te kunnen verwerken in dezelfde faciliteit kunnen bidirectionele systemen uitkomst bieden. Een dergelijk systeem kan in twee richtingen werken waardoor beide stromen over dezelfde bandtransporteurs gaan. Voor een dergelijk systeem is ook een sorteerder nodig die in twee richtingen werkt, hiervoor kunnen wielsorteerders gebruikt worden die op basis van frictie een pakket uitsorteren.

Ondanks dat er al vele wielsorteerders bestaan, is er nog weinig bekend over de achterliggende principes. Hierdoor wordt elk systeem individueel ingeregeld gebruikmakend van dynamische aansturing waarbij de hoek instellingen van de wielen varieren op basis van de positie van het pakket. Dit resulteert in dure inbedrijfstelling, problemen met timing en hoge gevoeligheid voor verstoringen. Verder is het onduidelijk welke variabelen invloed hebben op het pakketgedrag en waarom sommige pakketten beter sorteren dan anderen. Daarom is er meer inzicht nodig in het pakketgedrag, invloed van parameters en effecten van verschillende layouts voor de sorter.

Om een objective keuze tussen de verschillende layouts mogelijk te maken is er gekozen voor de Set-Based Concurrent Engineering methode welke een gestructureerde aanpak volgt om verschillende concepten te elimineren. Om deze eliminatie mogelijk te maken is er een test nodig om concepten te kunnen meten, daarom is er een simulatie model gemaakt waarmee verschillende layouts getest en geelimineerd kunnen worden.

Door het uitvoeren van experimenten op de huidige wielsorteerder kon het model gevalideerd worden. Verder zijn deze experimenten gebruikt om de invloed van verschillende parameters te onderzoeken. Hieruit volgde een duidelijke afhankelijkheid van de pakket ratio, andere pakket parameters hebben significant minder invloed op het pakketgedrag. Op product niveau heeft de hoogte van de wielen weinig invloed terwijl het wel verstoringen introduceert in de snelheid van het pakket. Een verhoogde snelheid van de sorteerder kan gebruikt worden om de snelheid van het pakket in transport richting gelijk te houden tijdens het uitsorteren. Verder heeft de hoek instelling van de wielen een duidelijke invloed op de positie en orientatie van het pakket en kan daarom gebruikt worden om dit te beinvloeden.

Contents

Acknowledgement

During my thesis several people provided their knowledge and time in order to enhance this research. First, I would like to express my gratitude to Matthieu Kouwenberg, Casper Vlug and Yvo Zethof for their continued support, feedback and flexibility.

Dr. Ir. Dingena Schott and Ir. Wouter van den Bosch provided me with valuable feedback, guiding me through several steps of the research process.

Finally, I wish to thank Naomi van Rooten for her help with constructing the experiments and Layla Teunissen and Philippe Pauli for reviewing my thesis.

List of Figures

List of Tables

1 Introduction

The e-commerce market is constantly increasing and has doubled over the last five years [8]. This growth results in a higher demand on parcel handlers such as DHL and UPS. To meet this demand, capacity of sorting facilities should be increased, which can be achieved by introducing bidirectional sorting systems [3]. Bidirectional systems can operate in reverse to accommodate vans and trucks at the same docks during morning and afternoon shifts in order to accommodate outbound and inbound using the same conveyors [11].

Steerable rollers are currently the only group of sorters which feature this property a high capacities [36]. Several steerable roller concepts have been developed which share a similar mechanism [9, 24, 32, 40]. In 2014 VanRiet Material Handling introduced the modular IQ-Grid (Figure 1.1) which also incorporates this mechanism [26]. The IQ-Grid has already been applied in several systems and proved the efficiency of a bidirectional system.

The constant aim for higher sorting capacities requires continuous improvement and innovation of equipment. Therefore, it is necessary to improve the current product leading to a higher efficiency and more knowledge on the influence of parcel properties.

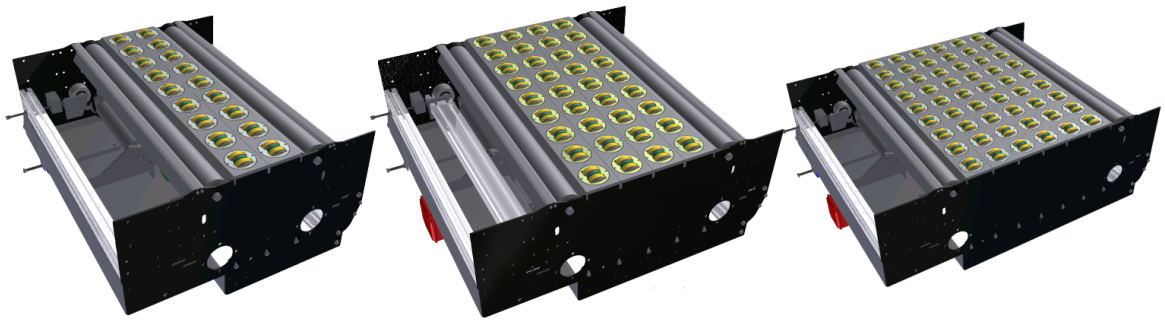

Figure 1.1: The bidirectional sorter designed by VanRiet called the IQ-Grid.

1.1. Problem Statement

The first generation of the IQ-Grid was developed using a qualitative approach, most of the design is based on experience of earlier developments and visual observations. However, this approach resulted in a black-box able of sorting parcels to an outlet without knowing where and how the parcel will end up there. Due to this uncertainty, commissioning is expensive since the controls of each system are tweaked to ensure reliable sortation for specific parcel sets of each customer. Furthermore, controls follow a dynamic profile based on parcel position resulting in systems which are complex and highly sensitive to disturbances.

Uncertainty about the parcel behaviour also results in design challenges since the influence of certain design parameters is not necessarily known. For example grid height which is set 5 mm higher than the adjacent conveyor to ensure better grip while diverting parcels. While also, introducing a ramp resulting in jumps of parcels leading to undesired behavior and lower sorting reliability since parcels have less contact with the sorter. Also influence of parcel parameters is unknown which leads to uncertainty on which types of parcels can be sorted by the IQ-Grid.

Furthermore, the layout is based on the cassette design resulting in divert angles set per row (lateral to the transport direction). This layout was prescribed by the mechanical design but may not provide optimal parcel behaviour and therefore, requiring unnecessary extra grid length.

1.2. Research Questions

The problem statement clearly indicates the need for better insight in the functioning of the grid which can lead to improved sorting behaviour and predictability. Therefore, the following research question was formulated to aim for optimized bidirectional sorting:

> *How can parcels be efficiently sorted in a bidirectional system independent of their position on the feeder?*

To answer this primary question the following sub-questions have been formulated:

- What are State of the Art bidirectional sorters and their required functions?
- How can a bidirectional sorter and surrounding equipment be modelled?
- How can the parcel behaviour be accurately described?
- Which parameters influence the parcel behaviour on a bidirectional sorter?
- Which layout configuration is most efficient in sorting parcels?
- How viable is the current design compared to the new developed concept?

1.3. Report Outline

First, the design methodology of this research was defined which provided a framework for the research. By this method the following steps were determined which starts by discovering the functional requirements of the product.

By examining a typical system in which the IQ-Grid is usually applied and literature survey, product requirements were defined. Which were used in order to eliminate concepts following a quantitative and structured approach.

According to the chosen design method (Set-Based Concurrent Engineering) a test was required to perform concept elimination . Because of the high costs and time required to physically test different concepts, a simulation model was constructed. First, the mathematical model required for this simulation was defined. From there, the model was computerized into a simulation and verified to ensure a proper implementation.

By conducting experiments more insight was gained into the impact of several parameters, but also a method was presented to validate the simulation model. After validation, the model was used to test the different configurations. Leading to an improved conceptual design for the layout of the bidirectional sorter, this is presented together with the gained insight on parameter influence and design choices. Which is finally, confirmed by repetition of the experiments on the new layout configuration.

In short, this method led to the following structure: Chapter 1 - Introduction, Chapter 2 - Research Methodology, Chapter 3 - Product Background, Chapter 4 - Parcel Behaviour Model, Chapter 5 - Parcel Simulation, Chapter 6 - Experiments & Model Validation, Chapter 7 - Design Selection IQ-Grid, Chapter 8 - Validation Improved Design, Chapter 9 - Conclusion & Recommendations.

2

Research Methodology

This chapter describes the method used during the research, this consist of two parts namely: design and simulation. First the design method was selected which provided guidelines to select a concept. For this selection a test was necessary. The kind of test is described in the second part of this chapter.

2.1. Design Method

The methodology prescribed the different steps to follow during the research and provided a tool for the successful redevelopment of the product. A distinction was made between different design methods from there, a method was selected and applied to this research by determining the different steps required.

2.1.1. Method selection

A distinction was made between different methodologies to be able to categorize these methods and clearly indicate their strengths and weaknesses. Which were used to select one of the two types of methodologies and from there, select a specific method.

Two types of design methods were distinguished: quantitative and qualitative methods. Both methods are described below:

- **Quantitative:** this type of methods is focused on selecting the design based on objective numbers. These can be acquired using measurements, calculations or simulations and are processed using numerical comparisons and statistical inferences. The selection of the final design can then be made based on an objective decision [28]. An example of a quantitative design method is Set-Based Concurrent Engineering, this method focuses on excluding solutions by tightening the boundaries (product requirements). To eliminate concepts, objective data is necessary in order to examine if the solution still meets the tightened boundaries [34].

- **Qualitative:** these methods rely on personal observations, designs selection using these methods mostly rely on subjective decisions and experience of earlier product developments [28]. An example of these methods are the Pugh matrix or Kesselring's selection matrix. The Pugh matrix indicates strengths and weaknesses of the solutions compared to a reference design. This is done using, a plus (better than reference), minus (worse than reference) and S (same as reference) from multiple criteria stated beforehand. In addition Kesselring's selection matrix adds weights which can add importance to certain criteria [35].

The current design of the IQ-Grid is developed using the experience of previous products and information from the field. This approach was chosen since little was known about the parcels that will be sorted by the product, usually only restrictions based on weight and dimensions are applied. Therefore, behaviour of parcels was assumed to be a non-deterministic process and hard to describe.

This information led to the decision to design the product using a qualitative approach, performed by selecting concepts based on criteria like: reliability, costs and robustness. These criteria were ranked using a Pugh matrix with information based on estimates and experiences.

Currently not much is known about the influence of different design parameters on the performance of the product. Also including influence of parcel properties such as friction coefficients, stiffness and inertia. These insights could be acquired using measurements, calculation and other quantitative information.

Therefore, a quantitative method was chosen for this research to approach the problem differently and gain more insight in the principles behind the product. More precise, the previously described Set-Based Concurrent Engineering method was chosen. Because of its quantitative properties, objective approach and its proven results in previous research [18, 34, 35, 39].

2.1.2. Description Applied Method

Set-Base Concurrent Engineering was chosen for this research and was applied to the research by indicating the required steps and fitting these to the research objective of Chapter 1.

Several concepts were found for the new product, these concepts were set into boundaries, defined by the product requirements. Ideas which lay outside the boundaries were eliminated from the set. From there, the boundaries were tightened even further to converge to a single concept.

To make an objective elimination during each iteration the level of detail was increased to the amount necessary at that stage. An overview of this process is shown in Figure 2.1.

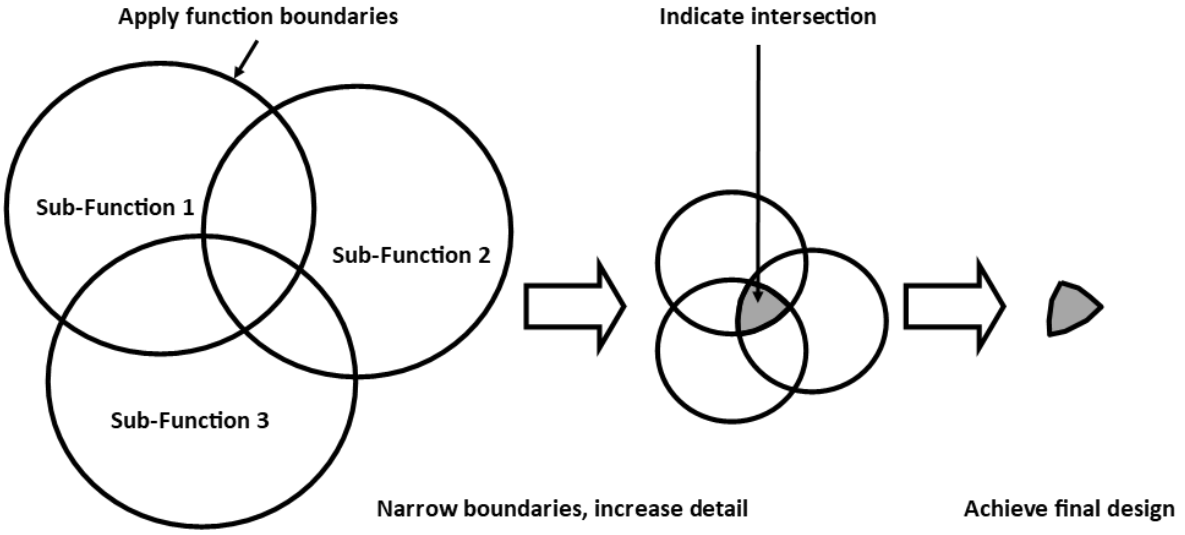

Figure 2.1: Schematic representation of the SBCE design method

After developing several concepts these were narrowed down to a definitive conceptual layout for the IQ-Grid. The selection process was done according to the described methodology, leading to the following steps:

1. Elimination based on tests using maximum parcel dimensions for sortation.
2. Elimination based on tests using maximum parcel dimensions for merge.
3. Elimination using several different parcel properties.
4. Concept selection by examining detailed parcel behaviour.

2.2. Development Simulation Model

Development of a conceptual layout for IQ-Grid required several tests to eliminate certain layouts according to the chosen design method. These results could be achieved using several methods, in Figure 2.2 different options for concept analysis are shown.

The physical model and experiment with the actual model require functioning products. During this research only the first generation of the IQ-Grid was available which is limited in angle settings (steps of 12.8°) and has a fixed length (0.6 m). These angle settings may not provide the flexibility required to test different layouts and parcels placed far away from the outfeed may not be sorted due to the limited grid length. Creating a new prototype with this flexibility will require time and resources which were not available in this phase of the design.

Therefore, only the analytic and simulation models remained for the redevelopment. Due to the expected complexity of the model a simulation seemed most appropriate [25]. Using simulation different configurations could be tested with multiple inputs (parcel properties, velocities, etc.).

The development of such model required the following steps: model qualification, model verification and model validation [31]. This process is shown in Figure 2.3 and described in detail below.

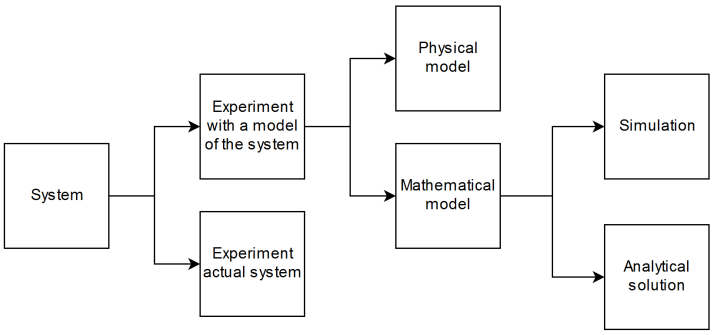

Figure 2.2: Different methods that can be used to provide tests for the configuration options. Obtained from [25].

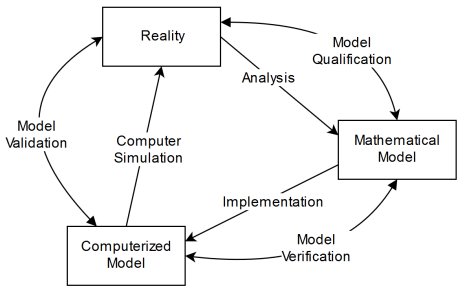

Figure 2.3: Steps necessary to create a simulation model which can then be used to simulate the physical product. Obtained from [31].

2.2.1. Model Qualification

First, a conceptual model was made which described the physical system. In this research the model consist of several formulas describing the translation and rotation of the parcel when travelling over the IQ-Grid. This step resulted in a mathematical model [31].

2.2.2. Model Verification

The mathematical model was used in a simulation, to construct this simulation the mathematical model was implemented into a computerized model. The implementation was verified to ensure the model showed correct responses as expected by the mathematical model.

The verification of this implementation could be done using static or dynamic testing [12]. Static testing is done by analyzing the computer program by checking the code in a structured way. Dynamic testing uses tools to check the results generated by the model, this research used the following tools available for dynamic testing to ensure a proper implementation [37]:

- **Animation:** using an animation a 'logical' path of the parcel was ensured. For instance strange jumps in position or unreasonable rotations of the parcel were detected. This provided a preliminary test for a correct implementation.
- **Face-validity:** after inspection of the animation, it was passed to an expert which indicated if the model showed behaviour which he expects from his experience.
- **Traces:** finally traces can be used to ensure proper implementation, this was done by varying the input parameters of the model and check if the response of the simulation model corresponds to the expected response by examining the mathematical model.

2.2.3. Model Validation

Finally, the model was validated to ensure the simulation model generated a result which was reliable to model the physical product [31]. Since a physical product (first generation IQ-Grid) was available for testing, the validation was performed using an objective approach consisting of experiments and statistical tests [37].

By performing experiments using the physical product while varying different parameters the model was validated. These results were compared to the results generated by the simulation model, if these were within defined bounds the model could be assumed to represent the physical model correctly.

These experiments were conducted using design of experiments which was used to limit the number of experiments necessary by varying multiple parameters simultaneously [4]. To determine which parameters needed to be varied in the experiment first a dimension analysis was performed. The analysis provided dimensionless groups which were used to setup the experimental plan [23], which is described in detail in Chapter 6.

After a successful verification and validation of the simulation model it was used to eliminate proposed layout designs by testing the layouts using different parameters as explained in Section 2.1.2.

2.3. Conclusion

Based on the design method applied during the development of the first generation grid, a different approach was chosen for this research to gain better insight in the working principles of the product. Therefore, a quantitative design method named Set-Based Concurrent Engineering was chosen due to its characteristics and proven success in previous research.

To eliminate several concepts using this method, a test was required to measure the feasibility of configurations towards the requirements. These tests were conducted using a simulation model in order to save costs and time, which are introduced when using a physical model.

For construction of this simulation several steps were taken to develop a reliable solution. First, the model was qualified by stating the mathematical model, after implementation of this model into a simulation it was verified. Finally, a validation step was taken by performing different experiments to check correspondence with the reality.

3

Product Background

In this chapter the background of the IQ-Grid is provided. Which is used to determine functional requirements for the product, in order to eliminate configurations which do not comply to these requirements as discussed in Chapter 2.

First, a system description is given which explains how a first generation IQ-Grid is usually applied in a project. Second, the State of the Art is discussed, this can be useful to gain insight in possible concepts and competitors products. This information is then used to define the requirements.

3.1. System Description

In Figure 3.1 a layout is shown which is applied in an actual project. This layout includes 14 IQ-Grids and uses the bidirectional functionality. This facility serves as a last hub before the customer and enables transfers from trucks to smaller delivery vans. During the morning schedule (5:00-8:00) parcels are unloaded from trucks and transferred to vans which then take parcels to the customer. After delivery, the vans bring back parcels collected at shops. These vans arrive in the afternoon (14:00-20:00) during this process parcels are unloaded from the vans into the trucks to be transported to other hubs.

3.1.1. Unloading Trucks

The first step of the process is the unloading of the trucks during the morning schedule, this process is shown in Figure 3.2. A truck arrives at the hub and connects to one of the docks (1), after this the containers can be unloaded using a forklift. These containers are then placed at the offload area (2).

From here the parcels are placed into the system by manual operators and transported by conveyors. These conveyors transport the parcels to the infeed (3) which then places the parcel on the sorter belt as shown in Figure 3.3. Using an IQ-Grid (4) the parcel is guided onto the sorter belt to prevent parcels from getting stuck.

3.1.2. Sorting to Correct Outfeed

This system has three types of outfeeds, namely: multi-purpose (5), B2C (6) and the vans (7) as shown in Figure 3.4. After placement on the sorter the parcels will be send to the correct outfeed using the IQ-Grids. Since the IQ-Grid currently has a limited length a presort grid is necessary to ensure reliable sorting. The presort IQ-Grids (in green) align the package to the side of the outfeed after which the sorter IQ-Grid (in blue) can sort the parcel to the outfeed.

If a parcel is not sorted it will end up in the hospital outfeed (8). In this section, the parcel is checked manually and fed back to the system if the problem is resolved, then it can be sorted to the correct outfeed.

3.1.3. Loading Vans

After a parcel has been sorted to the van outfeed (7) the parcel will arrive at the Pick-up and Delivery finger shown in Figure 3.5. Here the parcels are sorted per three vans by an IQ-Grid (in blue). In this stage presort is not necessary since this is already performed during sorting (Figure 3.4). A parcel is send to the correct roller conveyor by the IQ-Grid which are positioned on both sides. This requires a IQ-Grid capable of three angles. The parcel is picked up from the roller conveyor and placed into the correct van by the operator.

3.1.4. Afternoon Process

During the afternoon process the system will operate in reverse using the bidirectional property of the equipment. First parcels are directly placed on the belt conveyor at the Pick-up and Delivery station (Figure 3.5) or at the multi-purpose station (5). The parcels are then sorted to the correct outfeed by the IQ-Grids (4) which feed the parcels to the offload area (2). In this area the parcels are manually placed into the containers and then loaded into the trucks (1).

3.2. State of the Art

To develop new products it can be useful to consider the already available technology. For bidirectional sorters several products have been made over the years. Which are used in several industries such as, parcel handling, tire industry and e-commerce. Studying these technologies can help with the design of a new product.

The literature study will provide an overview of the available products. This will be done by consulting literature, patent databases and company brochures. This information can also later be used to create a competitive product which features better functionality or specs, or to check patent infringement.

First, different methods for sorting parcels will be discussed and compared. Secondly, the patents found will be discussed, patents showing an innovative solution are also individually described in Appendix B. An overview of all patents found on bidirectional sorters can be found in Appendix D Lastly, the products found which share functionality with the IQ-Grid or capable of bidirectional sorting are discussed, an individual description for each product can be found in Appendix C.

3.2.1. Sorters

To enable sortation to specific shipping lanes usually extra equipment is used besides the transport equipment e.g. belt conveyors or roller conveyors. These sorters can be used to sort parcels according to their destination for instance, this is similar to the system described in Section 3.1. In this section each method for sortation will be briefly described.

- **Deflector:** this type of sorter uses a movable arm to deflect parcels onto a different conveyor. The product is laterally transferred to the outfeed i.e. parcel orientation adapts the outfeed orientation [29].
- **Pusher diverter:** this type is similar to the deflector and also uses a arm to divert parcels. However, the parcel's orientation is not maintained since the pusher diverts the parcel at a right angle and therefore, places the parcel turned on the take away conveyor [29].
- **Pop-up wheel:** these wheels are usually placed in between two conveyors or in between narrow belt conveyors. The wheels are positioned with a certain angle to divert parcels to the take away conveyor. Parcels are diverted when the wheels pop-up above the conveyor surface. Certain types also feature sortation in three directions [29].
- **Swivel wheel sorter:** in contrast to the pop-up wheels the height of steerable rollers is fixed and equal to the conveyors' surface. The wheels can obtain several angles to transport parcels in different directions [29].
- **Sliding shoe:** this type combines the conveyor and sorting equipment, the conveyor is constructed using slats, each slat is equipped with a shoe (sliding pusher) which can be moved laterally across the width of the slat. When a parcels needs to be diverted to an outlet the shoes move towards the outlet and therewith, push the parcel to the outlet [29].
- **Tilt tray:** these trays are mounted to a continuous track, each tray can tilt individually and usually carries a single parcel. When the tray reaches its outlet the tray will tilt in direction of the outlet causing the parcel to slide onto the outlet using gravity. The tray can tilt in either direction enabling three sort directions [29].

- **Cross belt:** similar to the tilt tray this equipment also uses a continuous track but instead of trays it uses belt conveyors constructed perpendicular to the transport direction. Each belt conveyor can be activated individually and can then transport a parcel onto the outlet [29].

These different products and their features are shown in Table 3.1. According to [29] only the steerable rollers sorter has a bidirectional property. However, in Section 3.2.2 & 3.2.3 this statement will be further examined by checking available bidirectional solutions using existing products and patents.

Important differences for the product design can be found by the handling of products and type of product. As indicated in Section 3.1 the products are currently used for parcel handling. This usually includes general merchandise (polybags) and cartons. These polybags can get easily stuck in the equipment which excludes the deflector and pusher according to Table 3.1.

Furthermore, these polybags require a gentle handling with little collisions with sorting or transport equipment. This is necessary to ensure the content of the bag is not damaged during sortation. Again excluding the deflector and pusher from the possibilities according to Table 3.1.

Table 3.1: Overview of different types of sorting equipment, obtained from [29].

Characteristics	**Deflector**	**Pusher**	**Pop-up wheels**	**Steerable rollers**	**Sliding shoe**	**Tilt tray**	**Cross belt**
Sorting speed	Low	Low	Medium	Medium	High	High	High
Load range	Low	Medium	High	High	Medium	Medium	High
Handling of product	Medium to rough	Medium	Gentle	Gentle	Gentle	Gentle to medium	Gentle
Cost	Low	Low to medium	Medium	Medium to high	High	High	High
Product orientation	Maintained	Turned	Maintained	Maintained	Maintained	Maintained	Maintained
Type of products	Cartons	Cartons	Cartons/ totes	Cartons/ totes	Cartons/ totes/ envelopes	Cartons/ break pack goods	Cartons/ break pack goods
Sort directions	2	2	2	3	3	3	3
Bidirectional	No	No	No	Yes	No	No	No
Application	Parcels and freight baggage	Parcels and freight baggage	General merchandise, cartons and totes	General merchandise, cartons and totes	General merchandise, cartons and totes	Catalog, postal parcel and freight	Catalog, postal parcel and freight

3.2.2. Patents

A patent search has been conducted to gain insights in bidirectional sorting solutions, this search was specifically used for this purpose and not to find possible violations. After conducting an initial search two classifications stood out, these are: B65G13/10 and B65G47/52. B65G indicates *Transport or Storage Devices*. The addition 13/10 indicates roller systems and specifically switching arrangements. 47/52 stands for devices used to transfer articles or materials between conveyors.

It can be seen that most patents providing bidirectional sortation indeed use steerable rollers to sort parcels. Furthermore, there is still innovation in the mechanisms for steerable rollers sorters, for instance patents [15, 33, 45] from 2007 and 2016 which can be considered as recent innovations.

Several patents [7, 10, 13, 22] have fixed divert angles which seem less applicable for the new bidirectional sorter since it should be able to both sort and merge parcels which usually require different angle settings.

By observing the patents found for bidirectional sorting it can be noted several options are available for transferring frictional force to the parcel. For instance wheels, rollers, balls and belts are featured in the several found patents which is also shown in Appendix D.

A selection of patents are discussed in appendix B providing insight in several solutions for bidirectional sorting. In Table 3.2 a summary is presented of all discussed patents. In Appendix D all patents found for a bidirectional sorter are shown indicating their working principles.

Table 3.2: Overview of the discussed patents.

Title:	**Divert Angle**	**Positions**	**Pop-up**	**Actuator**	**Remarks**
Electromagnetically actuated sorter [33]	30, 45, 90	Predetermined	No	Magnets	Spring plunger to stabilize the divert angle
Steerable Divert System [10]	0-90	Variable	No	Pneumatic/Electric	Gear plate to set the divert angle
Bidirectional Transfer Mechanism [13]	90	Fixed	Yes	Pneumatic+electric	O-ring used to transfer the packages
ARB Conveyor [22]	30, 45, 90	Predetermined	No	Electric	Belt or rollers underlying the conveyor to rotate the wheels
High Speed Take-Off [7]	30	Fixed	Yes	Pneumatic+electric	Wheels mounted on a chain to transfer package
Conveying Apparatus [30]	30, 45, 90	Predetermined	No	Pneumatic/Electric	Small belt conveyors to transfer package, incline possible
Transmission Variable Output [45]	All	Variable	No	Pneumatic/Electric	Wheel rotation by underlying conveyor, rotation and divert angle decoupled

3.2.3. Products

By visiting company websites and consulting previous products several products were found. Furthermore, documentation available at VanRiet about competitors was used to complete the product search. The products are discussed individually in appendix C, in this section a summary will be provided.

The products found include some very similar products to the IQ-Grid, like the products of ZiPLine, OCM, Dematic and FBA Italy. These products have a similar transmission and layout as the IQ-Grid. The product of FBA Italy stands out because of the two separate control blocks in the sorter. This enables the possibility to have opposite divert angles on both sides of the grid which can be useful to center parcels (wheels toward each other) or to diffuse parcels (wheels away from each other).

A number of competitors also include an option to have a full electric actuated product introducing variable angle settings. For instance sorters of ZiPLine, OCM and Siemens featuring similar functionality as the IQ-Grid. Variable divert angles enable better parcel control. The VarioRoute of Siemens features the largest range with variable divert angle from 0 to 45°.

The sorters with an open deck like the products of Intelligrated, Damon and Vanderlande can be considered to be outdated due to safety reasons, the open mechanism can result in injuries. These systems are usually not applied nowadays. However, the pop-up mechanism in these products does offer an advantage since the parcel is lifted off the belt conveyor. This helps to divert parcels since the belt conveyor will no longer have influence on the parcel movement.

The Swivel Belt Sorter stands out most in originality with its belt drivers instead of wheels. The product is similar to the patent in Section B.6. These belts support the parcel well and ensure a less wobbly behavior which results in better handling.

A summary of products discussed in appendix C is shown in Table 3.3, different characteristics of each sorter are stated. A dash (-) indicates that the information is not available.

Table 3.3: Overview of the discussed products with their specifications.

Name	Divert Angle [deg]	Positions	Pop-up	Actuator	Package Weight [kg]	Capacity [packages/hour]	Roller Speed [m/s]
Wheel Sorter, Gubunki [17]	30 to 90	Variable	No	Electric	40	6000	2,5
NBS Wave 200, TGW [41]	30	Fixed	Yes	Pneumatic+electric	34	12000	2,15
Wave Sorter, Garam [16]	30 to 40	Variable	No	Electric	50	10000	1,8
PWDSorter, ZiPline [40]	0 to 30	Variable	No	Electric	23	4500	0,61
ProSort, Hytrol [19]	30	Fixed	No	Electric	34	4800	1,5
ARB, Intralox [22]	30, 90	Fixed	No	Electric	90,7	6000	0,77
Belt Sorter [15]	30, 45, 90	Fixed	No	Pneumatic+electric	-	-	-
Wheel Sorter, OCM [32]	30, 45, 90	Fixed	No	Pneumatic or electric	50	10,000	2
Steerable Wheel Divert, Dematic [9]	30	Fixed	No	Pneumatic+electric	50	4800	-
OneSorter, FBA Italy [24]	30, 90	Fixed	No	Pneumatic+electric	50	4000	1,5
Truxorter, Vanderlande [44]	45	Fixed	Yes	Pneumatic+electric	50	5000	2
Swivel Wheel, Damon [5]	30	Fixed	No	Pneumatic or electric	35	4200	1,5
RC22, Transnorm [42]	45	Fixed	No	Pneumatic+electric	50	5000	1,5
Intellisort WD, Intelligrated [20]	30	Fixed	Yes	Pneumatic+electric	-	6000	-
VarioRoute, Siemens [38]	0 to 45	Variable	No	Electric	50	13000	2,5

3.3. Product Requirements

Since this research will not focus on the mechanical design but only on the conceptual layout, the requirements are restricted to functional design. These requirements are determined to be:

- Product should be capable of sorting and merging bidirectional.
- Align parcels on the conveyor for presorting.
- Product functions are independent of parcel position on conveyor.

These requirements are formed using the product specification for the IQ-Grid [43] and confirmed by the state of the art which presents products containing similar functionality. Sorting and merging bidirectional (Figure 3.6) is required to enable switching the system between morning and afternoon shifts as described in Section3.1. Also the alignment of parcels on the outlet can be useful to enable 'pre-sort' of parcels (Figure 3.7), this can save length for sortation grids following since the parcel has to travel less distance to the outlet. Such a configuration can be useful in systems having many exits and therefore, multiple sortation grids.

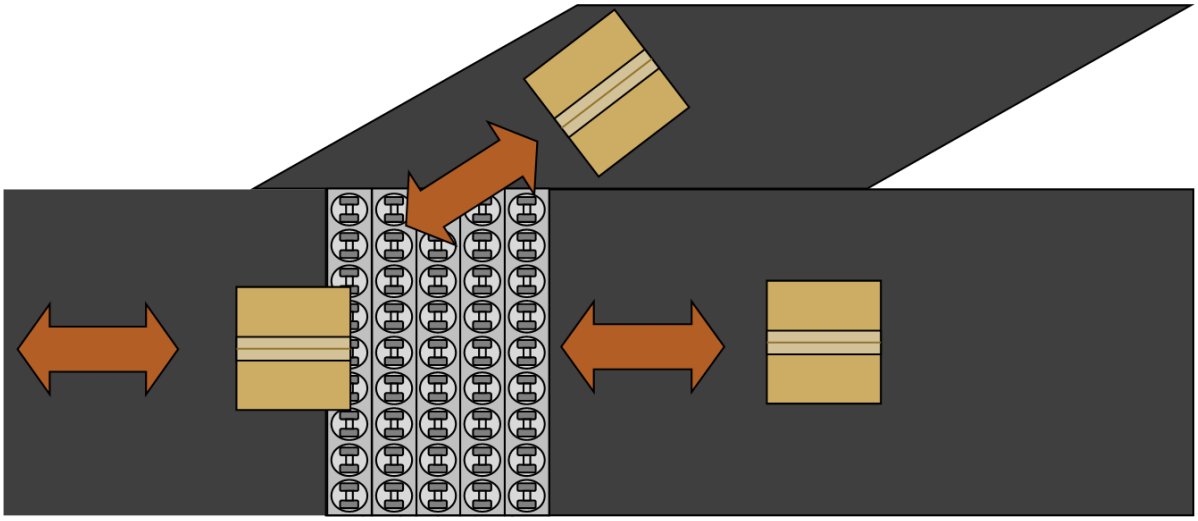

Figure 3.6: Bidirectional sort configuration in which parcels can be sorted to the outlets by the grid, but can also merge the parcels back on the conveyor when operating in reverse.

Finally, products hypothetically have to be moved from the far right to an outlet by a single grid. This may be necessary in systems which have no grids for pre-sortation. However, this requirement may be overcome by creating a larger grid to ensure proper sortation without requiring different layouts as is the case for the other requirements.

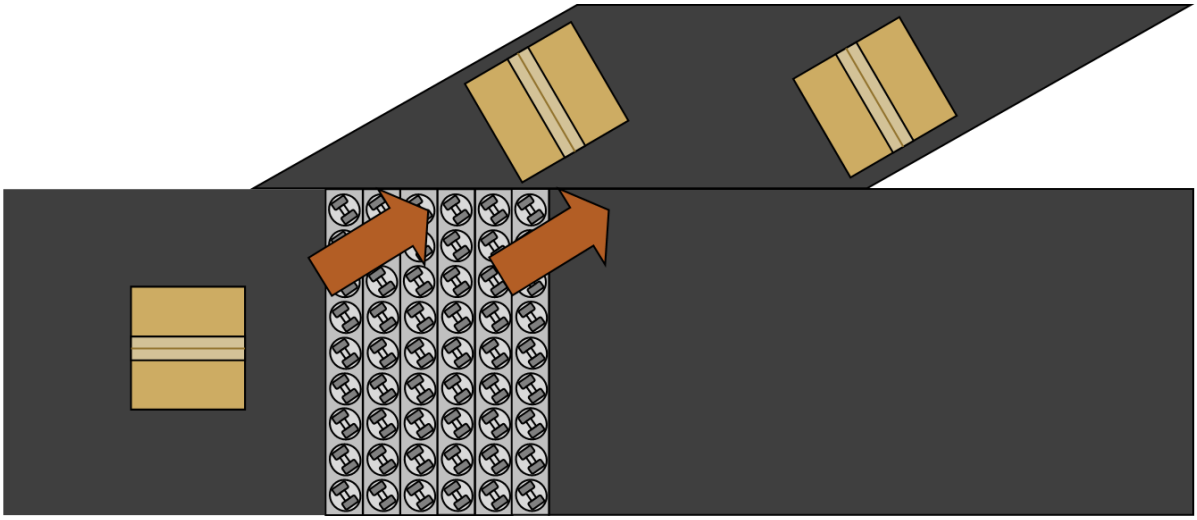

Figure 3.7: To save grid length at multiple exits the parcels can be pre-sorted by a grid such that parcels have less distance to travel towards an outfeed at the following grids.

3.4. Conclusion

In this chapter one of the sub questions was answered in order to provide background information on bidirectional sorters. This sub question was defined as:

What are State of the Art bidirectional sorters and their required functions?

According to Table 3.1 the only feasible option for bidirectional sorting is a steerable rollers sorter. Furthermore, the deflector and pusher were already unsuitable due to the introduced collisions which can cause damage to the content in polybags or they can get stuck in the diverter while sorting.

To further investigate the possibilities for bidirectional sorting different patents and products were explored. These products and patents showed an overlap in solutions, each mechanism is based on friction between the equipment and parcel to divert the parcel instead of force driven sortation. This results in a gentle handling and usually bidirectional properties when the product can operate in reverse. This approach will be used to define the mathematical model in the following chapter.

Using the information gathered, the product requirements are determined to be: bidirectional sorting and merging independent of the position of the parcel and ability to align parcels at different positions in the outlet.

4

Parcel Behaviour Model

In this chapter a parcel behaviour model is constructed to predict the position and orientation of the parcel during transportation over conveyors and the IQ-Grid. The model is described by several functions which relate the parcel and equipment properties to a change of position and orientation of the parcel. These functions are later implemented in a simulation model which (after validation) is used for the design of the second generation IQ-Grid.

This chapter holds four sections namely: Product decomposition, Parcel translation, Parcel rotation and Element forces. The first section decomposes the product by using the similarity between different bidirectional sorters as described in Chapter 3 which stated that all of these sorters use frictional forces to divert the parcel.

Secondly, the translation of the parcel is described using the forces induced on the parcel. These forces are then also used in the next section to determine the rotation of the parcel. Finally, the calculation of these forces is described by splitting the parcel into different elements. These aspects will form the basis of the simulation described in Chapter 5.

4.1. Product Decomposition

The product can be abstracted to its core principle, this can help to develop the mathematical model and to find a new configuration on conceptual level. By taking the products and patents discussed earlier into account, it can be seen all products sort parcels based on a frictional force rather than a restricting one (pusher, guiding rails, etc.).

It is assumed all equipment is at equal heights and each piece of equipment can be modelled by a plate having a certain divert angle, friction and velocity. Therefore, the mathematical model is limited to x,y-coordinates. This assumption is made, since the equipment is usually aligned in z-direction and to simplify the model by neglecting bumps and imperfections caused by the wheels and transitions between equipment.

As seen in Chapter 3 the frictional force can be applied by different members, e.g. wheels, belts,

Table 4.1: All three variables corresponding to a bidirectional sorter including their category and remarks on how these will be used during this research.

Variable	**Category**	**Remarks**
Velocity	Controlled	Could be adjusted but is determined to be equal for different parcels to lower the necessary mechanical requirements
Divert Angle	Independent	Adjustable, can be used to influence parcel behaviour
Friction Coefficient	Dependent	Determined by mechanical design and parcel, cannot be adjusted to influence parcel behaviour

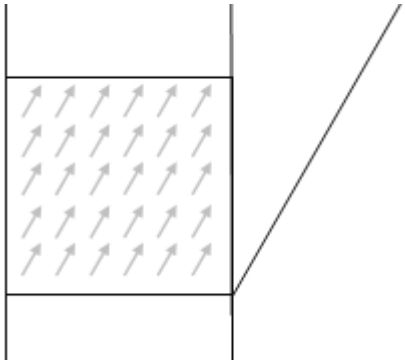

Figure 4.1: Abstract representation of bidirectional sorter which exerts a force on the parcel in a different direction in order to divert the parcel.

balls, etc. This medium may be determined during the mechanical design, since it will not influence the working principle namely, the force which diverts the parcel from its path towards a different direction. This member does determine the friction coefficient which should be optimized to provide enough grip on the parcels. But, this variable cannot be adjusted during operation and can therefore, not be used to optimize the parcel behaviour and is a fixed property. This only leaves the velocity and divert angle as variables to influence the parcel behaviour.

An abstract representation of a bidirectional sorter is shown in Figure 4.1 in which the product is converted to a vector field of frictional forces of which the direction can be adjusted by choosing different divert angles. Used to influence the parcel translation and rotation to efficiently sort the parcel.

The different products found in the State of the Art show a difference in the layout of these forces for instance, an angle set per member, per row or column. The patterns of these angles may be used to optimize the parcel behaviour. By optimizing these angles it does not matter which members and other mechanical components may be used as long as they are able to fulfill the prescribed abstract layout.

Another variant could be the drive speed of the wheels to accommodate a diversion of the parcel. This however, will require constant adjustment of the velocity of the members and is assumed to be more demanding than a rotation of the members. Therefore, the focused is laid on optimizing the parcel behaviour by adjusting the rotation angles. While using a fixed setting for the velocity of the grid. The different variables belonging to the wheel sorter are shown in Table 4.1.

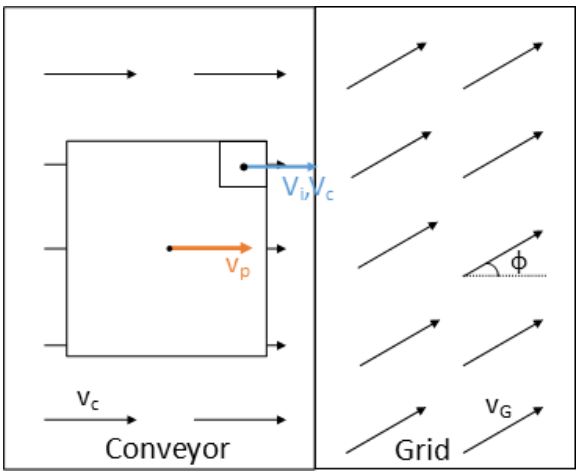

Figure 4.2: Parcel is in contact with one piece of equipment. Velocity of the parcel is equal to the magnitude and direction of equipment velocity and resultant force on an element is equal to zero.

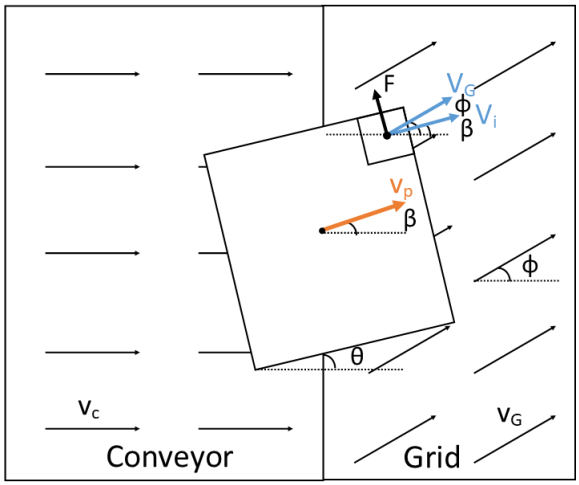

Figure 4.3: Parcel is in contact with two pieces of equipment, the resultant force on an element depends on the difference between the element velocity and equipment velocity.

4.2. Parcel Translation

In Figure 4.2 & 4.3 two different situations are shown which can occur during transportation of the parcel over different pieces of equipment. These situation can be described as follows:

- Parcel is in contact with one piece of equipment: in this case the parcel will adapt the velocity of the equipment, which is in the direction of ϕ. Consequently, the element velocity will have the same direction as the equipment velocity, resulting in a difference of zero leading to a resultant force of zero.
- Parcel is in contact with two or more pieces of equipment: the parcel will have a static friction with one piece of equipment which has the largest frictional force and dynamic friction with the other ones. The parcel will be influenced by the forces induced by all equipment and its displacement will depend on the sum of these forces.

The acceleration is calculated for each individual element in Section 4.4.2 and found by the forces in each direction, this also included terms for acceleration and deceleration if the velocity of the parcel and equipment differs. The accelerations found at the elements within the parcel are then averaged by Equation 4.1 & 4.2 resulting in respectively acceleration in x- and y-direction for the complete parcel at a certain time step, $(t+\Delta t)$. The number of elements, n_e is determined by the size of the parcel and element size.

$$a_x(t+\Delta t) = \frac{\sum_{i=1}^{n_e} a_{xi}(t+\Delta t)}{n_e} \tag{4.1}$$

$$a_y(t+\Delta t) = \frac{\sum_{i=1}^{n_e} a_{yi}(t+\Delta t)}{n_e} \tag{4.2}$$

These results can then be used to find the velocity and displacement for both the x- and y-direction using Equations 4.3 & 4.4.

$$v(t+\Delta t) = v(t) + a(t) \cdot \Delta t \tag{4.3}$$

$$s(t+\Delta t) = s(t) + v(t) \cdot \Delta t + \frac{1}{2} \cdot a(t) \cdot \Delta t^2 \tag{4.4}$$

4.3. Parcel Rotation

During transportation the parcel can rotate when in contact with multiple pieces of equipment, due to element acceleration and torque induced by the resultant force shown in Figure 4.3. This torque is assumed to take place in the center of the parcel, resulting in a rotation of the parcel around its center.

By combining the torque (of the element forces) and moment of inertia the angular acceleration of the parcel can be found, which can then be used to find the rotation (θ) of the parcel induced by torque. First the total torque acting on the parcel is computed by taking the sum of the torques induced by each element. This is calculated using Equation 4.5. The total torque and moment of inertia can then be used to find the angular acceleration (α) of the parcel shown in Equation 4.6.

$$\tau = \sum_{i=1}^{n_e} \tau_i \tag{4.5}$$

$$\alpha = \frac{\tau}{I} \tag{4.6}$$

Using the angular acceleration, the added rotation of the parcel can be computed using similar equations as for the displacement in Section 4.2. First, the angular velocity (ω) will be computed by Equation 4.7, which can then be used to calculate the resultant parcel rotation (θ) by Equation 4.8.

$$\omega(t+\Delta t) = \omega(t) + \alpha(t) \cdot \Delta t \tag{4.7}$$

$$\theta(t+\Delta t) = \theta(t) + \omega(t) \cdot \Delta t + \frac{1}{2} \cdot \alpha(t) \cdot (\Delta t)^2 \tag{4.8}$$

4.4. Element Forces

To account for possible slip occurring between the parcel and equipment the model calculates the forces acting on the parcel for several elements. These forces are then averaged to calculate the resultant force and torque used in Sections 4.2 & 4.3, while elements can move relative to each other. This calculation concept is also shown in Figure 4.4 in which the complete parcel is shown but also a single element.

4.4.1. Element Mass

First, the mass of a single parcel has to be found, this mass depends on the chosen element size, parcel size and weight distribution within the parcel. The model uses square elements which results

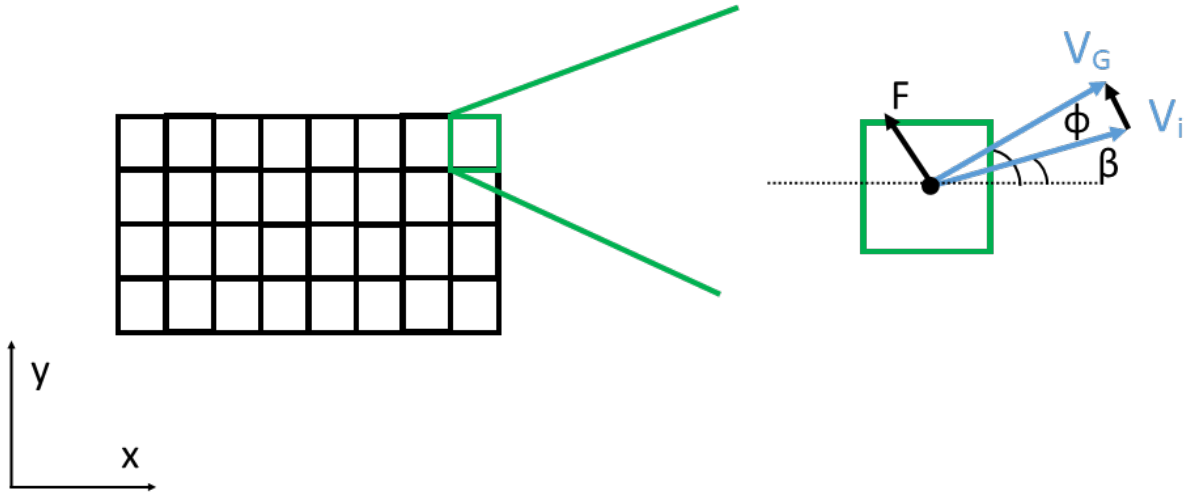

Figure 4.4: A parcel split into different elements shown on the left, a zoomed in view of a single element is shown on the right including the resultant force exerted by the equipment (F), element velocity (V_i) and equipment velocity (V_g).

in equal dimensions for the length and width of the element ($A_i = B_i$). The element mass is given by Equation 4.9, in which the following parameters are used:

- $\rho(\hat{x}, \hat{y})$**:** the density of the parcel at the position of element.
- ΔA**:** length of the element.
- ΔB**:** width of the element.

$$\hat{m_e} = \Delta A \cdot \Delta B \cdot \rho(\hat{x}, \hat{y}) \tag{4.9}$$

When considering a homogeneous plate the mass for an element simplifies to Equation 4.10 in which the density distribution is replaced by the following parameters:

- m_p**:** mass of the parcel.
- A: length of the parcel.
- B: width of the parcel.

$$\hat{m_e} = \Delta A \cdot \Delta B \cdot \frac{1}{A \cdot B} \cdot m_p \tag{4.10}$$

4.4.2. Forces Acting on an Element

Following Figure 4.4 the force acting on an element can be found. This forced is induced by the equipment underlying the element and depends on the friction force and the vector between equipment- and element velocity.

Using the mass of a single element the friction force between the equipment and the element (F_w) will be described, this force is given by Equation 4.11. In which the following parameters are used:

- m_e**:** mass of the element.
- g: gravitation constant ($9.81 m/s^2$).
- μ**:** friction coefficient which depends on the equipment the element is in contact with, which is described further in Section 4.4.3.

$$F_{w_i} = m_e \cdot g \cdot \mu \tag{4.11}$$

In order to find the corresponding x- and y-forces a vector is determined to describe the difference between the equipment- and element velocity. The resultant force has the same direction therefore, the x- and y-components are determined using the vector.

In Equation 4.12 the vector is determined using the angles and velocities shown in Figure 4.4 in order to determine F_x & F_y. These are calculated using the following variables:

- V_e: equipment velocity.
- V_i: element velocity.
- ϕ: angle between the x-axis and velocity of the equipment.
- β: angle between the x-axis and velocity of the element.
- F_w: friction force as determined by Equation 4.11.
- F_x: resultant force on the element in x-direction.
- F_y: resultant force on the element in y-direction.

$$\begin{bmatrix} F_x \\ F_y \end{bmatrix} = F_w \cdot \begin{bmatrix} V_e \cdot cos(\phi) - V_i \cdot cos(\beta) \\ V_e \cdot sin(\phi) - V_i \cdot sin(\beta) \end{bmatrix} \tag{4.12}$$

The acceleration for an element is found by taking the force in x- or y-direction and dividing by the element mass as shown in Equation 4.13 & 4.14. These results are then used to determine the average acceleration of the parcel.

$$a_{x_i} = \frac{F_{x_i}}{m_e} \tag{4.13}$$

$$a_{y_i} = \frac{F_{y_i}}{m_e} \tag{4.14}$$

To preserve the shape of the parcel, the new positions for each element are calculated using the average displacement as shown in Equation 4.15 & 4.16. By calculating the element positions from the average parcel displacement it is possible to have slip during a time step and preserving the shape of the parcel by modelling stiff connections between the elements. The variable θ represents the rotation of the parcel compared to the lateral direction (x), this variable will be calculated using the equations in Section 4.3.

$$s_{x_i}(t+\Delta t) = s_x(t+\Delta t) + \left[s_{x_i}(0) - s_x(0)\right] \cdot cos(\theta) - \left[s_{y_i}(0) - s_y(0)\right] \cdot sin(\theta) \tag{4.15}$$

$$s_{y_i}(t+\Delta t) = s_y(t+\Delta t) + \left[s_{x_i}(0) - s_x(0)\right] \cdot sin(\theta) + \left[s_{y_i}(0) - s_y(0)\right] \cdot cos(\theta) \tag{4.16}$$

4.4.3. Friction Coefficients

The friction coefficients used in the equations depend on the piece of equipment, state of the parcel, its orientation and surface of both the equipment and parcel. The parcel can have two states with the equipment underneath it namely: static and dynamic. These states introduce a difference in friction coefficient whereas the static friction is higher. The parcel is assumed to have static friction with the piece of equipment which has the largest total frictional force on the parcel of all the pieces of equipment.

Furthermore, the shape of the equipment can have an influence on the friction coefficient, which is the case when using wheels to transport the parcel. The friction between the wheel and the parcel will depend on the orientation of the wheel towards the parcel. This friction coefficient if found by using the ellipse shown in figure 4.5 , whereas θ is the angle difference between the parcel and the wheel ($\theta = \phi - \beta$), with is 0° if the parcel is aligned with the wheels and 90° if the wheel is perpendicular to the parcel. The resultant friction coefficient if found by using Equation 4.17 which can be used to either calculate the static or dynamic friction [2]. In which the following parameters are used:

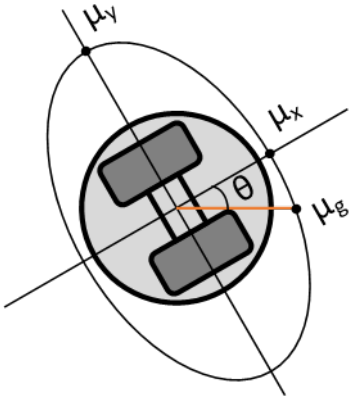

Figure 4.5: Ellipse which is use to determine the friction coefficient between the wheels and the parcel, if the parcel travels longitudinal to the wheel $\theta = 0°$ and so the friction coefficient (μ_g) is equal to μ_x if the parcel travels lateral $\theta = 90°$ to the wheel then $\mu_g = \mu_y$. For the other values of θ Equation 4.17 will be used.

- μ_{w_x}: friction coefficient between the equipment and parcel in radial direction.
- μ_{w_y}: friction coefficient between the equipment and parcel in axial direction.

$$\mu_w = \sqrt{\left(\mu_{w_x} \cdot cos(\phi - \beta)\right)^2 + \left(\mu_{w_y} \cdot sin(\phi - \beta)\right)^2} \tag{4.17}$$

4.5. Torque Induced by Element Forces

The torque is assumed to be in the center of the parcel and is induced by the forces induced by each element and the equipment. In Figure 4.6 the definition of R_{x_i} & R_{y_i} is shown which are used to calculated the torque. Furthermore, the definition of the torque direction is shown from which the signs for each force are derived.

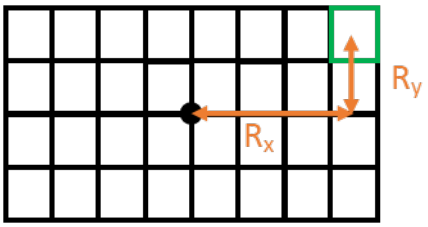

Figure 4.6: Definition for R_x&R_y for the single element shown in green. These dimensions are calculated for each individual element to compute its contribution to the torque acting on the parcel.

The torque of a single element is calculated using Equation 4.20 in which R_{x_i} & R_{y_i} are found using Equation 4.18 & 4.19 which calculate the difference between the parcel centre and element centre.

$$R_{x_i} = s_{x_i} - s_x \tag{4.18}$$

$$R_{y_i} = s_{y_i} - s_y \tag{4.19}$$

$$\tau_i = F_y \cdot R_{x_i} - F_x \cdot R_{y_i} \tag{4.20}$$

4.5.1. Moment of Inertia of the Parcel

The parcel has a resistance to angular acceleration, this acceleration is necessary to cause an rotation of the parcel. The moment of inertia is a measure of this resistance and will be used to calculate the angular resistance together with the torque calculated in Section 4.5.

When considering a non-homogeneous parcel the inertia is computed using the density distribution $(\rho(x,y))$ also used in Section 4.4.1. This density is used to integrate over the volume of the parcel, for each element at a distance of r from the centre of the parcel. This results in Equation 4.21, which can be used to compute the inertia of a non-homogeneous parcel.

$$I = \int_V r^2 \rho \, dV \tag{4.21}$$

When considering a parcel with an homogeneous weight distribution this formula reduces to a simpler form depending only on the total mass, length and width of the parcel. This formula is shown in Equation 4.22.

$$I = \frac{1}{12} \cdot m_p \cdot (A^2 + B^2) \tag{4.22}$$

4.6. Conclusion

In order to qualify the model this chapter answered the following sub question which was defined in Chapter 1.

How can a bidirectional sorter and surrounding equipment be modelled?

By using an element approach for both the parcel and equipment it was possible to find a mathematical model for the equipment while taking into account slip. This model comprising of functions for the displacement (s) and rotation (θ) can now be implemented into a simulation to evaluate the parcel behaviour.

By considering the different equations parcel behaviour can be described by knowing the dimensions and density distribution of the parcel, and the velocity and friction coefficients of the equipment. By performing different experiments conducted in Chapter 6 it can be validated if these are indeed the only variables necessary to describe the position and orientation of the parcel.

5

Parcel Simulation

After describing the mathematical model in Chapter 4, it is implemented into a simulation used for studying the influence of different parameters and observing output. In this chapter the implementation of the mathematical model is described. First, the implementation itself and structure of the simulation is shown. Second, output of the simulation is shown, which later will be used to show the difference in results when varying parameters such as; parcel dimensions, friction coefficients or divert angles.

From there, the implementation is verified by observing if the response of the simulation is according to expectations derived from the mathematical model. If the implementation seems to be correct, the mathematical model and simulation are validated using experiments to compare its output with reality, which will be done in Chapter 6.

Finally, element size and time step are determined to ensure a reliable output of the simulation. This is a consideration between computational time and accuracy.

5.1. Implementation of the Mathematical Model

To make use of the proposed mathematical model a simulation is created which can be used to visualize and compute parcel behaviour described by the mathematical model. This simulation uses the equations described in Chapter 4. To understand the working principle behind the simulation this section will clarify the structure and computational steps performed during a single run.

5.1.1. Simulation Structure

In Figure 5.1 an overview is provided of the simulation which has been implemented. A step wise description is provided below:

1. Start of the simulation: time is set to 0, and parameters are loaded into the simulation such as the gravitational force g, inertia and layout parameters.

2. Get element info: position data and mass of the element at i=1 are loaded from the data set.

3. Find position parameters: info of equipment directly underneath the element is loaded to compute corresponding forces.
4. Compute beta: direction of the parcel velocity is computed which will be used for calculation of the resultant force.
5. Compute forces: with all information gathered the force working on the element can be calculated according to Equation 4.12.
6. Compute element acceleration: using the element mass the acceleration of the element can be calculated, which is used to determine the velocity of the parcel using the previous known velocity.
7. Compute torque: using the calculated forces and distance between the element and the center of the parcel (R_x&R_y) the torque induced by the element is computed according to Equation 4.20 this is then added to the total torque working on the parcel.
8. Increase element number: if not all elements are computed for the current time point, the index i will be increased to compute the next element and start over at step 2.
9. Compute resultant velocity, position and rotation: if all elements are computed the overall parameters for the parcel are determined using previously computed torque and velocity.
10. Increase time: if the end of the simulation is not reached yet, the time will be increased by the time step provided. Then the progress will start over again and calculate all elements for the next time point starting at element i=1, step 2.
11. End of simulation: if the ending time is reached, the calculated data is processed and the output is generated after which the simulation ends.

5.2. Simulation Output

The simulation calculates the parcel behaviour for a predefined period of time, the results of this simulation are archived and can be reviewed after completion. In this section the output of the simulation is described, this output holds two parts, namely: a numerical output and a graphical output. Both outputs will be described below.

5.2.1. Numerical Output

This output consists of data sets describing different properties of the parcel at each time step. When using the standard configuration the simulation provides three data sets namely: Pc, Vc and Pphi. The first set (Pc) contains the parcels centre points defined by x- and y-coordinates at each time step. Vc, contains respectively the velocity in x-direction and in y-direction again, at each time step. Lastly, Pphi contains the rotation angle θ of the parcel compared to the transport direction (x) at each time step.

These data sets were chosen as the output of the simulation since these parameters will be measured during the experiments conducted in Chapter 6 and can therefore, be used to compare the results of the simulation and reality. Alternatively, logs can be created for several other parameters such as: the force acting on each element, torque on the parcel or resultant acceleration.

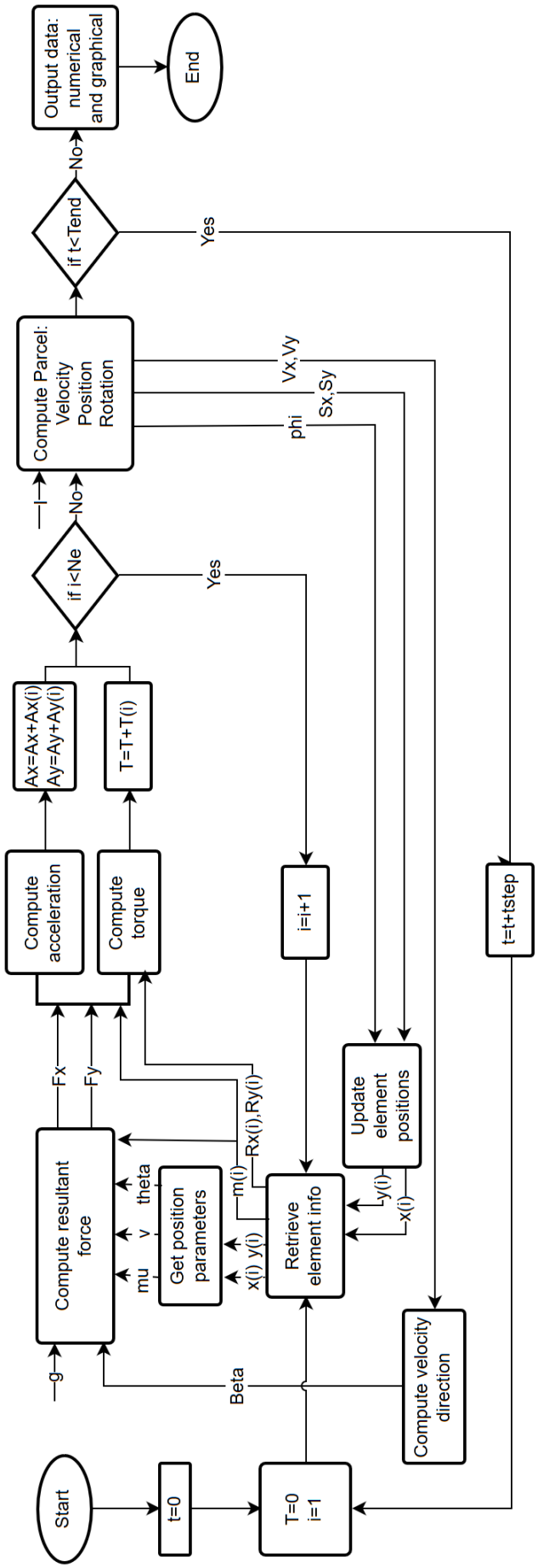

Figure 5.1: Overview of the simulation structure and computation steps.

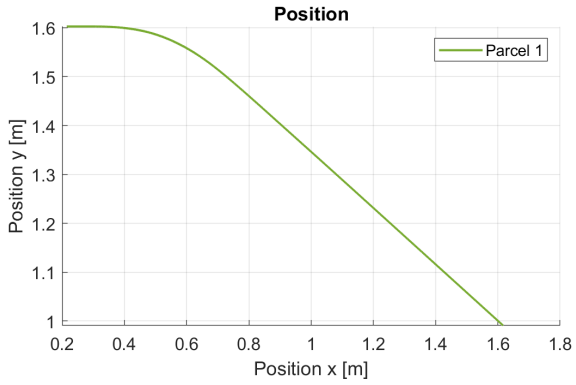

Figure 5.2: Graphical output simulation model showing the path followed by the parcel for the x- and y-coordinates.

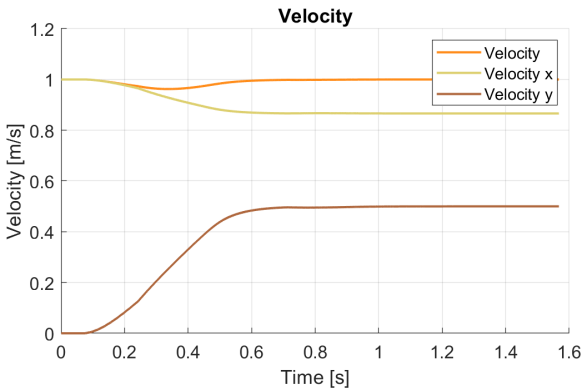

Figure 5.3: Graphical output simulation model showing the velocities of the parcel for both x- and y-direction and also the combined velocity.

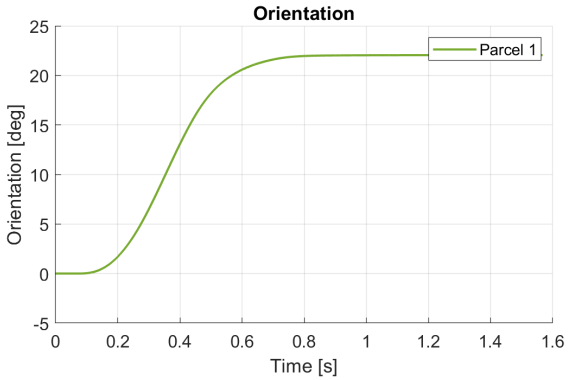

Figure 5.4: Graphical output simulation model showing the orientation of the parcel during

5.2.2. Graphical Output

The data sets are also represented by the graphical output of the simulation which includes plots of the velocity, position and orientation of the parcel. As shown in Figure 5.2-5.4, each data set has its own graph and can include separated or combined information of the x- and y-coordinates.

These figures will also be used to compare the model prediction and experiments, since the same parameters will be measured during the experiments. A second graphical output shows the progress of the simulation which can be useful as an indication for the remaining simulation time when using large sets of different parcels or other properties such as: friction coefficients or divert angles.

5.3. Verifying the Implementation

In this section several checks will be performed to verify the simulation model which is necessary to check a correct implementation of the mathematical model of Chapter 4. If errors were introduced during scripting, the mathematical model may seem incorrect during the validation phase while actually the errors are introduced by the implementation.

First, the simulation results will be observed to identify if the parcel shows a reasonable and expected behaviour. This will be done by checking the graphical and numerical output of the simulation. Second, parameters will be varied of which the influence will be observed compared to the expected outcome of the mathematical model. If both checks are met it can be assumed that the implementation of the mathematical model suffice.

5.3.1. Observing Simulation Results

First the initial model has been run to check a correct response of the parcel to the different pieces of equipment. This simulation was performed on the same parameters as the base model which will be discussed in Chapter 6. For the verification the value of the parameters are less important but mostly the response to a change in parameters will be tested. The validation phase in Chapter 6 will check if the output is correct according to the value of the parameters.

In Figure 5.5 the graphical representation is shown of a parcel travelling over respectively: the conveyor, grid and outfeed. The parcel is shown at multiple time steps of 0.25 s starting at x = 0.02 m. It first can be observed that the parcel indeed follows the direction of the conveyor which is to the right. Furthermore, the parcel is diverted by the grid in the same direction as the wheels are pointing. Finally, the parcel again follows the outfeed in the transport direction, which seems logical.

The direction of travel at the end is found to be at an angle of 30° with the x-axis, this is exactly the direction of the outlet. Since no other equipment is in contact with the parcel it is correct that the parcel will follow the transport direction of the belts on the outfeed.

Another check has been made on the velocity of the parcel, since the equipment has all been set to 1.00 m/s this should be the maximum velocity found for the parcel. By computing Equation 5.1 the maximum combined velocity is found to be 1.00 m/s which corresponds with the expectation.

$$v_{max} = \max\left[\sqrt{v_x^2 + v_y^2}\right] \tag{5.1}$$

Furthermore, the maximum parcel rotation is found at x = 1.18 m, which is between the grid and the outfeed. Since the friction coefficients of the grid are larger than the ones on the outfeed this seems correct. This is because the parcel will tend to true back towards the x-axis since the back of the parcel is pushed upwards due to the higher friction coefficients. This phenomenon is illustrated by Figure 5.6. Therefore, it seems logical that the maximum θ is found in between the grid and the outfeed.

Another observation on the parcel orientation can be made during the first and last part of the transport. The orientation of the parcel stays constant, since the parcel is travelling on a single piece of equipment is stopped turning since the forces around the parcel cancel out and no longer induce a torque.

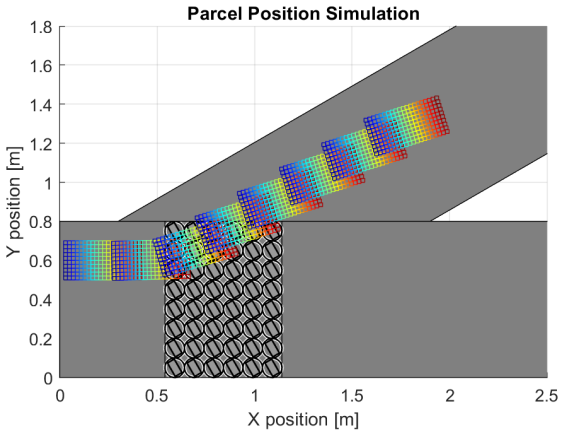

Figure 5.5: Simulation of the base model containing a parcel of 0.4x0.2 m, start position at 0.6 m, velocities at 1 m/s and a divert angle of 30°.

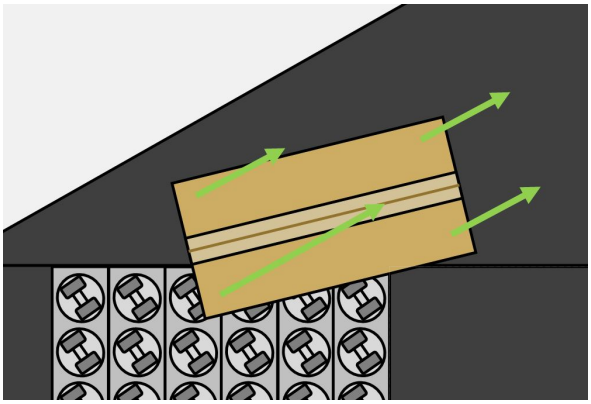

Figure 5.6: Phenomenon in which the parcel slightly rotates back towards the original position, which causes the maximum parcel rotation to be in between the grid and outlet.

5.3.2. Observing Parameter Response

By observing the formulas defined in Chapter 4 several parameters can be identified which will have influence on the parcel behaviour. These parameters will be varied in this section to check if the response corresponds to the expectation by observing the formulas. The parameters which will be varied are:

- Ratio B/A: parcel ratio found by dividing the width by the parcel length. An increase of the ratio will result in a higher inertia following Equation 4.22. Furthermore, the time available to rotate the parcel will stay constant or become less. Due to the higher resistance to rotate and equal or less transition time between equipment the parcel will rotate less.

- V: the velocity setting for the equipment. According to Equation 4.12 an increase in velocity results in increased forces exerted by the equipment on the parcel. This should result in a larger distance travelled between time steps. Furthermore, the torque is also increased which (in case of the grid) will result in a larger rotation of the parcel.

- μ: friction coefficients between the equipment and parcel. A higher friction coefficient results in increased F. When adjusting the friction coefficient for a single piece of equipment this should lead to an earlier and longer contained alignment for the direction and velocity of the parcel with the equipment. Due to the larger friction the equipment can have a higher influence on the parcel compared to other equipment.

- θ: the divert angle of the grid. A steeper divert angle should result in a larger a_y and lower a_x when the parcel is on the grid. This should result in a shorter path towards the outfeed.

Because the forces induced by the grid (F_x&F_y) will respectively decrease and increase due to the increase of the term $tan(\phi)$ corresponding to the steeper divert angle.

- I: inertia of the parcel. According to Equation 4.6 an increase in I will result in a decrease of α, this should eventually result in less rotation of the parcel since the resistance to rotate is higher.

Since the expected effects on parameter changes are determined, these can now be verified by the simulation model. Each run will have constant parameters as used in the base model of Section 5.3.1 with time step: 0.0005 s and element size 0.02 m which were determined before.

In Figure 5.7 the base model is shown with an overlay of the result of the dimension increase of two times (A=0.8 m, B=0.4 m). It can be seen visually that the parcel has rotated less, more specific the smaller ratio results in a rotation of 17.48° and the higher ratio 10.43°. This corresponds to the expected outcome.

In Figure 5.8 the base model is shown with an overlay of the results of the velocity increase from 1 m/s to 1.5 m/s. It can be seen that the parcel moved a longer distance is both x- and y-direction while the number duration was kept equal. Furthermore, the amount of rotation increased from 17.48° to 21.42°. Both observation correspond to the expected outcome.

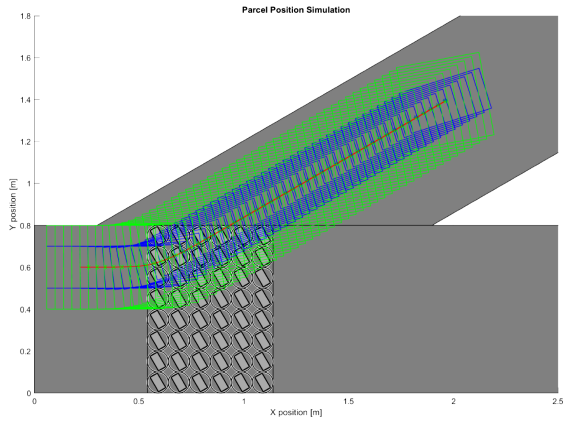

Figure 5.7: Base model (blue) with the adjusted parcel ratio to 1 resulting in dimensions: 0.4x0.4m as an overlay (green)

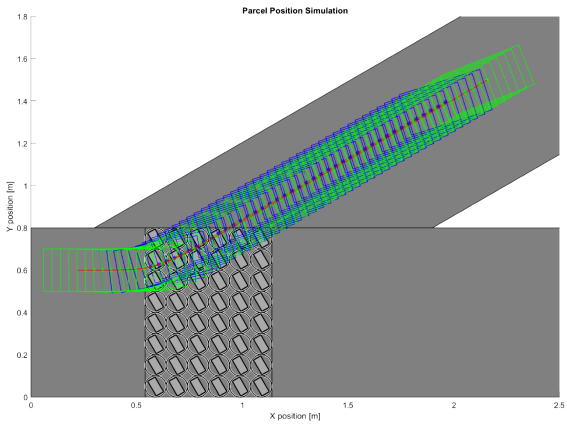

Figure 5.8: Base model (blue) with the adjusted grid velocity to 1.5 m/s instead of 1 m/s as an overlay (green)

The effect of the friction coefficient increment can be seen in Figure 5.9, in this run the friction coefficients of the grid were increased by a factor of 1.5. It can be seen that the parcel starts to rotate earlier and also the parcel transport direction adjusts in an earlier stage (difference can be seen by the red lines). In Figure 5.10 the friction coefficient of the conveyor was multiplied by 1.5 times compared to the base model. Here, it can be seen that the parcel contains its orientation and position for a longer amount of time compared to the base model. Both observation were expected to happen and therefore, show the desired result.

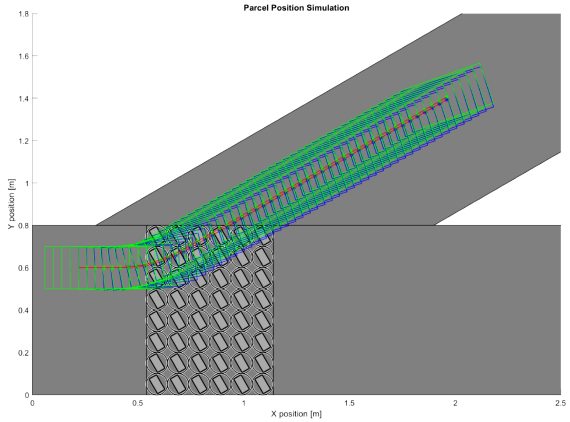

Figure 5.9: Base model (blue) with the adjusted grid friction coefficients increased by 1.5 times as an overlay (green)

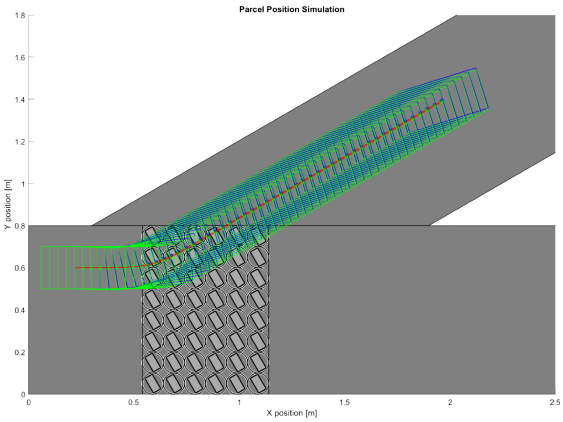

Figure 5.10: Base model (blue) with the adjusted conveyor friction coefficients increased by 1.5 times as an overlay (green)

To check the response to a increase in θ, the base value was adjusted from 30° to 45°. The effect of this increase can be seen in Figure 5.11. The adjusted simulation turns more quickly to the outfeed due to the steeper divert angle. This corresponds to the expected result which is described above.

Finally, inertia of the parcel was increased by a factor two, to indicate the response to an increased inertia. The effect of this can be seen in Figure 5.12. The parcel has rotated less but the position is remained. The rotation angle is found to be 8.93° compared to the 17.48° of the base model. The result corresponds with the expectation which indicated a decrease in rotation and constant position.

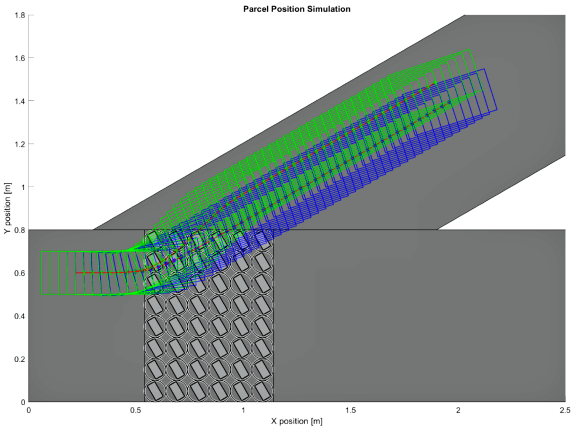

Figure 5.11: Base model (blue) with the adjusted grid divert angles from 30° to 45° as an overlay (green)

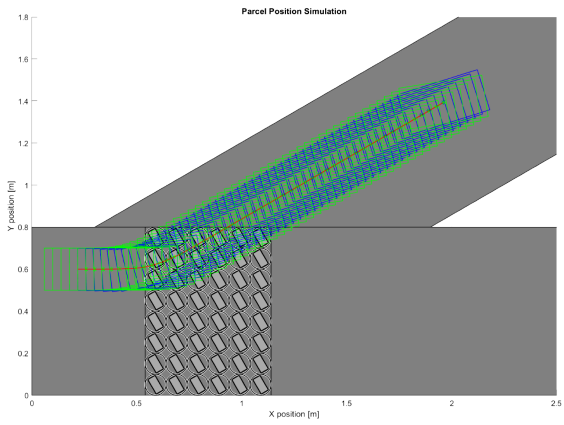

Figure 5.12: Base model (blue) with the inertia multiplied by a factor of two as an overlay (green)

5.4. Reliable Element Size and Time Step

In the simulation there are two important parameters which determine the accuracy and run time of a calculation, these are: element size and time step. The element size determines the dimensions of a single element and therefore, the number of elements used to simulate a single parcel. Since the

Table 5.1: Element sizes with their corresponding results, error towards the true value and computational time for a 0.4x0.2m parcel and time step: 0.00005 s.

Gridsize [m]	No. Elements	Position X [m]	Difference	Position Y [m]	Difference	Orientation [deg]	Difference	Time [s]
0,2	2	2,0762	3,74%	1,5187	2,58%	17,3411	0,99%	3,78
0,1	8	2,1076	2,28%	1,5744	-0,99%	18,1700	-3,74%	4,84
0,05	32	2,1376	0,89%	1,5502	0,56%	17,6181	-0,59%	8,12
0,02	200	2,1501	0,31%	1,5569	0,13%	17,4654	0,28%	34,51
0,01	800	2,1545	0,11%	1,5582	0,04%	17,5087	0,03%	130,35
0,005	3200	2,1568	0,00%	1,5589	0,00%	17,5148	0,00%	551,32

position of an element is rounded to a single piece of equipment the accuracy increases when using more elements since the rounding error will decrease. This however, also increases the calculation time since the calculation has to be performed for every element.

Furthermore, the time step determines the amount of time between two calculations points at which the new position of the parcel will be determined. Since the parcel will pass several different pieces of equipment it can be useful to detect these in an early stage and therefore, using small time steps in which the influence of each equipment is taken into account directly from the arrival of the parcel.

In this section the consideration between the accuracy and calculation times of these parameters will be discussed. This will result in a final value for the element size and time step which will be used during the continued development, validation and concept design.

5.4.1. Element Size

To determine a reliable element size the parameter will be varied and compared to the result of the smallest possible element size due to computational limits. This smallest size is determined to be 0.005 m and results in a number of elements of 3200 for a parcel having dimensions 0.4x0.2 m. The result of this measurement will be assumed to be the true value.

Each result for the position in x- and y-direction and orientation will be compared to the 'true' value to indicate the error between. In Table 5.1 and 5.2 the results are shown for two different parcels and different element sizes while using the most accurate time step possible namely: 0.00005s. A smaller time step results in an unresponsive simulation. In the next section the time step parameter will be varied to find the optimal balance between computational time and accuracy. Furthermore, these parcel sizes were chosen since these will be also used during the experiments and can indicate the influence of the element sizes for two different width/length ratios: 0.5 & 1.

The element size of 0.02 m has been chosen as the default size for the simulation, this is because of the accurate results while having acceptable computation times. This is mainly because of the accuracy of the parcel orientation during a rectangular parcel whereas other settings give inaccurate results (error>5%) or require computational times more than 1 minute. The large computational time will result in inefficiency when large data sets of parcels will be tested to check the correct operation of the new designed product.

Table 5.2: Element sizes with their corresponding results, error towards the true value and computational time for a 0.4x0.4m parcel and time step: 0.00005 s.

Gridsize [m]	No. Elements	Position X [m]	Difference	Position Y [m]	Difference	Orientation [deg]	Difference	Time [s]
0,2	2	2,0597	4,34%	1,6055	1,47%	11,2200	-9,51%	4,06
0,1	8	2,0997	2,48%	1,6489	-1,19%	10,5220	-2,69%	5,99
0,05	32	2,1328	0,95%	1,6292	0,02%	10,7606	-5,02%	12,86
0,02	200	2,1482	0,23%	1,6333	-0,23%	10,4090	-1,59%	66,76
0,01	800	2,1527	0,02%	1,6354	-0,36%	10,3208	-0,73%	257,59
0,005	3200	2,1532	0,00%	1,6295	0,00%	10,2460	0,00%	739,69

5.4.2. Time Step

In the last section the element size was determined to be 0.02 m, in this section the time step will be varied to further optimize the computational time. The most accurate setting possible is 0.00005 s which was also used for the determination of the element size. In Table 5.3 and 5.4 the results are given for respectively the parcel with width/length ratio 0.5 and 1. The errors are again determined by taking the smallest time step possible as 'true' value.

It can be seen that setting the time step to 0.0005 s, leads to errors close to zero while reducing the computational time by 4.5 times. Therefore, it has been decided to set the default time step to 0.0005 s which will result in a maximum error of 1.79% (0.2%+1.59%) for the orientation of a square parcel. The average error is determined to be 0.51%.

Table 5.3: Time steps with their corresponding results, error towards the true value and computational time for a 0.4x0.2m parcel and an element size of: 0.02 m.

Time step	Position X [m]	Difference	Position Y [m]	Difference	Orientation [deg]	Difference	Time [s]
0,5	0,2118	90,15%	3,0466	-95,68%	0,0000	100,00%	0,61
0,05	2,1863	-1,68%	1,5393	1,13%	14,5555	16,66%	4,61
0,005	2,1554	-0,25%	1,5591	-0,14%	17,7133	-1,42%	4,95
0,0005	2,1501	0,00%	1,5566	0,02%	17,4774	-0,07%	7,82
0,00005	2,1501	0,00%	1,5569	0,00%	17,4654	0,00%	35,79

Table 5.4: Time steps with their corresponding results, error towards the true value and computational time for a 0.4x0.4m parcel and an element size of: 0.02 m.

Time step	Position X [m]	Difference	Position Y [m]	Difference	Orientation [deg]	Difference	Time [s]
0,5	0,2770	87,11%	3,2003	-95,94%	0,0000	100,00%	0,86
0,05	2,1524	-0,20%	1,6478	-0,89%	18,8033	-80,64%	6,35
0,005	2,1526	-0,20%	1,6339	-0,04%	10,5660	-1,51%	6,84
0,0005	2,1483	0,00%	1,6331	0,01%	10,4303	-0,20%	12,45
0,00005	2,1482	0,00%	1,6333	0,00%	10,409	0,00%	67,04

5.5. Conclusion

In this chapter the model of Chapter 4 was implemented in order to answer the following sub question:

How can the parcel behaviour be accurately described?

By creating a simulation according to the mathematical model an output was achieved showing the parcel behaviour over the grid. The output was then verified to ensure a correct implementation and will later be validated to ensure an accurate description of the parcel behaviour.

According to the verification it can be assumed that the mathematical model of Chapter 4 has been

implemented correctly. All verification steps gave a similar response as expected by observing the underlying equations, which leads to the assumption that the simulation is correctly implemented.

The verification also showed which responses can be expected when varying parameters. However, these values still need to be validated by real world experiments before any conclusions can be draw upon the impact of each parameter and outcome. These experiments should also show if the simulation is indeed accurate.

Furthermore, the element size and time step have been set to 0.02 m and 0.0005 s which showed a reliable outcome while reducing the computational time by several minutes compared to the maximum setting. This also showed that the a time step smaller than 0.0005 s significantly increases computational time but only slightly increases accuracy.

6

Experiments & Model Validation

In this chapter the simulation model constructed in Chapter 5 using the mathematical model of Chapter 4 is validated. This is an important step towards a reliable model by ensuring that the assumptions of the mathematical model and implementation are correct.

As described in Chapter 2 validation is performed by experiments using the first generation IQ-Grid. Via these experiments the model output is compared to a physical model. If these results agree, it is assumed that the model can also be used for several other layout since the underlying physics are correct.

First, an experimental plan is developed using a dimensional analysis and design of experiments methodology. From there, experiments are carried out and parameters are analyzed to show which parameters have significant influence on the sorting reliability.

Finally, the experiments are compared to the results obtained from the simulation for different parameters. If these overlap the model can be used to test different layout configurations in Chapter 7.

6.1. Experimental Plan

To gain reliable and relevant information from the experiments a clear experimental plan needs to be developed. This plan includes information about the measurement setup, variables and experiments to be conducted. These steps will be described in this section.

6.1.1. Dimensional Analysis

The variables which have been indicated to have influence on the sorting behaviour are shown in Table 6.1, these were found using the mathematical model (Chapter 4) and experience from the development of the first generation product.

Table 6.1: Different variables indicated to have influence on the parcel behaviour by the mathematical model and experience of earlier development.

Length parcel	L_p	Wheel height	h_w	Friction parcel-grid	μ_g
Velocity conveyor	V_c	Divert angle	α	Friction parcel-conveyor	μ_c
Acceleration	a_g, a_c	Surface	S_m	Position	x_p, y_p
Gravitational	g	Parcel ratio	$\frac{W_p}{L_p}$	Orientation	ϕ
Start orientation	ϕ_0	Velocity	$\frac{V_g}{V_c}$	Roll friction	C_r
Start position	x_{p0}, y_{p0}	Inertia	$\frac{I}{L_p^2 m_p}$	Weight	m_p
Transport width	T_w	Stiffness	S		

Dimensions of each variable are also shown in Table 6.1, these are used to determine main variables for the dimension analysis in such a way that each dimension is represented. The following variables were chosen:

$$(L_p, S, I, m_p, v_g, a_g)$$

These main variables can then be used to determine linear terms (e.g. terms consisting of two equal dimensions or no dimension). The following linear terms were found:

$$\left(\frac{L_g}{L_{tw}}, \frac{W_p}{L_p}, \frac{h_w}{L_p}, \frac{y_{p0}}{L_p}, C_r, \varphi, \mu_g, \mu_c, \alpha, \frac{V_c}{V_g}, \frac{a_c}{a_g}, \frac{g}{a_g}\right)$$

According to the Buckingham Pi Theorem shown there should be (6-3) = 3 more independent dimensionless groups which can be found using the method of indices [27]. Using this method the following three dimensionless groups were found:

$$\left(\frac{m_p \cdot V_g^2 \cdot a_g}{L_p^5 \cdot S^2 \cdot I}, \frac{I}{L_p^2 \cdot m_p}, \frac{L_p \cdot a_g}{V_g^2}\right)$$

Using the defined dimensionless groups there should exist a formula which describes the sort behaviour of the IQ-Grid. Optimizing this sorting behaviour should lead to a smaller grid necessary to sort parcels therefore, the term L_g/L_{tw} was chosen to be described by the dimensionless groups. This is useful to indicate which groups has a large influence on the sort behaviour, which can be achieved by conducting several experiments in which these groups are varied. The varying of these parameters will be described in Section 6.1.4.

6.1.2. Parcel tracking

During the experiments measurements should be conducted on the parcels to determine their position and orientation. Since the design method described a quantitative approach (Chapter 2) these measurements should provide accurate data on the behaviour instead of for instance visual observations or ranking.

Therefore, it is decided to use video measurements to acquire information on the position, velocity and orientation of the parcel. These variables were chosen to measure since they can be directly

compared to variables of the model output (Chapter 5) and describe the behaviour of the parcel well.

Different patterns were used to decide which pattern would provide the most accurate results. Two types of trackers were selected namely: Whycon and checkerboard. Whycon trackers provide better results over several other tracking methods [1]. Furthermore, the checkerboard pattern was selected since it is a proven method for camera calibration, has a low error and a robust Matlab algorithm [14].

In Figure 6.1-6.3 the different patterns can be seen, for the whycon trackers minimal two circles are necessary to measure the orientation of the parcel furthermore, a tracker with four circles was used to indicate if the number of data points available has a positive effect on the accuracy. The checkerboard is a standard pattern and has been fitted to the smallest parcel which will be used during the experiments.

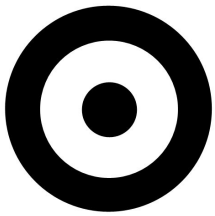

Figure 6.1: Whycon tracker using two circles.

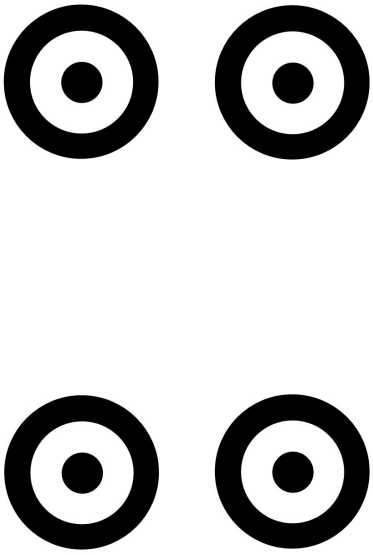

Figure 6.2: Whycon tracker using four circles.

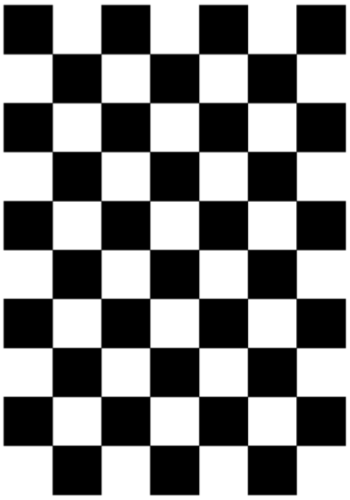

Figure 6.3: Checkerboard pattern as supplied by Matlab for camera calibration.

To show the difference in accuracy the velocity measurements were used, these measurements are shown in figure 6.4-6.6. These plots are acquired by measuring the difference in position between two frames and dividing by the recording speed of the camera. This results in a clear indication of the stability and noise for each tracker.

The graphs show a clear difference between the checkerboard and Whycon trackers, the checkerboard shows a more reliable and stable characteristic with less noise. This behaviour can be addressed by the increased amount of data available in the checkerboard tracker and more reliable detection algorithm used. Therefore, it was decided to use the checkerboard tracker for the experiments, due to the reduced noise and presumably higher accuracy. Additionally, the four Whycon trackers did not show a significant improvement over the two tracker configuration.

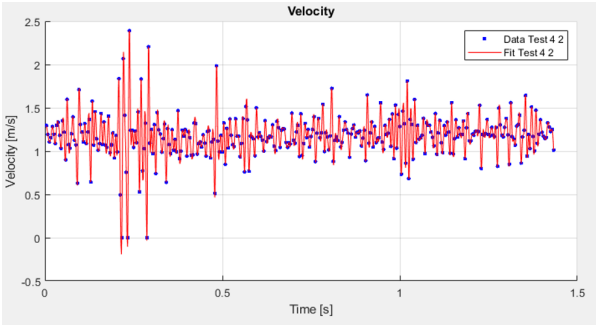

Figure 6.4: Measured velocity of the parcel using a Whycon tracker with two circles.

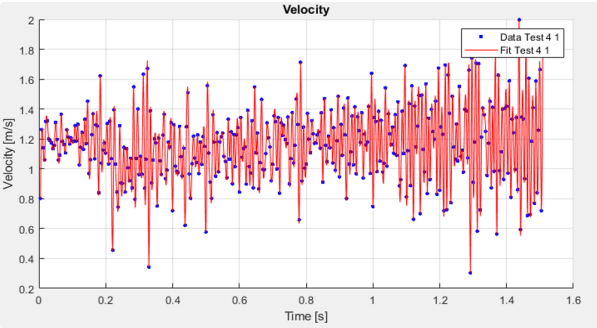

Figure 6.5: Measured velocity of the parcel using a Whycon tracker with four circles.

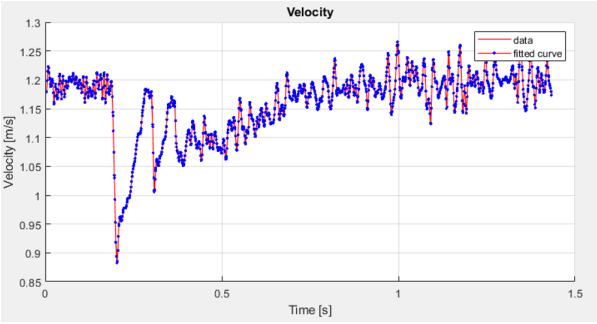

Figure 6.6: Measured velocity of the parcel using a checkerboard and Matlab detection algorithm.

6.1.3. Disturbances

During the setup of the experiments different disturbances were indicated and if necessary reduced. These were defined to be:

- **Lighting conditions:** by disabling the LED lights close to the setup the flickering visible in the slow motion video was reduced. Adding extra lights to the setup resulted in reflections from the equipment which leaded to reduced tracking results as can be seen in Figure 6.8 compared to the original measurement in Figure 6.7.
- **Parameter variance:** to ensure parameters were set to the same level during different experiments several precautions were made. To ensure the correct start position a stop was added at the side of the conveyor. Furthermore, settings for equipment height, speed and angle were marked and written down.
- **Video processing:** the camera processing indicated an error in the linearity of the time in between frames. This error was induced by the slow processor which resulted in a sinus pattern of 30 Hz visible in the captured velocity (Figure 6.7). By disabling other functions available in the camera such as GPS, Wifi and onscreen display, the processor has more resources for the video processing. This resulted in less noise as can be seen in Figure 6.9.
- **Equipment interaction:** in the testing facility also several other experiments were conducted during the setup, these interfere with the setup by vibrations which were also visible in the velocity plot. After switching off the other experiments the noise in the measurement was even further reduced which can be seen in Figure 6.10.

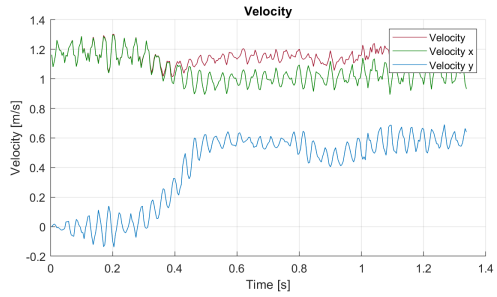

Figure 6.7: First acquired measurement without any disturbance reductions.

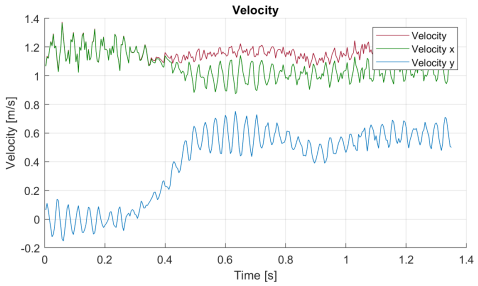

Figure 6.8: Measurement with added lights close to the field on interest (IQ-Grid), resulting in less accurate results.

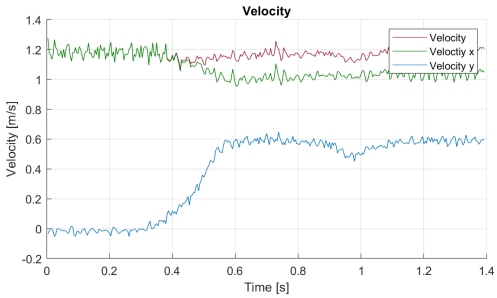

Figure 6.9: Reduced noise within measurement by enhancing the video processing speed of the camera resulting in a more linear frame capturing.

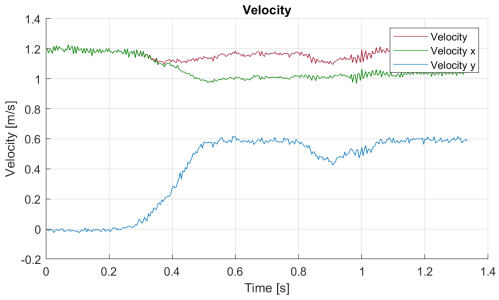

Figure 6.10: Disabling of other tests running in the facility, resulting in less vibrations and therefore, a more stable capturing.

6.1.4. Variables Definition

The dimensionless groups which were defined in Section 6.1.1 are used to determine which variables are controlled, dependent and independent. First, a definition of these different variables is given:

- **Controlled variables:** these variables will be kept constant during all experiments [4], an example of a controlled variable in this experiment is the start position of the parcel which is controlled by the stop described in Section 6.1.3.
- **Independent variables:** these variables are varied between different experiments and indicate the variables of which the influence on the parcel behaviour will be determined. They are independent of each other and can therefore, be varied without influencing other independent variables [4].
- **Dependent variables:** these variables need to be measured before or during the experiments, this is because these variables are influenced by the independent variables and will therefore, vary between experiments [4].

Table 6.2: Variable definition into controlled, independent and dependent groups. Constructed using the defined dimensionless groups to test the influence of each parameter in these groups.

Controlled Variables		**Independent Variable**		**Dependent Variables**	
Parameter	**Symbol**	**Parameter**	**Symbol**	**Parameter**	**Symbol**
Length parcel	L_p	Wheel height	h_w	Friction parcel-grid	μ_g
Velocity conveyor	V_c	Divert angle	α	Friction parcel-conveyor	μ_c
Acceleration	a_g, a_c	Surface	S_m	Position	x_p, y_p
Gravitational	g	Parcel ratio	$\frac{W_p}{L_p}$	Orientation	ϕ
Start orientation	ϕ_0	Velocity	$\frac{V_g}{V_c}$	Roll friction	C_r
Start position	x_{p0}, y_{p0}	Inertia	$\frac{I}{L_p^2 m_p}$	Weight	m_p
Transport width	T_w	Stiffness	S		

The velocities of the equipment are set to a certain value before the parcel arrives therefore, has the acceleration of the equipment no influence and is set to zero. Furthermore, is the rolling friction assumed to only have an influence on the necessary motor power but not on the parcel behaviour. The transport width is defined by the available equipment and therefore, set to 800 mm.

The independent variables were chosen in such a way that the influence of each dimensionless group can be tested. Only the start position and orientation were set as controlled variables to reduce the number of experiments and because the available equipment would otherwise not be able to sort each parcel. It is assumed that the behaviour of the parcel on the grid will not be influenced by these parameters. This results in the independent variables shown in Table 6.2. Since the material of the equipment is fixed μ_g&μ_c will be varied simultaneously by changing the surface of the parcel.

These friction coefficients will be measured before the experiments using an unster since they depend on the surface of the parcel. Other dependent variables are the position and orientation of the parcel (measured by camera) and the weight of the parcel which will depend on the parcel ratio and added inertia. This will also be measured before the experiments using a scale.

Finally the controlled variables are defined, as described earlier the transport width, acceleration, start position and orientation of the parcel will be kept constant. Furthermore, the length of the parcel is kept constant since it influences many dimensionless groups and will therefore, provide less information on the influence of each group.

6.1.5. Measurement Definition

To compare the results between different experiments or between the experiments and simulation, a definition has to be made about the reference point. Since the goal is to position the parcel neatly in the outfeed, the final position in the outfeed will be chosen as the measurement point.

Furthermore, the position will be measured using the distance to the edge of the outlet. This measure is chosen since this can later be used to align the parcel at a certain position in the outfeed. The orientation of the parcel is also measured at this point and will be determined using the initial orientation of the parcel before it arrived at the grid. These definitions are shown in Figure 6.11.

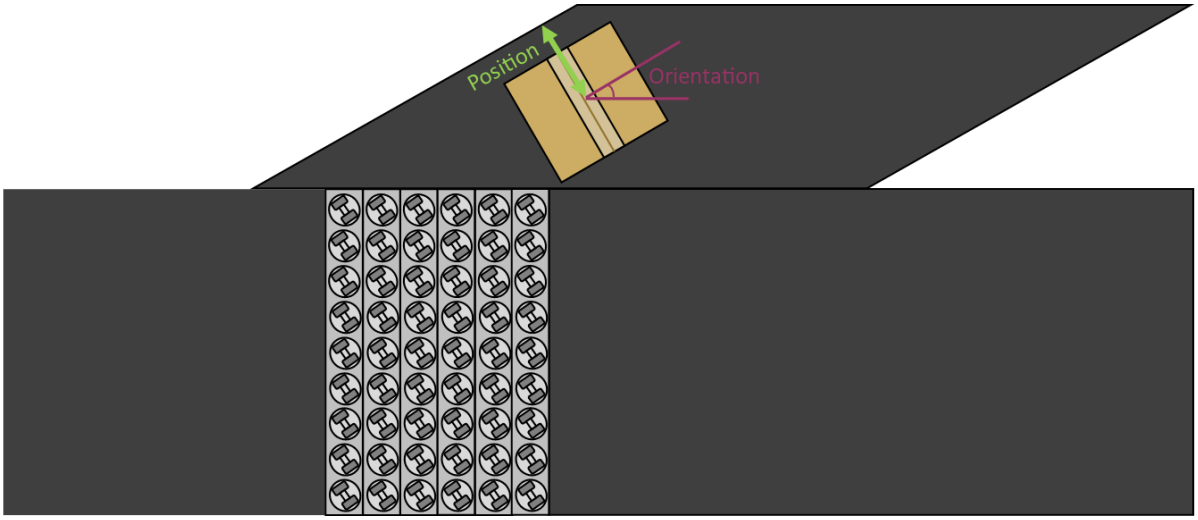

Figure 6.11: Defined measurement reference for the position and orientation of the parcel, used to compare different experiments to each other or to the simulation.

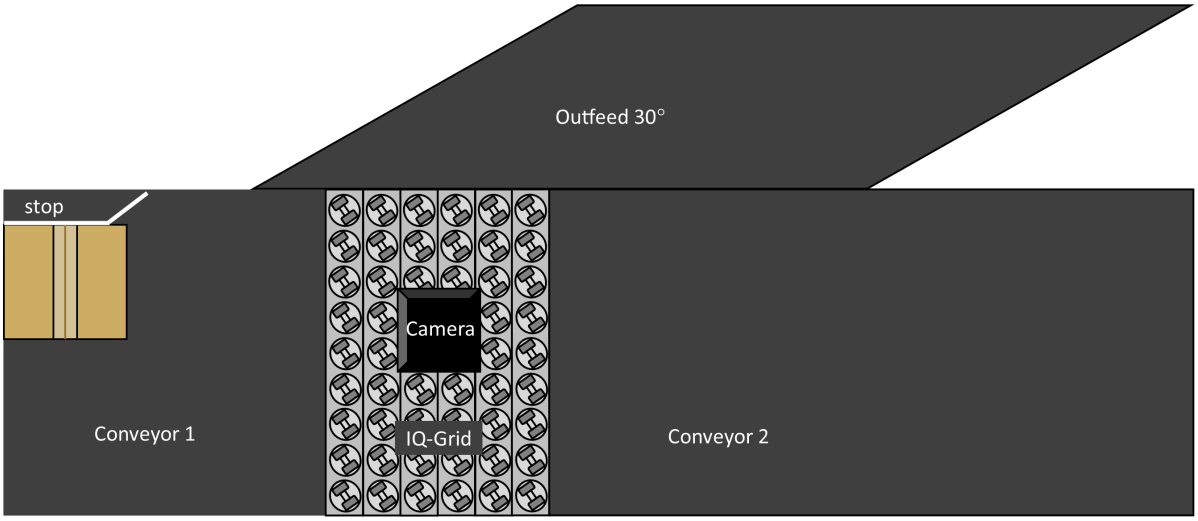

Figure 6.12: Experimental setup that will be used, comprising two conveyors, IQ-Grid with two settings (30°&45°), outfeed with fixed 30° angle, stop to align parcels and camera to measure the position and orientation.

6.1.6. Experiment Setup

The layout comprising two conveyors, IQ-Grid and an outfeed has already been used numerous times in this report however, the experimental setup also relies on this layout. In Figure 6.12 the experimental setup is shown. The conveyors are standard VanRiet equipment of 800 mm width with a stop mounted at the first conveyor to properly align the parcels on the conveyor.

The IQ-Grid used has a length of 600 mm and has the same width as the conveyors. The grid has a stationary divert angle which can be set to 30° or 45° according to the experiment. The outfeed has a fixed angle of 30°. The camera will be positioned right above the grid shifted 200 mm towards the outfeed to also capture the parcel when it is fully sorted.

Table 6.3: High- and low settings for the independent variables which will be varied during the experiments.

Parameter	Symbol	-1	1
Wheel height	h_w	$0mm$	$5mm$
Divert angle	α	30°	45°
Surface	S_m	Telfon	Rubber
Parcel ratio	$\frac{W_p}{L_p}$	0.5	1
Velocity	$\frac{V_g}{V_c}$	1	1.173
Inertia	$\frac{I}{L_p^2 m_p}$	1	1.5
Stiffness	S	MDF	Foam

Table 6.4: Parameters determined for the controlled variables, these parameters are constant throughout the different experiments

Parameter	Symbol	Value
Length parcel	L_p	$400mm$
Velocity conveyor	V_c	$1m/s$
Acceleration	a_g, a_c	$0m/s^2$
Gravitational	g	$9,81m/s^2$
Start orientation	ϕ_0	0°
Start position	x_{p0}, y_{p0}	$0,100mm$
Transport width	T_w	$800mm$

6.1.7. Experiment Design

Using the theory of design of experiments an experimental plan has been developed to discover the influence of the parameters which were indicated by the dimensional analysis. The independent variables of Table 6.2 will be varied between two levels: high and low setting while keeping the control variables constant [4]. The corresponding values of these independent- and control variables are respectively shown in Table 6.3 & Table 6.4 and were determined using the following reasons:

- **Wheel height:** during pre-tests it was indicated at which point the parcel and the grid will have a sufficient grip with respect to the conveyor, this turned out to be at 0 mm (top of the wheels equal to the conveyor). Furthermore, the grid was raised until a different behaviour was visually observed namely, a sharper sortation behaviour this took place at 5 mm.
- **Divert angle:** the grid available for testing has three settings: 30°, 45° and 90°. Since the outlet is restricted to 30°, the 30° and 45° were chosen for the two levels (Figure 6.13 & 6.14) since otherwise the parcel may fall of the outlet due to the sharp sortation angle.
- **Surface:** the parcel spectrum can consists of numerous materials, to test the extremes of this spectrum teflon and rubber were chosen (Figure 6.15 & 6.16). These should be able to give a clear indication on the influence of the friction.
- **Parcel ratio:** using the already constructed simulation model and pretests it was determined to set the length at 400 mm, which enables the possibility to have 0.5 and 1 for the parcel ratios (Figure 6.17 & 6.18). With different settings the parcel would miss the outlet or show an irregular behaviour since the width would be close to the wheel pitch.
- **Velocity:** these settings were chosen in such a way to detect if the parcel can be sorted while keeping an equal lateral velocity (high setting). Furthermore, the base velocities were set to 1 m/s to ensure the parcel remains in contact with the IQ-Grid after the parcel hits the first row of wheels. At higher velocities the parcel had small jumps due to the high wheel pitch and increased kinetic energy.
- **Inertia:** the inertia setting was found by performing pretests and ensuring the added weight had a significant contribution to the parcel weight. These weights were placed at the edges of the parcel to increase the inertia while retaining the center of mass in the middle of the parcel (Figure 6.21).

- **Stiffness:** for the stiffness two materials were required ensuring that one setting would stay on top of the wheels and the other one would come in contact with the base plate. To ensure this behaviour a MDF panel was chosen for the stiff setting and a foam stuffing was used to ensure the parcel would fall over the wheels (Figure 6.19 & 6.20).

To discover the individual influences as well as the two-factor interactions between the independent variables a Resolution IV design was chosen [4]. This results in an experimental plan in which one or two variables are set to the high setting while keeping the other settings low. Furthermore, these settings are blocked e.g. the settings are grouped as much as possible and hard to adjust settings are kept together to reduce variance errors. These settings are the divert angle of the grid and the height of the wheels.

Each experiment will be conducted a single time except for the base experiment at which all variables are kept low. To indicate the standard deviation and systematic errors this experiment is performed at different moments (start of the experiment, in between and at the end) resulting in a total of three replicates. These measurements can eventually be used to determine the confidence intervals of the other experiments [4].

The resulting experimental plan following this described method can be found in Appendix E.

Figure 6.13: Low setting for the divert angle namely: 30° which correspond with the angle of the outlet.

Figure 6.14: High setting for the divert angle namely: 45° which is higher than the angle of the outlet.

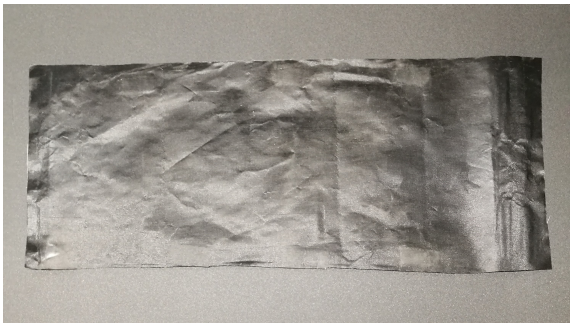

Figure 6.15: Low setting for the parcel friction resulting in a smooth surface by using Teflon

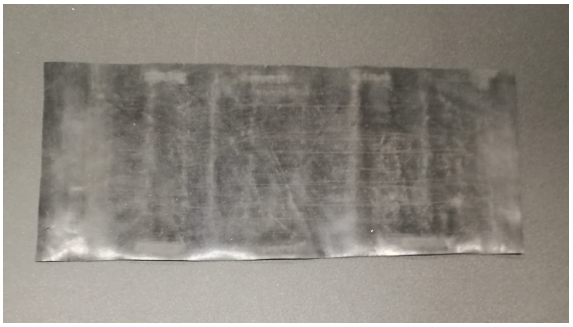

Figure 6.16: High setting for the parcel friction to simulate rough parcels using rubber.

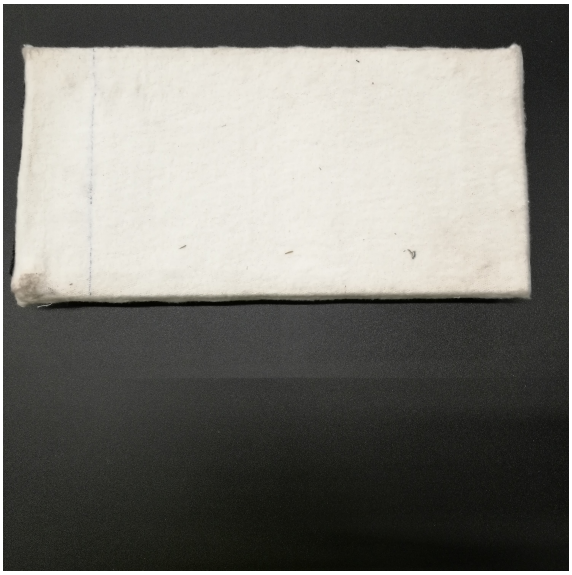

Figure 6.17: Low setting for the parcel ratio namely 0.5.

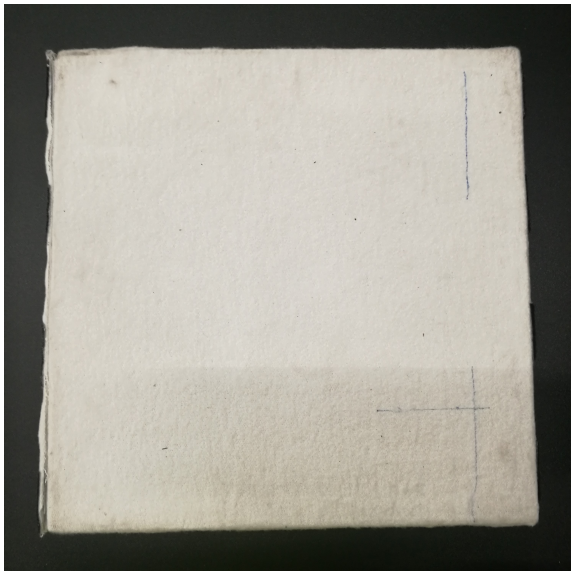

Figure 6.18: High setting for the parcel ratio of 1 resulting in a rectangular shape.

Figure 6.19: Low setting for the parcel stiffness using a MDF panel to ensure the parcel stays on top of the wheels.

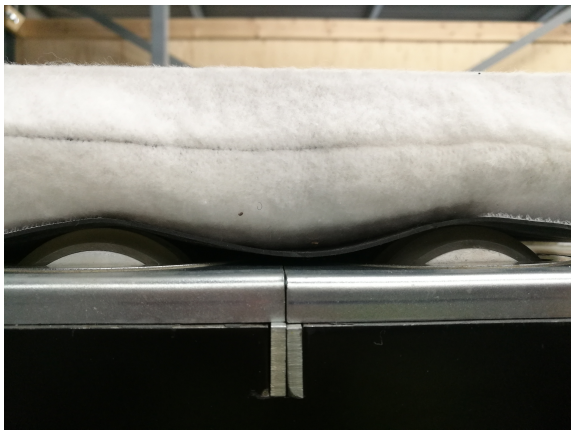

Figure 6.20: High setting for the parcel stiffness using foam stuffing which leads to a parcel which also has contact with the base plat of the IQ-Grid.

Figure 6.21: High setting for the parcel inertia by adding weight to the edges of the parcel to increase inertia, low setting is shown in Figure 6.17.

6.2. Experiment Results

In this section the results will be discussed which were obtained during the measurements executed according to the experimental plan. First, the results of the base measurement will be discussed since these can then be used to construct the confidence intervals for the other measurements. From here, the influence of each parameter will be discussed after which, the simulation model can be validated by comparing the model output to the results of the experiments. If these show similar results the model can be assumed to represent the physical model correctly and be used for the design of the new product.

6.2.1. Base Measurement & Error

As described in the experimental plan, the base measurement has been performed three times, namely: at the start, middle and end of the experiment. This was done to indicate the standard deviation and to see if a systematic error was introduced during the experiments. This systematic error can be introduced due to changing the parameters or another time dependent process such as heating up of the equipment.

In Figure 6.22 the position is shown for the three base measurements these show a clear overlap in position. In Figure 6.23 the orientation is shown, during the transport over the grid (0.2 - 0.5 s) the measurement show a similar curve, during its path over the outlet measurement 2 & 3 shown again a clear overlap. Measurement 1 has a small offset of one degree and a slight different curve. However, since the orientation during its transport over the grid is seems like a random error and not a standard error induced by changing of parameters. Therefore, the measurements are assumed to be correct for its purpose, namely: validating the simulation model to later differentiate between multiple configurations.

From these measurements the standard deviations are calculated at the earlier reference point (end of the measurement). These deviations turned out to be: 3.25 mm for the position and 0.69° for the orientation. Using Equation 6.1 the confidence intervals are calculated at 95% using a single sample, this results in 6.37 mm and 1.35°. These values will be used for the other measurements, since these should have a similar variance since the experiments are assumed to have the same random process and therefore, the same standard deviations [4].

$$\text{Confidence Interval} = \pm z_{0.95} \cdot \frac{s}{\sqrt{n}} \tag{6.1}$$

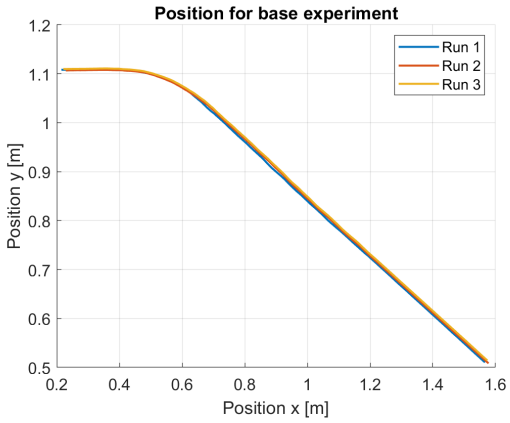

Figure 6.22: Position graph of the three conducted base measurements used to indicate the standard deviation and possibly systematic errors.

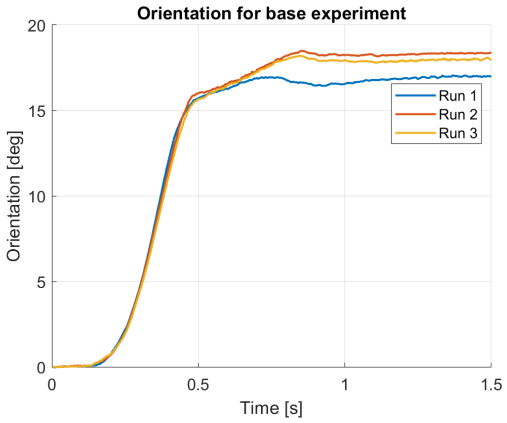

Figure 6.23: Orientation graph of the three conducted base measurements used to indicate the standard deviation and possibly systematic errors.

6.2.2. Parameters Influence

In Figure 6.26 & 6.27 the effects are shown for each parameter for respectively position and orientation. These effects are defined by Equation 6.2, and are used to show the influence of a single parameter (i) by evaluating it's measurements with interactions (i, j) minus the individual parameter measurement it interacts with (j). The red line indicates the level set by the boundaries (position= $\pm 50mm$, orientation= $\pm 5°$)to properly sort a parcel which will be discussed further in Chapter 7. Furthermore, a yellow bar indicates a decrease of the distance as defined in Section 6.1.5, for the orientation a yellow bar means the parcel rotated less.

$$\text{Effect i} = \text{Result i,j} - \text{Result j} \tag{6.2}$$

All parcels with a high ratio show less rotation and increased distance. Compared to other parameters, parcel ratio has significantly more influence. The reduced rotation can be addressed by their short length compared to their width. This leads relative short period of torque compared to its inertia, which will results in less rotation (Chapter 4). The increased ratio also causes more frequent contact with the second conveyor which, results in increased distance between parcel and outfeed side.

Other parcel parameters (stiffness, friction and inertia) show less influence on both the orientation as well as position. Only slight crossings of the boundary occur when involving increased ratio, wheel height or divert angle. However, when taking into account each boundary has a positive and negative part it can be assumed these parameters can still lay within the set boundaries in order to properly sort a parcel. To reduce the effect of parcel stiffness the mechanical design should be revised to better support the parcel and therefore, reducing the impact of parcel stiffness.

The high effect at VR (high velocity and ratio) in position is due to the increased parcel ratio combined with the fact that parcels are sorted a bit further from the outlet edge. This results in the parcel being carried away by both the outlet and second conveyor, eventually this resulted in the parcel disappearing in the gap between both pieces of equipment.

In the position graph it can be seen that the divert angle has a clear unanimous effect on the position. Due to the sharper divert angle all parcels arrive closer to the edge of the outlet which can be seen as a positive result since this would increase the sortation reliability (assuming position in the outlet is less important).

Other mechanical design parameters (wheel height and grid velocity) show little effects besides the earlier discussed VR. Indicating no clear advantage of an increased wheel height while it does introduce a bump during parcel translation over the grid (Figure 6.24). Therefore, is the increased wheel height abandoned from the design and fixed to 0 mm. Furthermore, the increased grid velocity can be used in order to keep parcel velocity in lateral direction equal during sortation (Figure 6.25). This property is useful in order to maintain gaps between parcels while sorting.

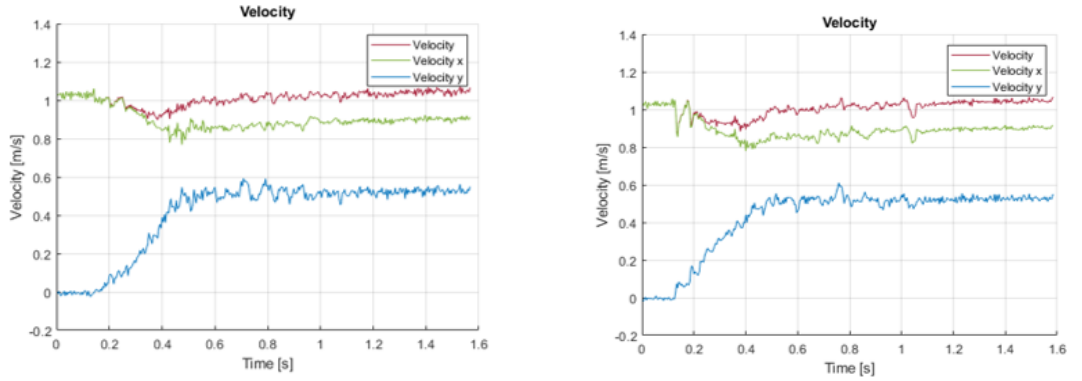

(a) Base measurement (b) Increased wheel height

Figure 6.24: Impact of increased wheel height showing a clear bump in velocity when the parcel reaches the wheels compared to the base measurement.

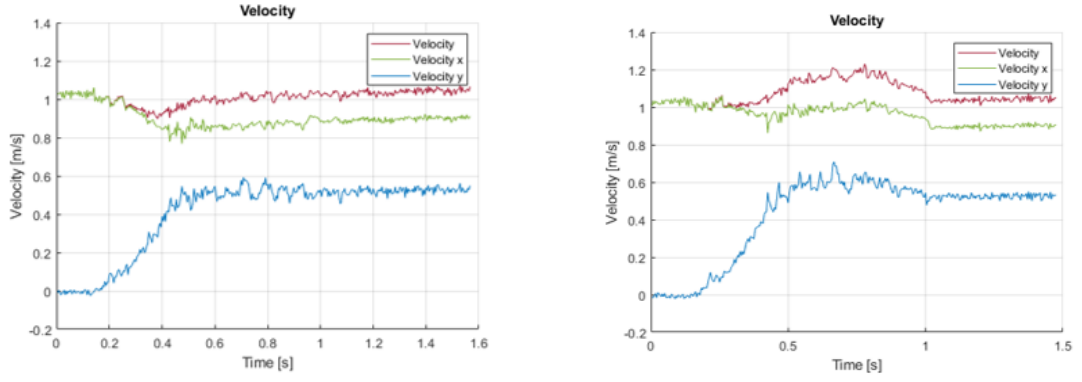

(a) Base measurement (b) Increased grid velocity

Figure 6.25: Impact of increased grid velocity showing maintained lateral speed (x) of the parcel compared to the base measurement.

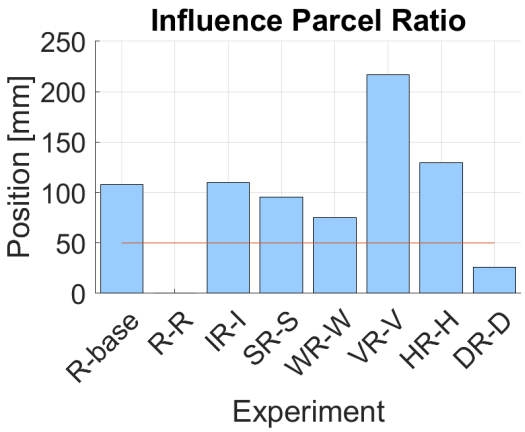

(a) Parcel ratio

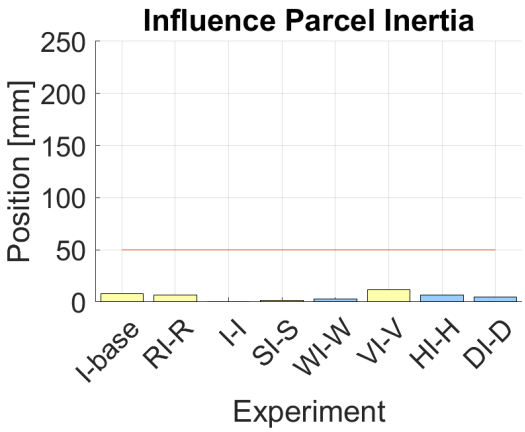

(b) Parcel inertia

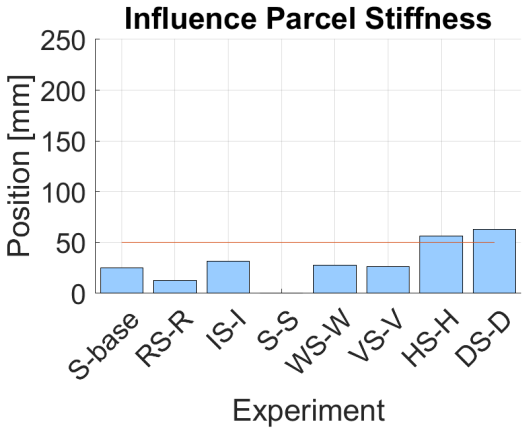

(c) Parcel stiffness

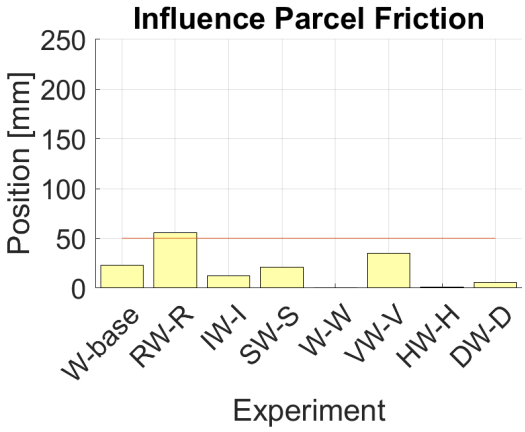

(d) Parcel friction

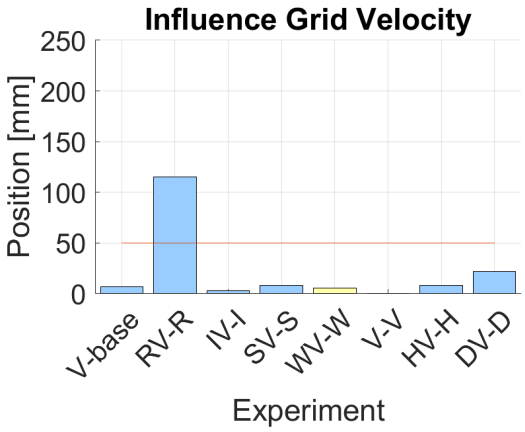

(e) Grid velocity

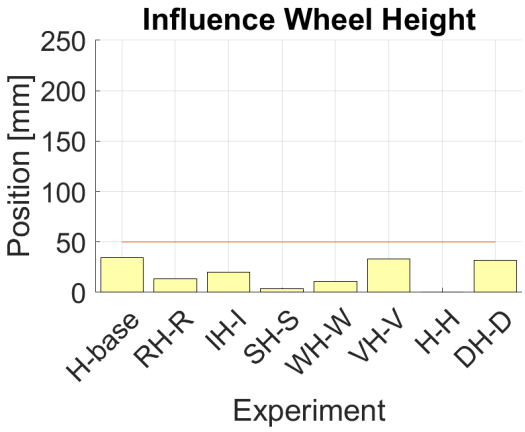

(f) Wheel height

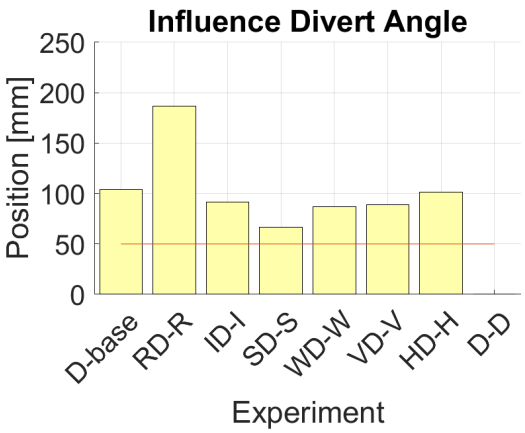

(g) Divert angle

Figure 6.26: Impact for all parameters on the parcel position measured as a distance between the parcel center and side of the outfeed. Yellow colors indicate a decrease and blue an increase of the distance.

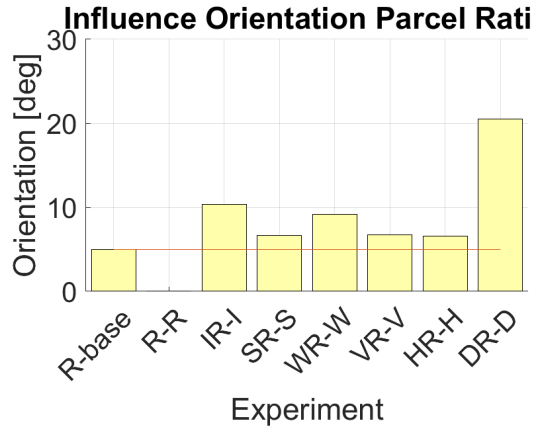

(a) Parcel ratio

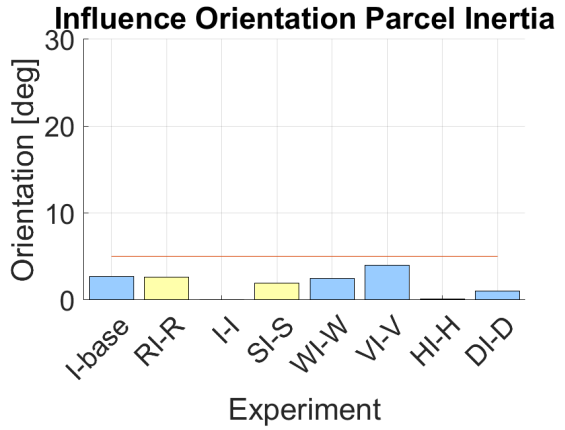

(b) Parcel inertia

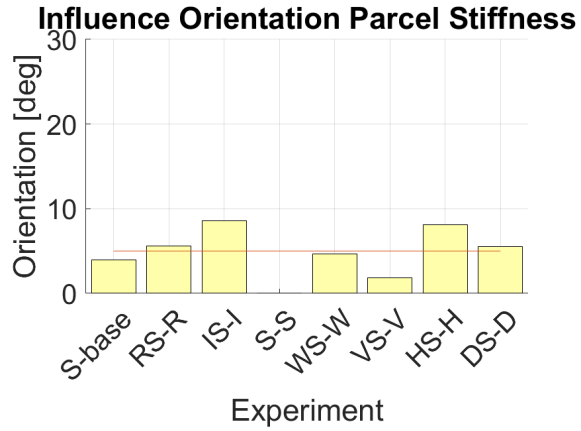

(c) Parcel stiffness

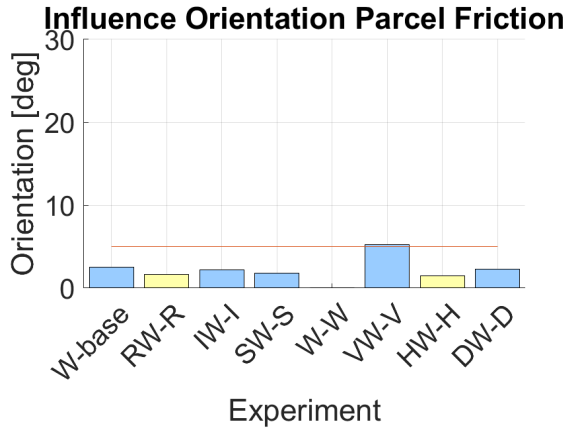

(d) Parcel friction

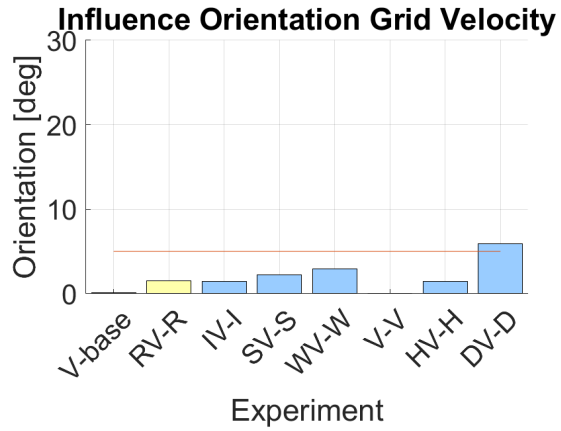

(e) Grid velocity

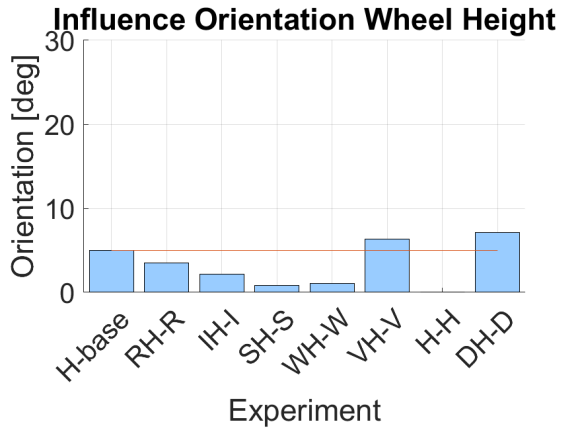

(f) Wheel height

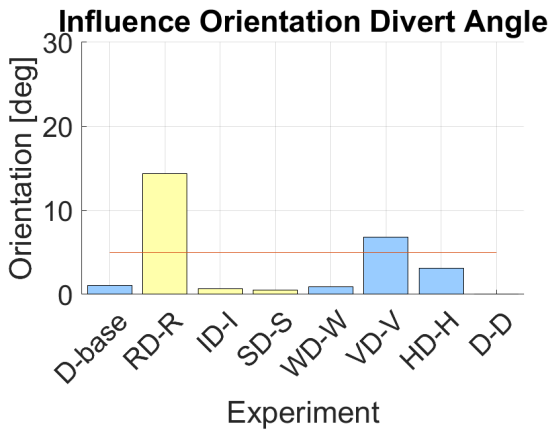

(g) Divert angle

Figure 6.27: Impact for all parameters on the parcel orientation measured relative to the main conveyor. Yellow colors indicate a decrease and blue an increase of the orientation.

6.2.3. Simulation Validation & Error Indication

After determining the measured influence of each parameter and their interactions, the simulation model will be validated in this section. In Figure 6.28 & 6.29 the errors between the real and simulated position and orientation are shown. These are again measured according to the definition in Section 6.1.7.

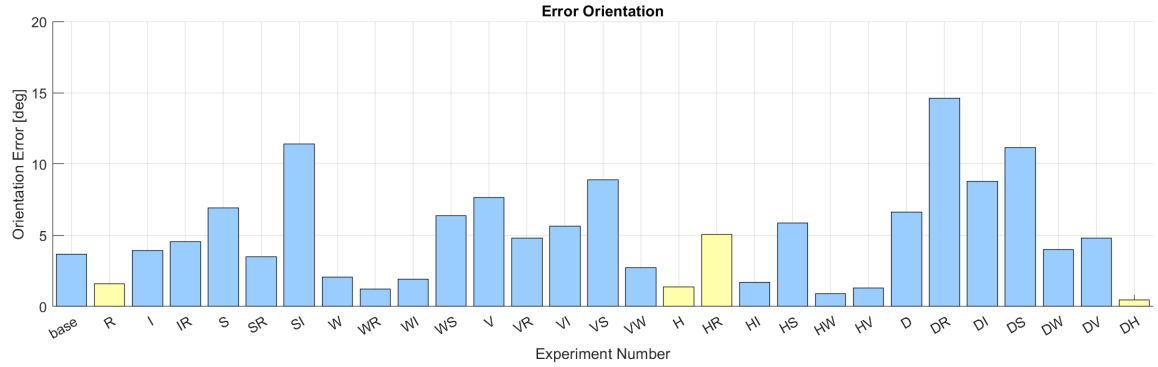

Figure 6.28: Difference between the expected orientation of the parcel and the measured one from the experiments. Yellow colors indicate a lower estimation and blue a higher estimation of the orientation.

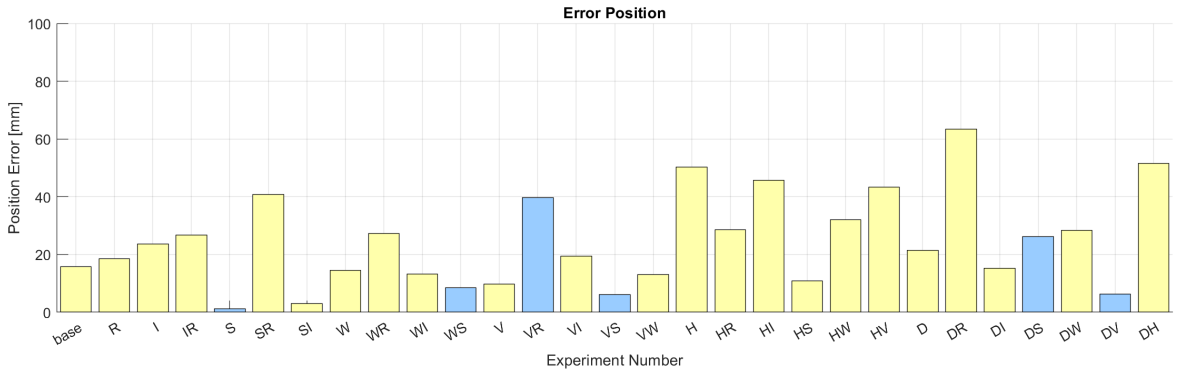

Figure 6.29: Difference between the expected position of the parcel relative to the conveyor and the measured one from the experiments. Yellow colors indicate a lower estimation and blue a higher estimation of the position.

The largest errors for both position and orientation occur with interactions containing the high parcel ratio setting. This is mainly because this setting results in frequent contact with the second conveyor, which leads to fuzzy behaviour. To overcome this the grid should be longer in order to support the parcel until it reaches the outlet and achieve a higher conformity with the model. However, in both simulation as reality the parcel reaches the outlet, which can be seen as a sufficient sortation.

Besides these differences the model and reality have roughly a difference of 60 mm and 5°. Since the goal of the simulation is to provide insight in the effects of different layouts this is assumed to be accurate enough. By improving the parcel behaviour the parcels should arrive in the outlet more reliably with less contact with the second conveyor. If this can be achieved the model could become even more close to the reality.

Other large differences can be found at settings with a high level for the wheel height. This seems logical since the wheel height is not modelled by the mathematical model of Chapter 4. This is because the model was constructed in two dimensions and therefore, does not account for the wheel height (third dimension). The increased wheel height however, showed a clear bump in velocity when the parcel hits the grid. Furthermore, the effects are negligible for the position of the parcel and the orientation gain is expected to be also achievable with other adjustments such as optimized divert angles. These reasons support the conclusion to set the wheel height to 0 mm, having a better parcel behaviour and be able to simulate the behaviour well.

6.3. Conclusion

In this chapter experiments were conducted in order to finalize the answer of the previous chapter to ensure an accurate parcel behaviour description. Furthermore, the subsequent question was answered, namely:

Which parameters influence the parcel behaviour on a bidirectional sorter?

By examining the different experiments it became clear that, usually unknown parcel variables only have a small effect on the position and orientation of the parcel and therefore, can be omitted during operation. Most dominant is the parcel ratio which is usually measured. This parameter results in fuzzy behaviour of the square parcel since it frequently touches the second conveyor and therefore, gets disturbed on its way to the outfeed. The stiffness also has some influence on the behaviour however, this could be resolved by reviewing the mechanical design of the IQ-Grid introducing better parcel support.

The errors between the model and experiments are relatively small and hence it can be concluded that the model is valid. Several differences occur at variables not present in the model (wheel height) or by disturbances of the second conveyor (high ratio parcels). However, for the purpose of the model it is assumed to be valid since the main goal is to differentiate between the different layout configurations rather than exactly predicting parcel behaviour.

As described in Chapter 2 validation was the last step towards an accurate parcel behaviour description therefore, it can now be used in Chapter 7 to eliminate configurations based on the defined requirements.

7

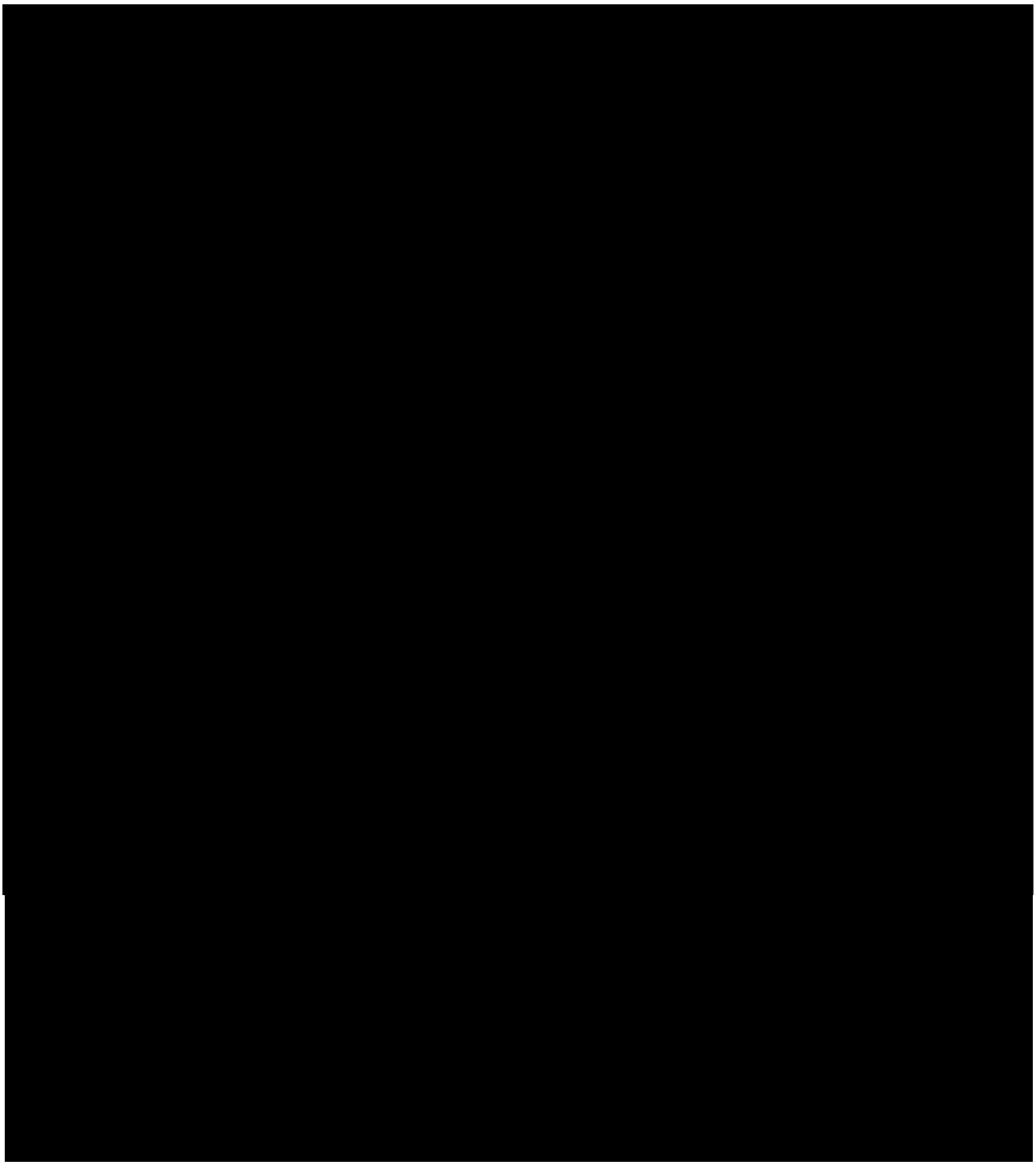

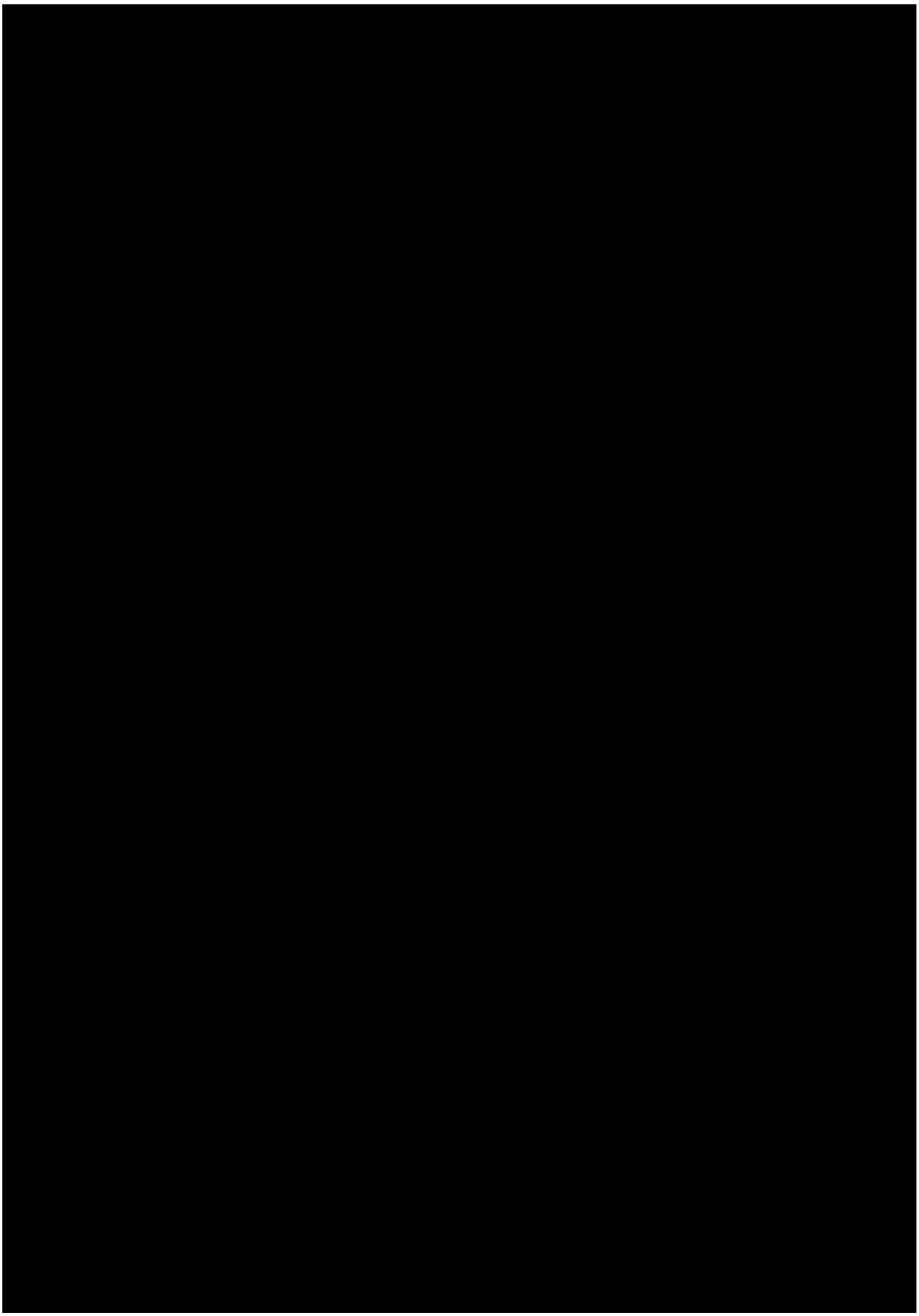

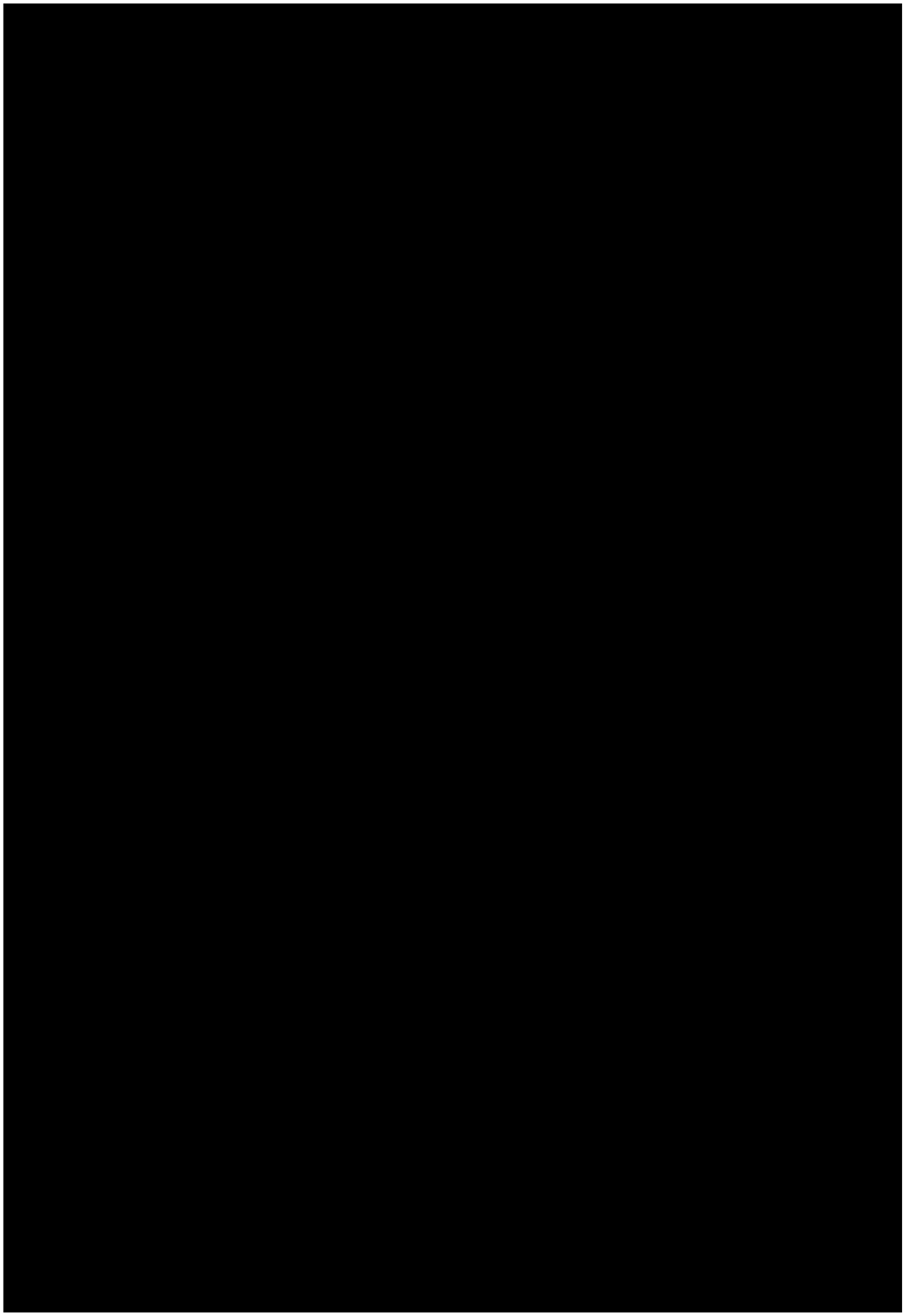

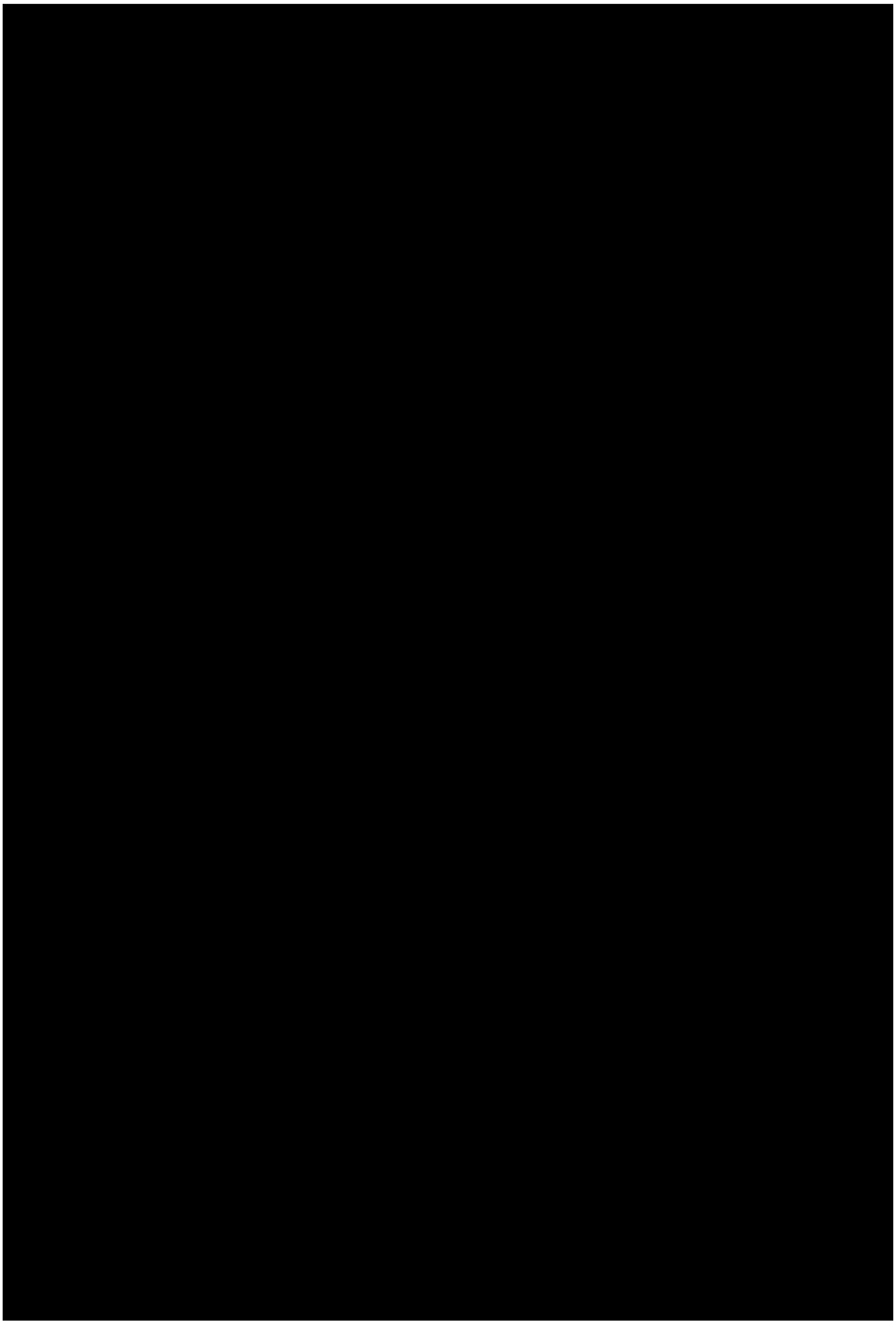

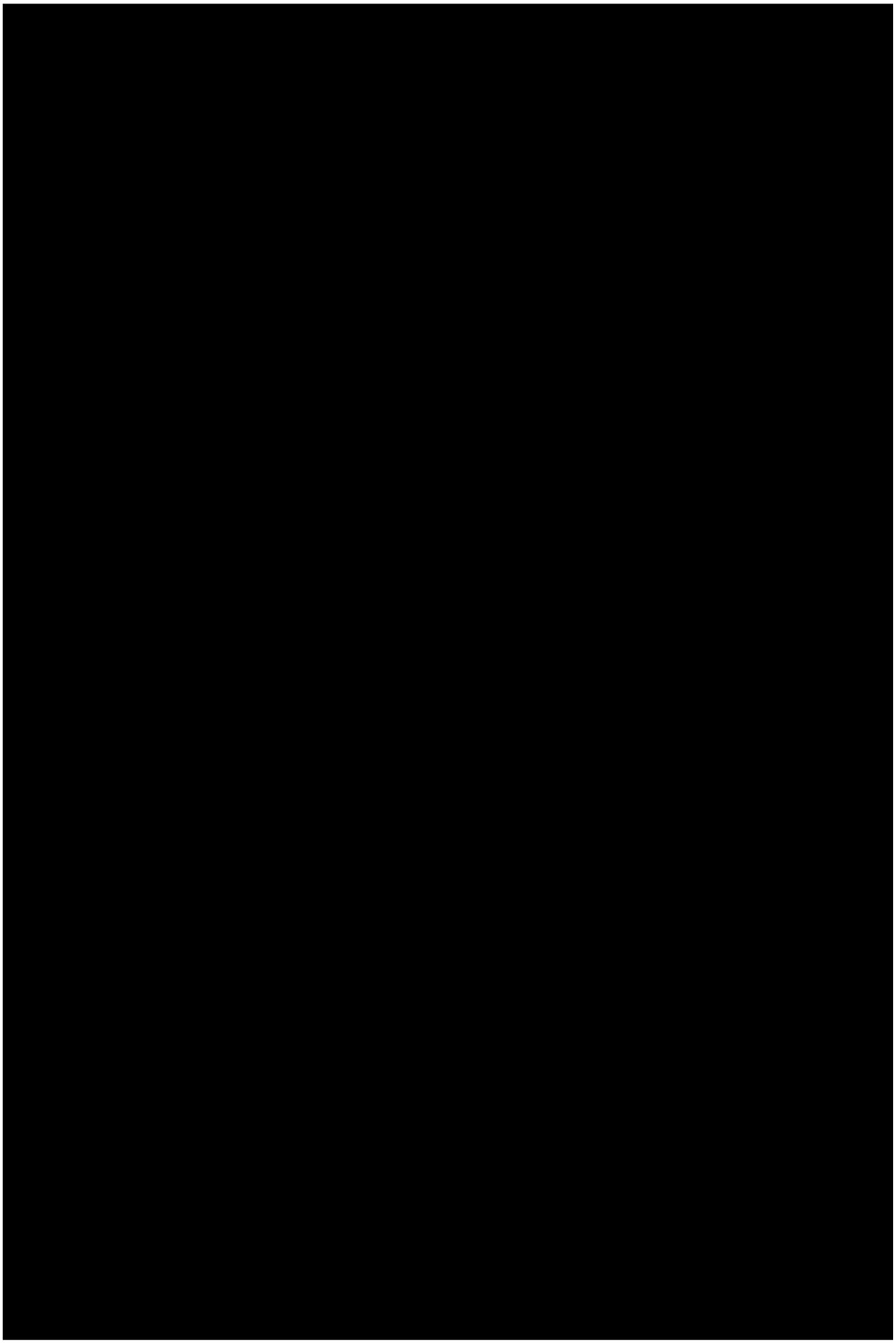

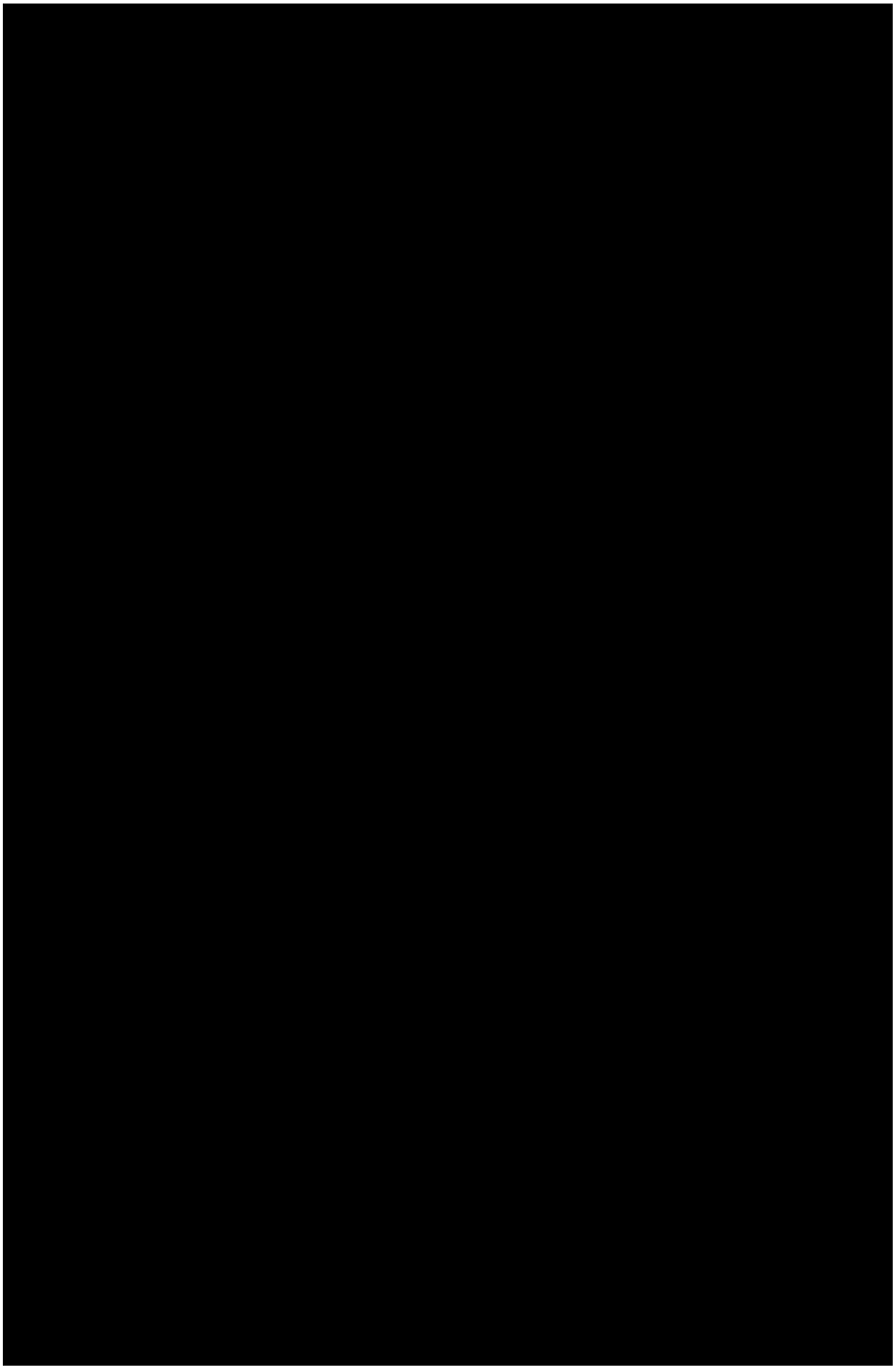

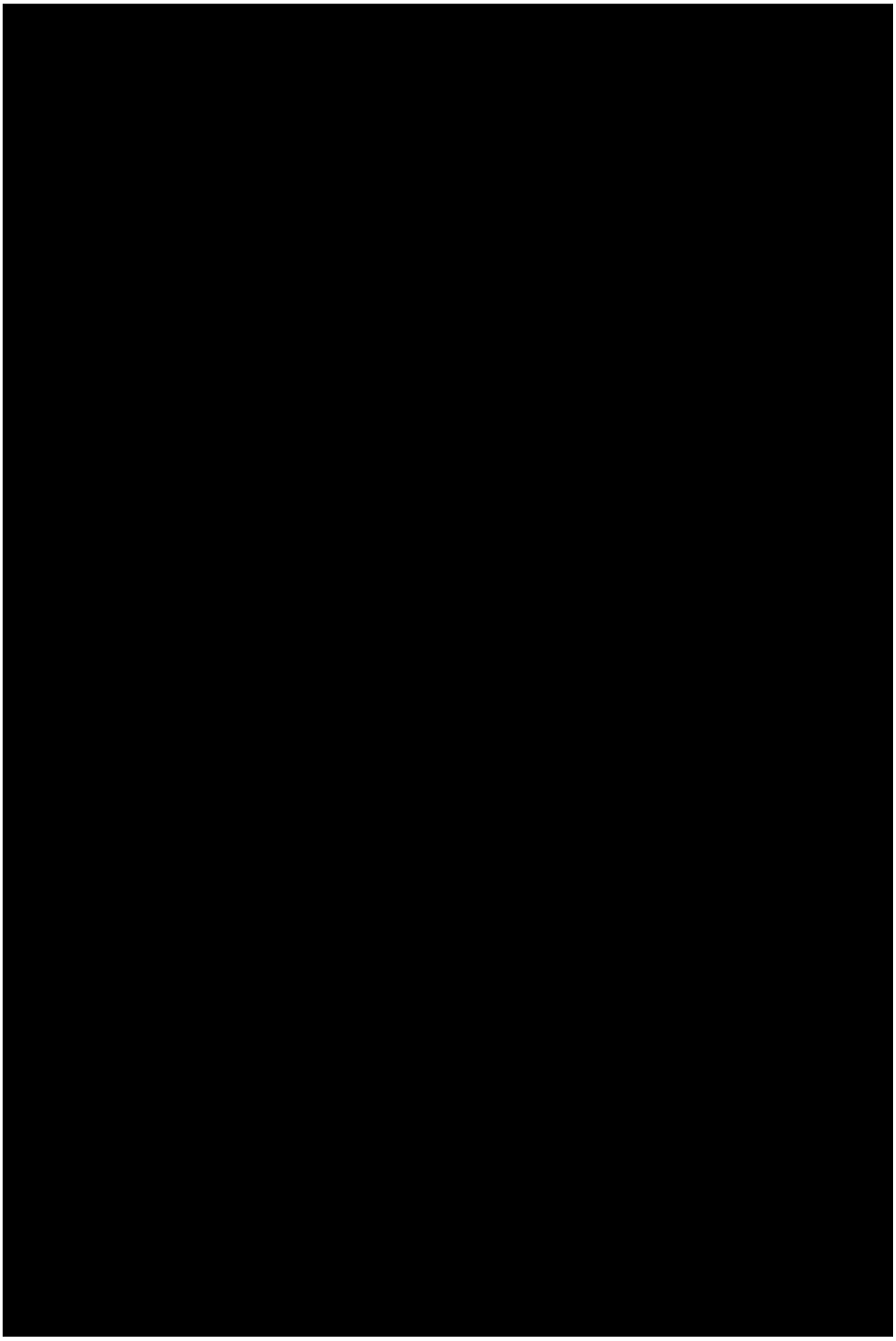

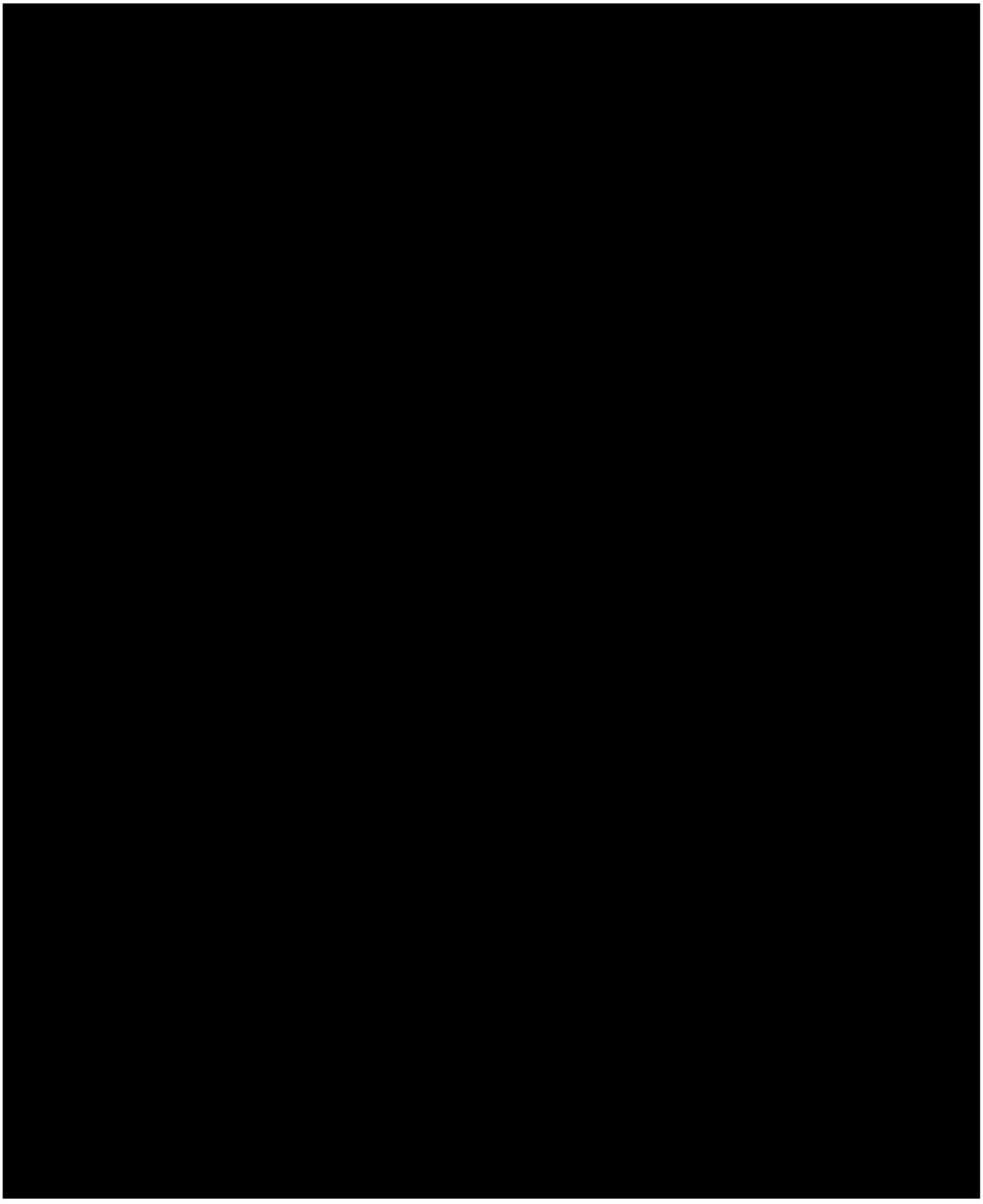

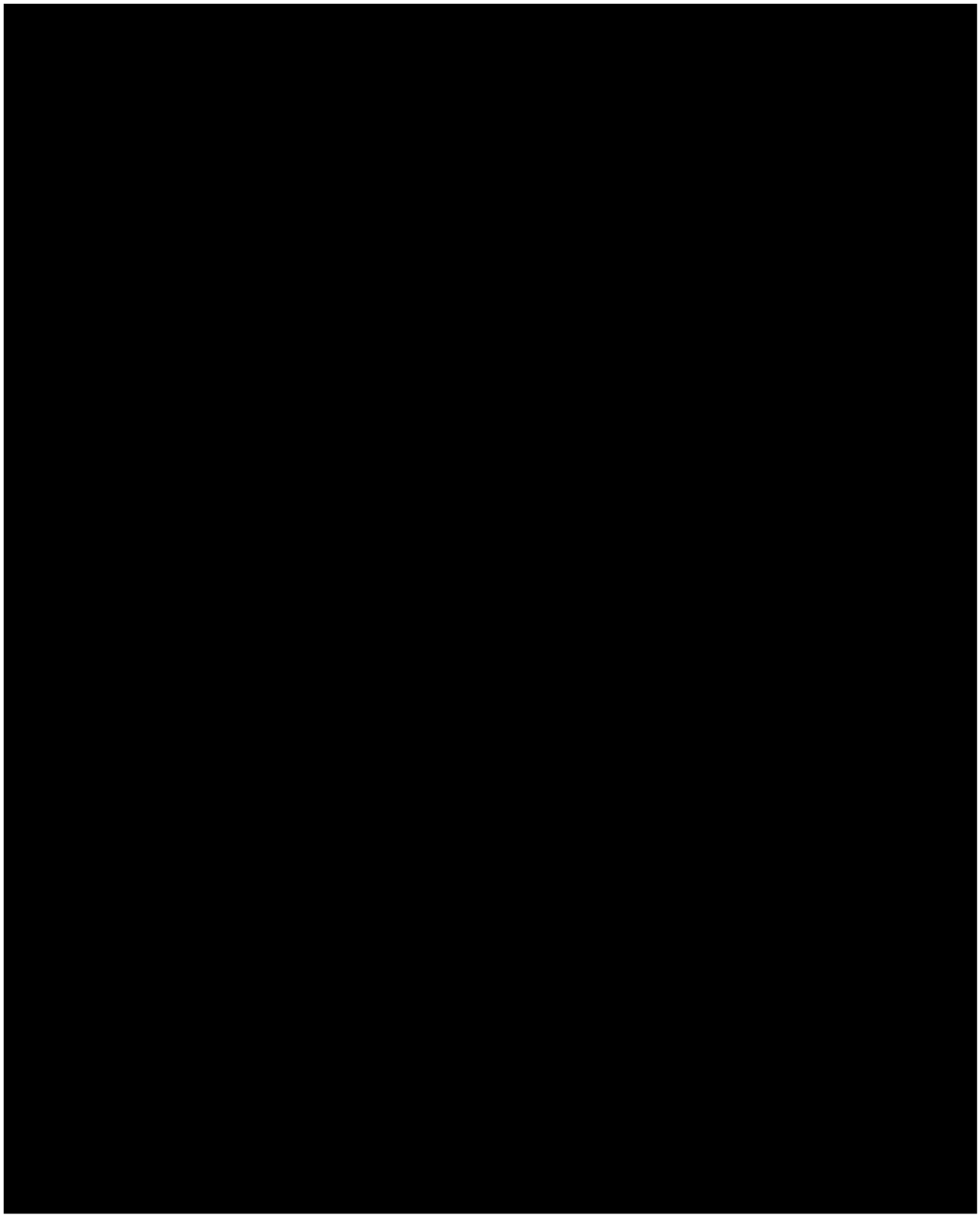

8

Validation Improved Design

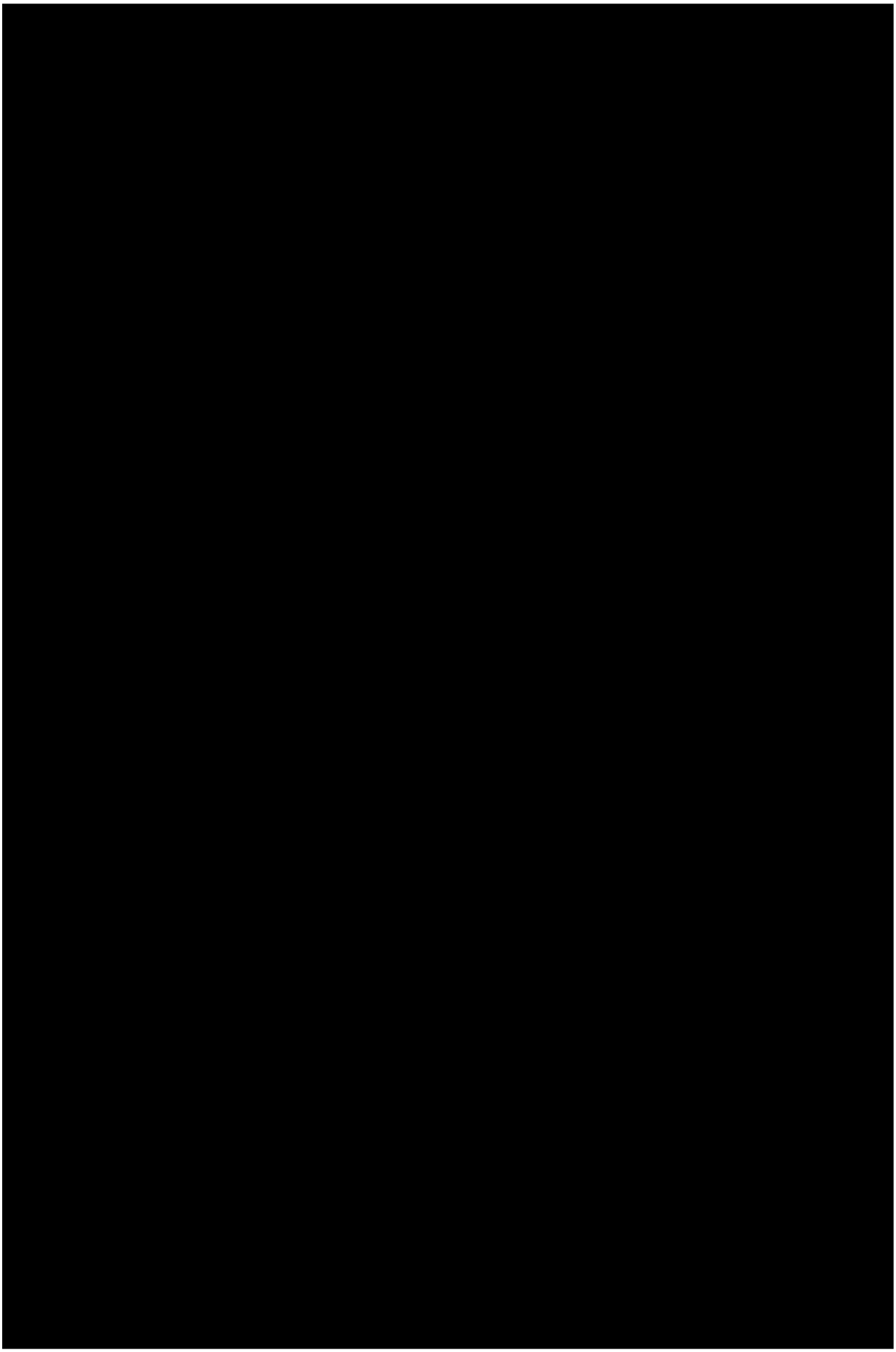

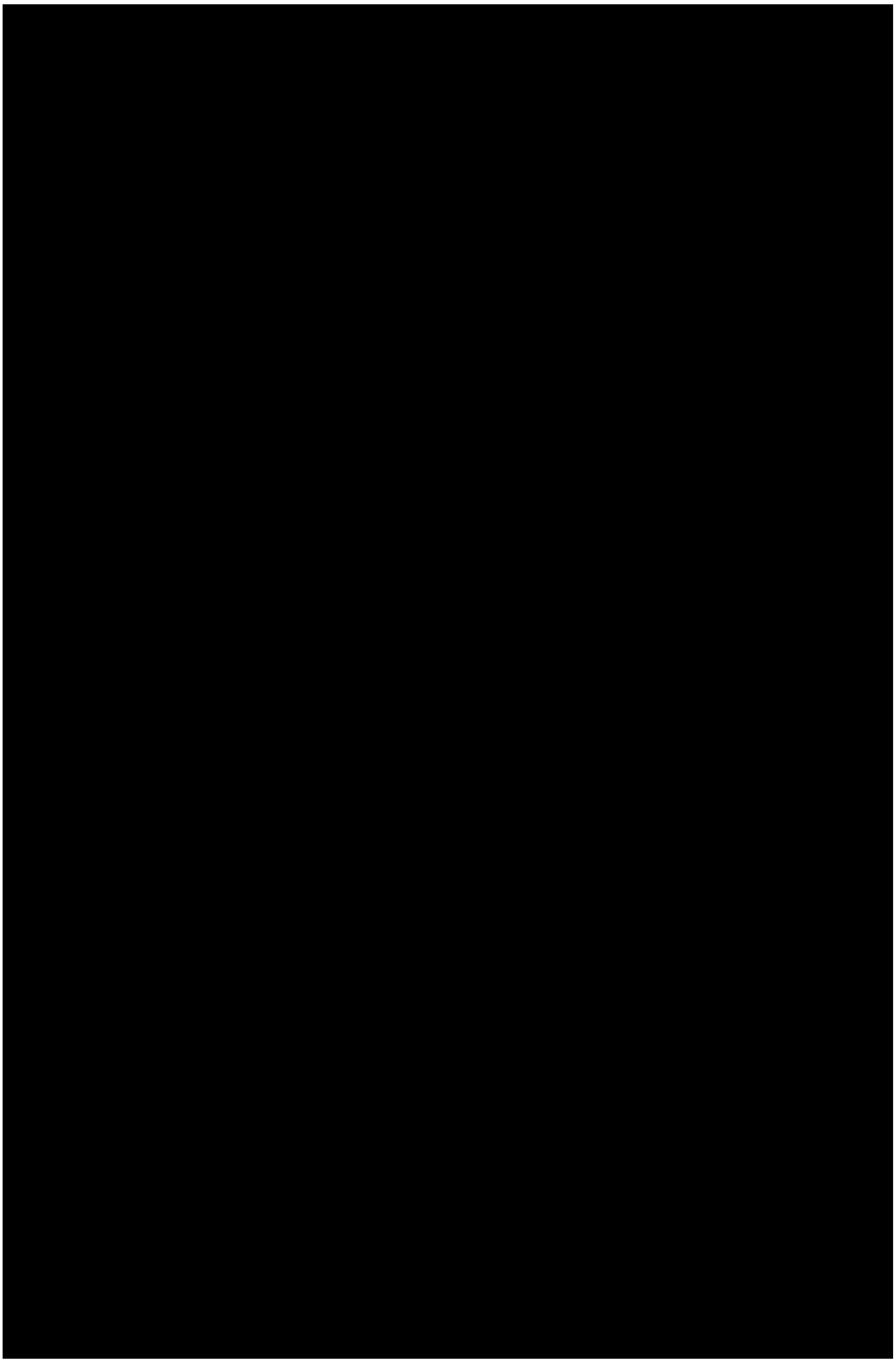

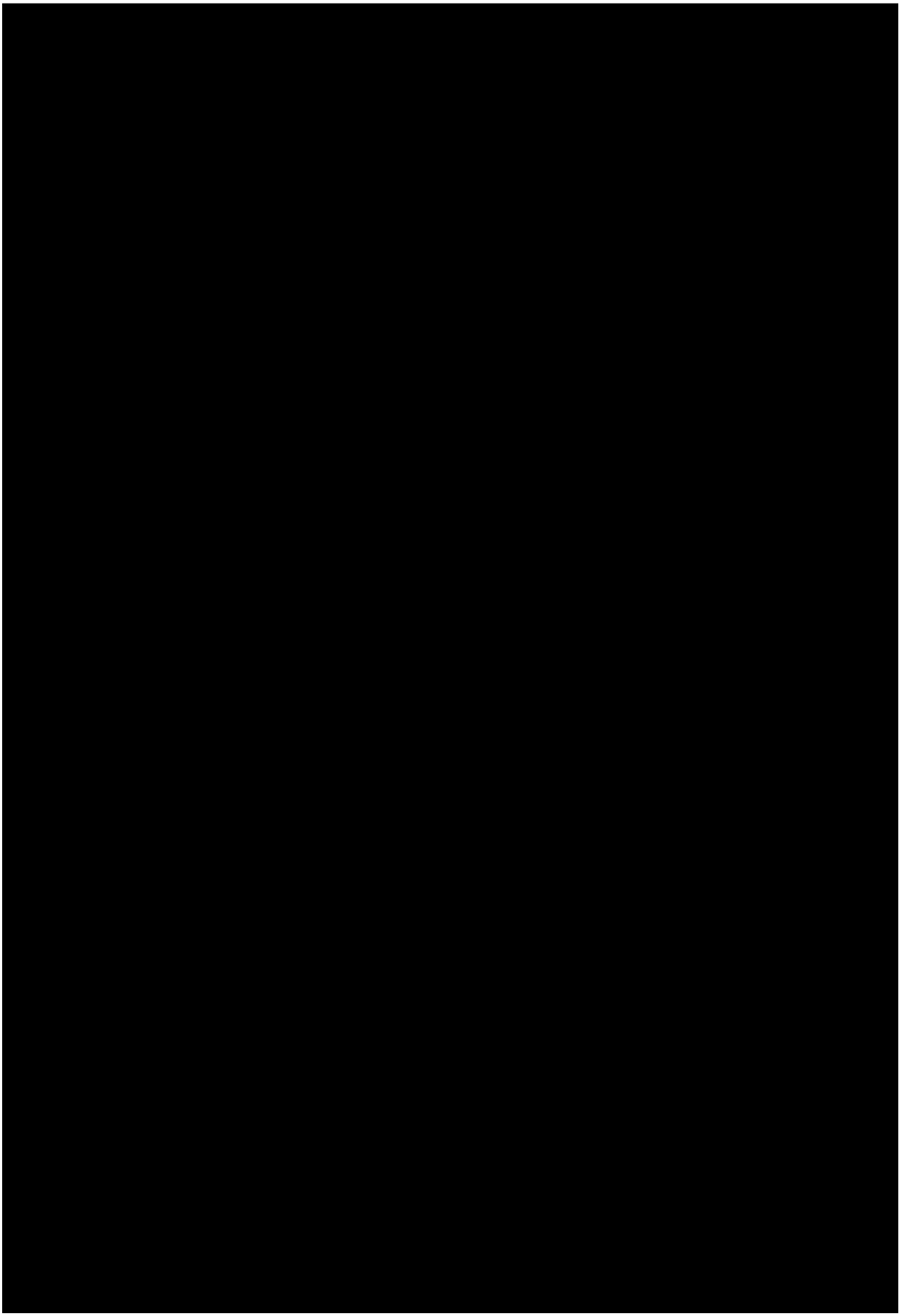

9

Conclusion and Recommendations

This research provides a new layout for the IQ-Grid which can ensure reliable and efficient sortation of parcels. In this chapter, conclusions will be drawn based on the different aspects as discussed in the previous chapters. Additionally, recommendations are formulated for further development of the simulation model.

9.1. Conclusion

This research initiated by the need for more insight in the behaviour of parcels on the IQ-Grid and influence of different layout configurations of the IQ-Grid on this behaviour. To provide this information the following research question was formulated:

How can parcels be efficiently sorted in a bidirectional system independent of their position on the feeder?

- The wheel height of the grid should be set to 0 mm in order to reduce jumps and deceleration of the parcels. This leads to more efficient sortation since the parcel behaviour is remains closer to the predicted behaviour.
- The largest impact on the parcel behaviour by parcel properties on the grid is caused by the parcel ratio (width/length). Square parcels tend to rotate less and are therefore, harder to accurately place into the outlet. Other, usually unknown parcel properties (stiffness, inertia, friction, etc) have significantly less influence and can therefore be ignored when determining angle settings.
- In order to determine angle settings only three variables are necessary namely: lateral parcel position and orientation before the grid and parcel ratio.
- To ensure sortation of parcels independent of their lateral position an extra block of three rows may be added to the grid resulting in a total of six rows.

This primary research question was answered using the defined sub-questions. These questions are answered below:

- What are State of the Art bidirectional sorters and their required functions?

Various bidirectional sorters were found which mostly shared functionality with the IQ-Grid. These sorters all use the same mechanism which diverts parcels from their path by introducing a frictional force on the parcel. This force can be induced by several different members such as: wheels, belts or balls. However, the abstract principle behind these products all comes down to a friction force acting on the parcel different than its path which leads to a diversion. This realization led enabled a redesign of the layout without needing to keep the mechanical design in mind, since the layout would only prescribe the directions for these frictional forces in the grid.

By observing different products, patents and system description functional requirements were determined. Following these requirements the bidirectional sorter should operate in both directions enabling sorting and merging, while functions are independent of the parcel position. Furthermore, the product is able of positioning parcels on the outfeed.

- How can a bidirectional sorter and surrounding equipment be modelled?

By introducing an element approach for both parcel and equipment, slip was taken into account using individual accelerations of each element in order to calculate displacement and rotation of parcels. To model the shape of the wheels an extra formula was introduced using the coulomb friction ellipse. Furthermore, equipment was modelled using only three variables namely: velocity, friction coefficient and divert angle.

- How can the parcel behaviour be accurately described?

Using a simulation based on the mathematical model parcel behaviour can be found. To achieve accurate results a time step of 0.0005 s and gridsize of 0.02 m should be used. These settings result in errors usually smaller than 0.05 m and 5°, whereas larger parcels have more significant errors due to contact with the conveyor behind the sorter. Small parcels which have no contact with the second conveyor show accurate results.

- Which parameters influence the parcel behaviour on a bidirectional sorter?

By conducting multiple experiments more insight was gained on parameter influence. It became clear that the behaviour of parcels on the equipment is mostly influenced by the ratio of parcels. An increased ratio leads to more resistance against the induced rotation. This can be beneficial if the orientation should remain the same, but for sortation towards an outlet this can provide difficulties.

Stiffness also has to some extent influence on the behaviour, but this could be solved during the mechanical design of the product by decreasing the wheel pitch or realizing a better support for the parcel (for instance belts).

- Which layout configuration results in most efficient parcel behaviour?

9.2. Recommendations

In this research assumptions were made to simplify the simulation model. For further research it can be beneficial to validate the influence of these assumptions. Furthermore, several insights were gathered during the simulations and experiments which also provides openings for continued research. The recommendations are as follows:

- Since the initial simulation model showed accurate results, it may be applied to actually predicting parcel paths or to determine control strategies. This option should be further researched in order to determine the necessary accuracy and the improvements necessary to the model.
- To further increase this accuracy the third dimension can be added to the model to account for bumps, shape of the wheels, parcel stiffness and transitions between equipment. This could also help to indicate the opportunities for the mechanical design of the grid.
- Parcel stiffness is hard to measure and model but does influence the orientation and position of parcels. Therefore, the mechanical design of the grid may be adjusted in order to better support parcels leading to reduced influence of parcel stiffness.
- The model assumed rotations occur around the center of the parcel however, this may not always be the case. By conducting experiments this behaviour could be further investigated and possibly implemented in the simulation.
- Since the element and corresponding simulation approach shown good initial results, it can possibly be used in other challenging projects that require simulation. For instance to accurately determine the position of a parcel on a shoe-sorter or to simulate the position shifts of parcels on a roller conveyor.
- The scope of the project should also be enlarged by examining the equipment around the grid. During the experiments and simulation it became clear that the second conveyor can have negative influence during sortation and merging. For example, parcel behaviour can be optimized even further by decreasing the friction coefficient of the conveyor behind the grid.

Bibliography

[1] Raul Acuna, Rosa Maria Carpio, and Volker Willert. Dynamic markers: Uav landing proof of concept. *arXiv preprint arXiv:1709.04981*, 2017.

[2] Raymond Brach and Matthew Brach. The tire-force ellipse (friction ellipse) and tire characteristics. Technical report, SAE Technical Paper, 2011.

[3] Dirk Briskorn, Simon Emde, and Nils Boysen. Scheduling shipments in closed-loop sortation conveyors. *Journal of Scheduling*, 20(1):25–42, 2017.

[4] Marco Cavazzuti. Design of experiments. In *Optimization Methods*, pages 13–42. Springer, 2013.

[5] Damon conveyor. Swivel wheel sorter, n.d. URL http://www.damonconveyor.com/en/product/product.aspx?id=11&bid=18&aid=4. [Online; accessed 05-04-2018].

[6] Mark Costanzo and Angela L Marshall. Switch conveyor, June 3 2003. US Patent 6,571,937.

[7] Good Maynard J De and Clyde L Bowman. High speed take-off, August 30 1966. US Patent 3,269,519.

[8] Peter de Weerd. Groei e-commerce bestedingen stagneert, 09-03-2018. URL http://www.logistiek.nl/supply-chain/nieuws/2018/03/groei-e-commerce-bestedingen\-stagneert-101162652. [Online; accessed 24-04-2017].

[9] Dematic. Steerable wheel divert, n.d. URL http://www.dematic.com/en/supply/-chain-solutions/by-technology/sortation-systems/divert-systems/. [Online; accessed 05-04-2018].

[10] Ronald C Ehlert. Steerable diverter system, May 9 2006. US Patent 7,040,478.

[11] Redactie Emerce. Vanriet lanceert bi-directionele sorteeroplossing, 06-10-2015. URL https://www.emerce.nl/nieuws/vanriet-lanceert-bidirectionele-sorteeroplossing. [Online; accessed 24-04-2017].

[12] RE Fairley. Dynamic testing of simulation software. In *Proc. 1976 Summer Computer Simulation Conf*, pages 40–46, 1976.

[13] Rosario Fazio and James L Frank. Bi-directional transfer mechanism, March 15 1988. US Patent 4,730,718.

[14] Azra Fetić, Davor Jurić, and Dinko Osmanković. The procedure of a camera calibration using camera calibration toolbox for matlab. In *MIPRO, 2012 Proceedings of the 35th International Convention*, pages 1752–1757. IEEE, 2012.

[15] Matthew L Fourney and Christoph Lemm. Sorter belt conveyor, October 23 2007. US Patent 7,284,653.

[16] Garam. Wave sorter, 2013. URL http://www.garam21.co.kr/page/page.php?pg_idx=25&thismenucode=2_garam0378. [Online; accessed 05-04-2018].

[17] Gubunki. High speed wheel sorter, n.d. URL http://gubunki.com/. [Online; accessed 05-04-2018].

[18] Merryn Haines-Gadd, Atsushi Hasegawa, Rory Hooper, Quentin Huck, Magdalena Pabian, Cesar Portillo, Lu Zheng, Leon Williams, and Angus McBride. Cut the crap; design brief to preproduction in eight weeks: Rapid development of an urban emergency low-tech toilet for oxfam. *Design Studies*, 40:246–268, 2015.

[19] Hytrol. ProSort SC1 & SC2, 01-01-2017. URL http://www.hytrol.com/mediacenter/catalog_sheets/c_prosortsc.pdf. [Brochure; accessed 05-04-2018].

[20] Honeywell Intelligrated. Sortation systems, n.d. URL https://www.intelligrated.com/solutions/sortation-systems#intellisort-wd. [Online; accessed 05-04-2018].

[21] Intralox. High-speed 90-degree sorting, 2018. URL http://www.intralox.com/High-Speed-90degree-sorting.aspx. [Online; accessed 05-04-2018].

[22] Intralox. ARB sortating systems, n.d. [Online; accessed 05-04-2018].

[23] M IslamA and LM LyeA. Combined use of dimensional analysis and statistical design of experiment methodologies in hydrodynamics experiments. 2007.

[24] FBA Italy. Onesorter, n.d. URL http://www.fbaitaly.com/images/pdf-eng/Pivot_wheel_sorter.pdf. [Brochure; accessed 05-04-2018].

[25] Averill M Law, W David Kelton, and W David Kelton. *Simulation modeling and analysis*, volume 2. McGraw-Hill New York, 1991.

[26] VanRiet Material Handling Systems BV. Vanriet introduces the iq-grid, the new generation of wheel sorting solutions, 15-05-2014. URL https://www.vanrietgroup.com/tire-expo/vanriet-introduces-the-new-iq-grid/. [Online; accessed 02-05-2017].

[27] Anthony F Mills and AF Mills. *Basic heat and mass transfer*, volume 2. Prentice hall Upper Saddle River, 1999.

[28] Victor Minichiello, Rosalie Aroni, and Victor Minichiello. *In-depth interviewing: Researching people*. Longman Cheshire, 1990.

[29] Philip Mitchel. *Tool and manufacturing engineers handbook: material and part handling in manufacturing*, volume 9. Society of Manufacturing Engineers, 1998.

[30] Robert J Nicholson. Conveying apparatus and article diverter, June 2 1992. US Patent 5,117,961.

[31] William L Oberkampf, Sharon M DeLand, Brian M Rutherford, Kathleen V Diegert, and Kenneth F Alvin. Error and uncertainty in modeling and simulation. *Reliability Engineering & System Safety*, 75(3):333–357, 2002.

[32] OCM. Wheel sorter, sorting system switch wheel technology, n.d. URL http://www.ocm.eu/download.php?idfile=133&dir=15&dir2=prodotti. [Brochure; accessed 05-04-2018].

[33] Bryant G Ragan. Electromagnetically actuated sorter, June 21 2016. US Patent 9,371,193.

[34] Dag Raudberget. *Industrial Experiences of Set-based Concurrent Engineering-Effects, results and applications*. PhD thesis, Chalmers University of Technology, Department of Product and Production Development, SE-412 96 Göteborg, 2012.

[35] Dag Raudberget et al. The decision process in set-based concurrent engineering-an industrial case study. In *DS 60: Proceedings of DESIGN 2010, the 11th International Design Conference, Dubrovnik, Croatia*, pages 937–946, 2010.

[36] Gavriel Salvendy. *Handbook of industrial engineering: technology and operations management*. John Wiley & Sons, 2001.

[37] Robert G Sargent. Verification and validation of simulation models. In *Simulation Conference (WSC), Proceedings of the 2009 Winter*, pages 162–176. IEEE, 2009.

[38] Siemens. Varioroute, highly efficient and cost-effective flow splitting, 2017. [Brochure; accessed 10-04-2018].

[39] Durward K Sobek, Allen C Ward, and Jeffrey K Liker. Toyota's principles of set-based concurrent engineering. *Sloan management review*, 40(2):67, 1999.

[40] Bastian Solutions. Pivot wheel sorters, 2017. URL https://www.bastiansolutions.com/solutions/technology/conveyor-systems/sortation/conveyor/pivot-wheel-sorter#zipline. [Online; accessed 05-04-2018].

[41] TGW. NBS wave 200, 2018. URL https://www.tgw-conveyor.com/technologies/sortation-conveyor/nbs-wave-200. [Online; accessed 05-04-2018].

[42] Transnorm. High outfeed and sorting performance with transnorm roller function conveyor with central drive, 2017. URL https://www.transnorm.com/en/products/horizontal-distributingsorting/swivel-wheel-conveyor.html. [Online; accessed 05-04-2018].

[43] Dirk van As. URS bi-directional redevelopment 2017, 28-05-2018. [Online; accessed 27-06-2017].

[44] Vanderlande. Truxorter (pop-up sorter), n.d. URL https://www.vanderlande.com/parcel/innovative-systems/sortation-parcels/truxorter. [Online; accessed 05-04-2018].

[45] John Joseph Wilkins. Transmission having variable output orientation, November 22 2016. US Patent 9,499,341.

A

Scientific Paper

Redevelopment of a bidirectional sorter to improve parcel behaviour

Transport Engineering and Logistics, University of Technology, Mekelweg 2, Delft, The Netherlands

E.M. Teunissen, Ir. W. van den Bos and Dr. ir. D.L. Schott

***Abstract*— Within this research parcel behaviour over a bidirectional sorter is optimized to increase efficiency. Currently, influence of parcel properties on the sortation behaviour is unknown and equipment settings are set by experience rather than objective information. To gain insight in the behaviour first, a simulation model has been developed and validated by experiments. These experiments also provided effects of parcel and equipment parameters. Using the obtained simulation model different layout configurations were examined to increase efficiency of the sorter by setting different divert angles.**

I. INTRODUCTION

The e-commerce market is constantly increasing and has doubled in the last five years [1]. This growth results in a higher demand on parcel handlers such as DHL and UPS. To meet this demand the capacity of sorting facilities should be increased. This can be achieved by introducing bidirectional sorting systems [2]. Such system can operate in reverse to accommodate vans and trucks at the same docks during morning and afternoon shifts enabling streams in both directions using the same conveyors [3].

Steerable rollers are currently the only group of sorters which feature this property [4]. Several steerable roller concepts have been developed which share a similar mechanism [5], [6], [7], [8]. In 2014 VanRiet Material Handling introduced the modular IQ-Grid (Figure 1) which also incorporates this mechanism [9]. The IQ-Grid has already been applied in several systems and proved the efficiency of a bidirectional system.

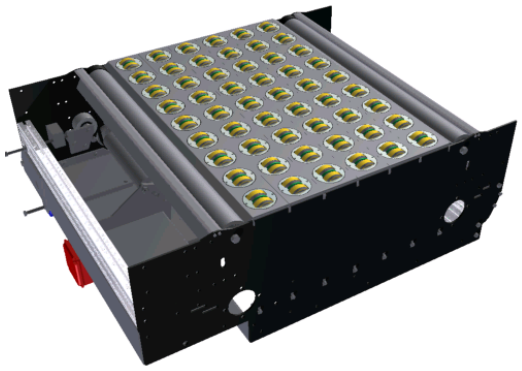

Fig. 1. Bidirectional sorter developed by VanRiet, called IQ-Grid [9].

The IQ-Grid was developed using a qualitative approach, the design is based on experience of earlier developments and visual observations. This however, resulted in a black-box which is able to sort parcels to an outlet without knowing where and how the parcel will end up at the outlet. This uncertainty about the parcel behaviour also results in design challenges since the influence of certain design parameters and impact of different types of parcels is unknown.

Therefore, this research aims to optimize the parcel behaviour on the IQ-Grid to increase the sorting efficiency by testing different layout configurations and gaining more insight in the influence of different parcel and equipment parameters.

II. METHOD

Optimization for the grid has been achieved by choosing an objective approach attaining information using measurements, calculations or simulations, to select a final design [10]. Therefore, Set-Based Concurrent Engineering design method was chosen due to its quantitative properties and proven results [11], [12].

To eliminate concepts based on quantitative information a test is necessary to assess compliance with product requirements, concepts which fail can then be eliminated. Due to high costs and time required to physically test different concepts, a simulation model will be constructed. The development of such model requires the following steps: model qualification, model verification and model validation [13]. This process is shown in Figure 2.

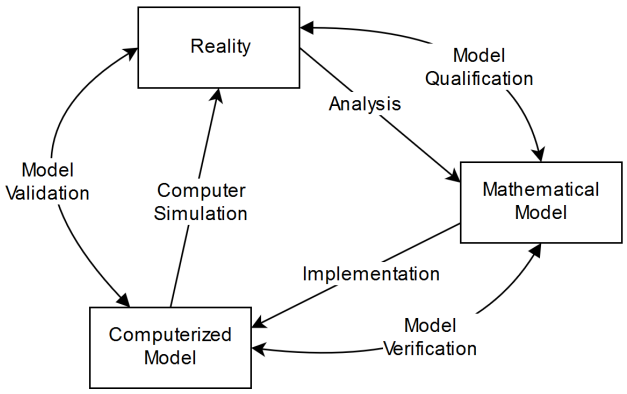

Fig. 2. Steps necessary to create a simulation model which can then be used to simulate the physical product. Obtained from [13].

III. THEORY

A mathematical description of parcels on the bidirectional sorter is necessary to develop a simulation. In Figure 3 a parcel is shown on two types of equipment: conveyor and bidirectional sorter. Resultant translation and rotation are found by determining forces induced on element level within the parcel. Using the element approach, slip can be taken into account to provide a more realistic model. These elements have a defined size which determines the number of elements

per parcel. By adding element forces a resultant parcel acceleration and rotational acceleration are found which are used to determine the position and orientation of parcels on the sorter. Two different situation can be distinguished, these are determined to be:

- Parcel is in contact with one piece of equipment: in this case the parcel will adapt the velocity of the equipment, which is in the direction of ϕ. Consequently, the element velocity will have the same direction as the equipment velocity, resulting in a difference of zero leading to a resultant force of zero.
- Parcel is in contact with two or more pieces of equipment: the parcel will have a static friction with one piece of equipment which has the largest frictional force and dynamic friction with the other ones. The parcel will be influenced by the forces induced by all equipment and its displacement will depend on the sum of these forces.

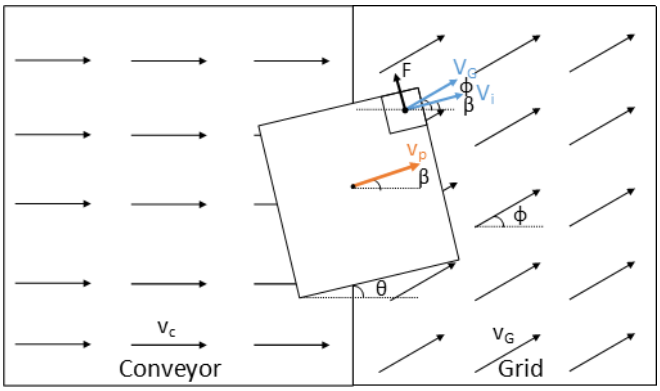

Fig. 3. Parcel in contact with conveyor and bidirectional sorter resulting in a translation and rotation due to frictional forces induced by the equipment. Showing divert angle (ϕ), parcel rotation (θ) velocity direction (β), resultant force acting on a single element (F) and velocities (v_p, v_c, v_g, v_i).

A. Parcel Translation

First, accelerations found at the elements within the parcel are averaged by Equation 1 resulting in acceleration for the complete parcel at a certain time step, $(t+\Delta t)$. The number of elements, n_e is determined by the size of the parcel and element size.

$$a(t+\Delta t) = \frac{\sum_{i=1}^{n_e} a_i(t+\Delta t)}{n_e} \tag{1}$$

Using the acquired parcel acceleration (a), velocity (v) and position (s) the parcel position at time $t+\Delta t$, is found by Equation 2. By these descriptions the position of the parcel can be found during translation over the grid.

$$s(t+\Delta t) = s(t) + v(t)\cdot\Delta t + \frac{1}{2}\cdot a(t+\Delta t)\cdot\Delta t^2 \tag{2}$$

To preserve the shape of the parcel, the new positions for each element are calculated using the parcel displacement of Equation 2. By calculating the element positions from the average displacement it is possible to have slip during a time step and preserving the shape of the parcel by modelling stiff connections between the elements.

B. Parcel Rotation

During transportation the parcel can rotate when in contact with multiple pieces of equipment, since the forces then no longer cancel out which results in a torque. This torque is assumed to take place in the center of the parcel, resulting in consequently a rotation of the parcel around its center. The parcel's resistance to rotation is given by the moment of inertia depending on the density (ρ) at all distances (r) throughout the parcel volume (V).

$$I = \int_V r^2 \rho \, dV \tag{3}$$

By combining the torque (of the element forces) and moment of inertia the angular acceleration of the parcel can be found, which is used to find the rotation (θ) of the parcel. First the total torque acting on the parcel is computed by taking the sum of the torques induced by each element using Equation 4. The total torque and moment of inertia can then be used to find the angular acceleration (α) of the parcel shown in Equation 5.

$$\tau = \sum_{i=1}^{n_e} \tau_i \tag{4}$$

$$\alpha = \frac{\tau}{I} \tag{5}$$

The rotation of the parcel is found using similar equations as for the translation using the calculated angular acceleration (α), angular velocity (ω) and rotation (θ) to find the parcel rotation at time step, $(t+\Delta t)$ by Equation 6.

$$\theta(t+\Delta t) = \theta(t) + \omega(t)\cdot\Delta t + \frac{1}{2}\cdot\alpha(t)\cdot(\Delta t)^2 \tag{6}$$

C. Element Level

The friction force (F_{w_i}) is determined by Equation 7 using mass of the element (m_e), gravitational constant ($g = 9.81$) and friction coefficient between the element and equipment underneath (μ).

$$F_{w_i} = m_e \cdot g \cdot \mu \tag{7}$$

Circular shapes of the grid wheels introduce a difference for the friction coefficient depending on the angle between parcel and wheel ($\theta = \phi - \beta$) illustrated in Figure 4. Using Equation 8 the adjusted friction coefficient is found [14].

$$\mu_w = \sqrt{\left(\mu_{w_x}\cdot cos(\phi-\beta)\right)^2 + \left(\mu_{w_y}\cdot sin(\phi-\beta)\right)^2} \tag{8}$$

In order to find the corresponding x- and y-forces a vector is determined to describe the difference between the equipment- and element velocity. The resultant force has the same direction therefore, the x- and y-components are determined using the vector. In Equation 9 the vector is

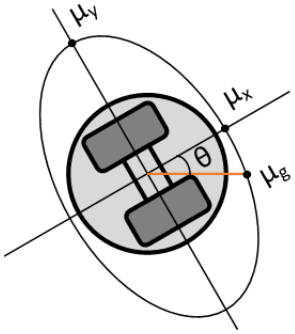

Fig. 4. Ellipse which is use to determine the friction coefficient between the wheels and the parcel, if the parcel travels longitudinal to the wheel $\theta = 0°$ and so the friction coefficient (μ_g) is equal to μ_x if the parcel travels lateral $\theta = 90°$ to the wheel then $\mu_g = \mu_y$. For the other values of θ Equation 8 will be used.

determined using the angles and velocities shown in Figure 3 in order to determine F_x & F_y.

$$\begin{bmatrix} F_x \\ F_y \end{bmatrix} = F_w \cdot \begin{bmatrix} V_e \cdot cos(\phi) - V_i \cdot cos(\beta) \\ V_e \cdot sin(\phi) - V_i \cdot sin(\beta) \end{bmatrix} \tag{9}$$

IV. MODEL

The mathematical model is implemented in Matlab to obtain a simulation model. Model output provides graphs on parcel position, orientation and velocity which is compared to experimental results and used to optimize parcel behaviour.

A. Verification

Implementation of the model was verified by observing the output results and parameter response compared to an expected response. In Figure 5 output of the model can be seen, in which a logical path can be distinguished according to the chosen divert angle and correctly maintained element positions relative to each other.

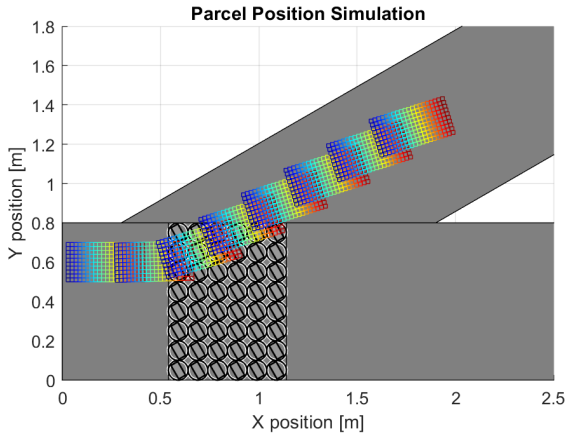

Fig. 5. Model output showing a parcel travelling over respectively conveyor, grid and outfeed. Input parameters are: $V = 1m/s, L_p = 0.4m, W_p = 0.2m, m_p = 1kg, x_0 = 0.25m, y_0 = 0.6m, \phi = 30°$.

B. Validation

Several experiments were performed using the IQ-Grid to validate the simulation model. These experiments were conducted using Design of Experiments in order to reduce number of measurements and to ensure validation of all relevant parameters. In Table I independent variables are shown with corresponding levels for a 2-level, Resolution IV design to examine individual and two-way interactions [15]. Wheel height determines the height difference between the conveyor and grid in order to possibly increase grip on parcels. Furthermore, different surfaces (rubber and Teflon) are used to vary friction coefficients between parcel and equipment.

TABLE I
HIGH- AND LOW SETTINGS FOR INDEPENDENT VARIABLES

Parameter	Symbol	-1	1
Wheel height	h_w	$0mm$	$5mm$
Divert angle	α	30°	45°
Surface	S_m	Telfon	Rubber
Parcel ratio	$\frac{W_p}{L_p}$	0.5	1
Velocity	$\frac{V_g}{V_c}$	1	1.173
Inertia	$\frac{I}{L_p^2 m_p}$	1	1.5
Stiffness	S	MDF	Foam

Dependent variables for position and orientation of the parcel were measured and compared to simulated results providing error indication between reality and model. Furthermore, friction coefficients between parcel and conveyor, grid and outfeed were determined using a unster and parcel weight using a scale. All other variables were kept constant during measurements as shown in Table II.

TABLE II
PARAMETERS DETERMINED FOR CONTROLLED VARIABLES

Parameter	Symbol	Value
Length parcel	L_p	$400mm$
Velocity conveyor	V_c	$1m/s$
Acceleration	a_g, a_c	$0m/s^2$
Gravitational	g	$9,81m/s^2$
Start orientation	ϕ_0	$0°$
Start position	x_{p0}, y_{p0}	$0, 100mm$
Transport width	T_w	$800mm$

By conducting these experiments results were gained and compared to the simulation model. In Figure 6 the error in parcel position is shown between model and experiments. Parcel position is measured as a lateral position on the outfeed, e.g. distance between parcel center and side of the conveyor. Parcel ratio results in most significant errors due to influence of the conveyor behind the grid which has more frequent contact with high ratio parcels, leading to disturbed behaviour. Further noticeable, is the wheel height which introduces relatively constant errors. This error was expected since wheel height was not taken into account by the mathematical model and only tested to gain insight in its influence.

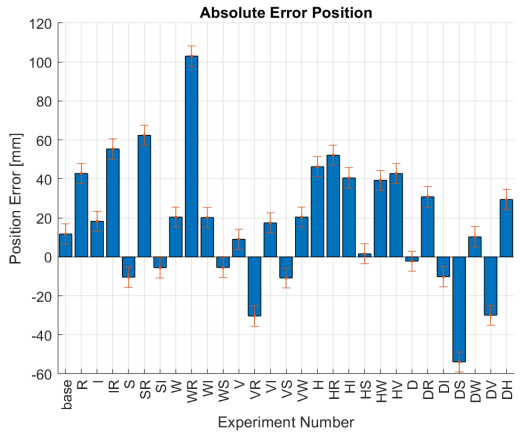

Fig. 6. Position error between model and experiments, a positive error indicates a larger distance between parcel and conveyor side, in the model. High errors are found at increased parcel ratio due to contact with the conveyor behind the grid. Wheel height is not modelled by the mathematical model and therefore, produces higher errors. Error bars indicate measurement errors of the experiments ($\pm 6.37mm$).

In Figure 7 errors in parcel rotation between the model and experiments are shown. Again, significant errors can be found at increased parcel ratios due to contact with the conveyor behind the grid. Most other experiments have errors of 5° or less combined with the position error of 60 mm or less the model is assumed to be sufficient to test different layout concepts to improve the parcel behaviour.

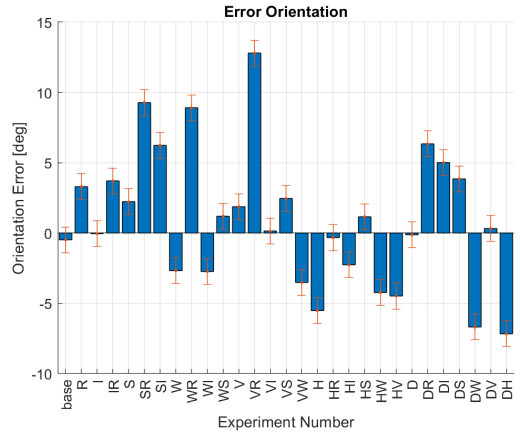

Fig. 7. Rotation error between model and experiments, a positive error indicates a larger parcel rotation in the model. Increased parcel ratio leads to higher errors. Furthermore, all remaining errors are relatively small. Error bars indicate measurement errors of the experiments ($\pm 1.36^\circ$).

V. RESULTS

The proposed improvements are found by both the performed experiments and testing of new layout configurations. Improvements based on the experiments are found by examining parameter influences to discover their effect on parcel behaviour. Finally, different configurations are tested using the validated simulation model to further optimize parcel behaviour.

A. Parameter Influence

Effects of parameter variation are calculated using Equation 10 which compares the experiment result to the base measurement (all settings at -1 in Table I). A higher value indicates a large effect on parcel position or rotation.

$$\text{Effect} = \frac{\text{Result measurement i}}{\text{Result base measurement}} \tag{10}$$

In Figure 8 effects are shown for all individual and combined parcel properties, but also effects of equipment parameters on the base measurement comprising grid velocity, wheel height and divert angle.

Effect:	W	WR	WI	WS	R	RI	RS	I	IS	S	V	H	D
Position	0,02	0,10	0,01	0,01	0,21	0,20	0,23	0,00	0,05	0,10	0,01	0,08	0,22
Orientation	0,15	0,40	0,30	0,17	0,30	0,43	0,61	0,18	0,37	0,21	0,01	0,29	0,08

Fig. 8. Influence of different individual and combined parcel properties for position and orientation. Parcel ratio is most dominant while other properties have only little effects. Furthermore, also equipment influence on the base measurement are shown comprising grid velocity, wheel height and divert angle.

Influence Parcel Characteristics

To develop a product suitable for numerous types of parcels it is important to examine the effects of parcel properties. According to Figure 8 parcel ratio is most dominant whereas other parameter have only little effects on position and orientation. The influence of parcel stiffness could be reduced by reviewing the mechanical design to better support the parcel and therewith, have behaviour closer to stiff parcels.

Because of this result, parcel behaviour should be optimized based on parcel ratio only. Therefore, only this parameter is necessary to measure in order to efficiently sort parcels. Other parameters comprising parcel stiffness, inertia and friction coefficients have only little effect and do not have to be taken into account for the layout configuration. Consequently, obtaining information regarding these properties is unnecessary.

Influence Equipment Characteristics

Furthermore, equipment variables were examined consisting of: grid velocity, wheel height and divert angle. In Figure 8, effects of these properties for the base measurement are shown. Grid velocity has no influence on both position and orientation of the parcel. Therefore, it may be increased compared to surrounding conveyors in order to keep longitudinal parcel speeds equal during sortation as shown in Figure 9, ensuring equal spacing between parcels.

Increased wheel height only effects parcel orientation and introduces a bump resulting in rough and unpredictable parcel behaviour (Figure 10). Since, parcel orientation can also be influenced by different layout configurations this property is defined as unwanted. Therefore, the wheel height should be set to 0 mm.

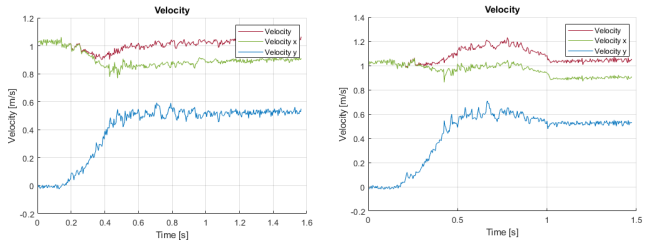

Fig. 9. Grid velocity equal to surrounding conveyors (left) compared to increased grid velocity (right) in order to maintain lateral parcel speed (green). This helps to ensure equal spacing between parcels while position and rotation are not influenced.

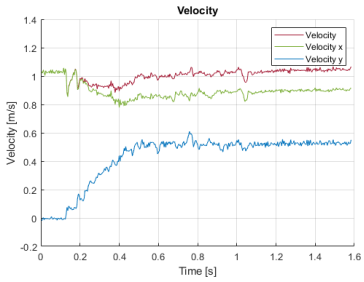

Fig. 10. Velocity profile for increased wheel height resulting in a bump as the parcel hits the grid (0.1 s). This bump introduces rough behaviour or even jumping parcels at higher velocities.

Finally, divert angle settings indicate effects on parcel position which can be used for the layout configuration in order to position parcels on the outfeed conveyor. Furthermore, different angle settings throughout the grid are assumed to also have influence on parcel orientation. Therefore, angle settings will be used to improve parcel behaviour.

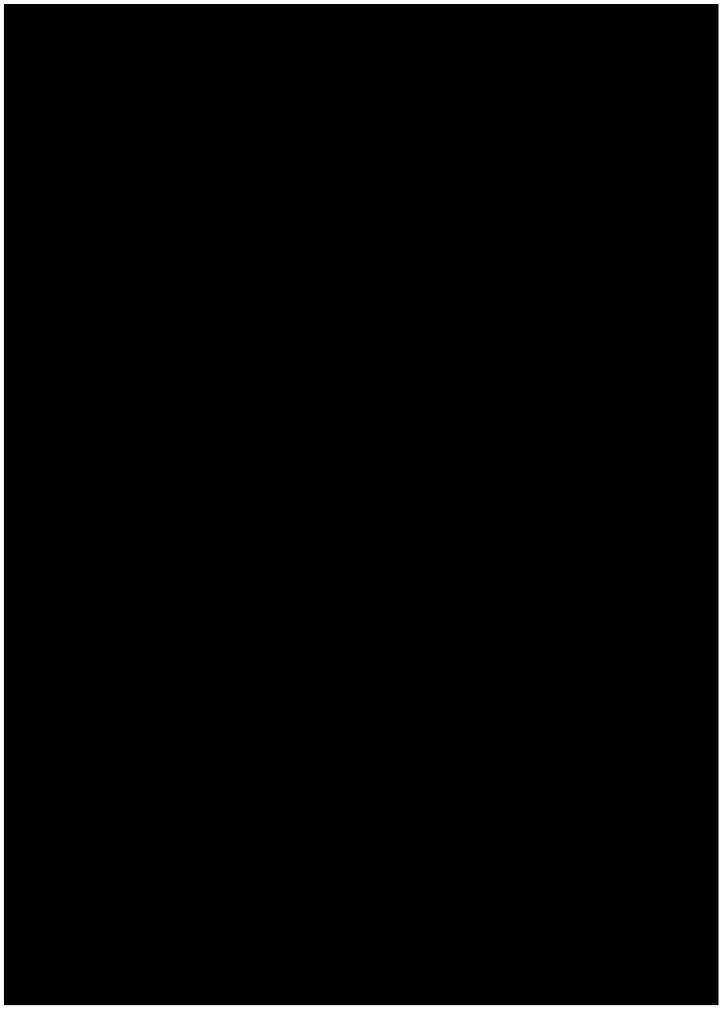

VI. DISCUSSION

This research provided more insight into parcel behaviour on a bidirectional sorter by developing a simulation model and conducting several experiments. Influence of variables was found using the experiments, while the simulation was used to optimize the layout configuration dictating blocks which share an equal divert angle.

Due to the low impact of most parcel properties, divert angles only need to be adjusted based on parcel ratio while other properties can be ignored. Furthermore, sorter velocity can be increased in order to maintain lateral parcel velocity without effecting position and orientation.

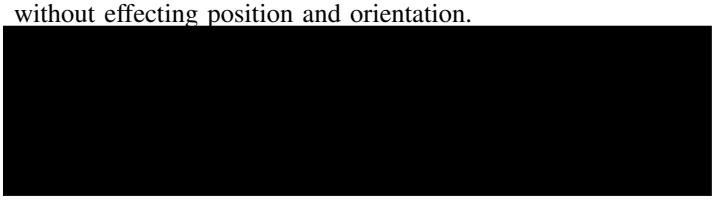

REFERENCES

[1] Peter de Weerd. Groei e-commerce bestedingen stagneert, 09-03-2018. URL http://www.logistiek.nl/supply-chain/nieuws/2018/03/groei-e-commerce-bestedingen -stagneert-101162652. [Online; accessed 24-04-2017].

[2] Dirk Briskorn, Simon Emde, and Nils Boysen. Scheduling shipments in closed-loop sortation conveyors. Journal of Scheduling, 20(1):2542, 2017.

[3] Redactie Emerce. Vanriet lanceert bi-directionele sorteeroplossing, 06-10-2015. URL https:// www.emerce.nl/nieuws/vanriet-lanceert-bidirectionele-sorteeroplossing. [Online; accessed 24-04-2017].

[4] Gavriel Salvendy. Handbook of industrial engineering: technology and operations management. JohnWiley & Sons, 2001.

[5] Bastian Solutions. Pivot wheel sorters, 2017. URL https://www.bastiansolutions.com/ solutions/technology/conveyor-systems/sortation/conveyor/pivot-wheel-sorter#zipline. [Online; accessed 05-04-2018].

[6] OCM. Wheel sorter, sorting system switch wheel technology, n.d. URL http://www.ocm.eu/ download.php?idfile=133&dir=15&dir2=prodotti. [Brochure; accessed 05-04-2018].

[7] Dematic. Steerable wheel divert, n.d. URL http://www.dematic.com/en/ supply-chain-solutions/by-technology/sortation-systems/divert-systems/. [Online; accessed 05-04-2018].

[8] FBA Italy. Onesorter, n.d. URL http://www.fbaitaly.com/images/pdf-eng/Pivot_wheel_sorter. pdf. [Brochure; accessed 05-04-2018].

[9] VanRiet Material Handling Systems BV. Vanriet introduces the iq-grid, the new generation of wheel sorting solutions, 15-05-2014. URL https://www.vanrietgroup.com/tire-expo/ vanriet-introduces-the-new-iq-grid/. [Online; accessed 02-05-2017].

[10] Victor Minichiello, Rosalie Aroni, and Victor Minichiello. In-depth interviewing: Researching people. Longman Cheshire, 1990.

[11] Dag Raudberget. Industrial Experiences of Set-based Concurrent Engineering-Effects, results and applications. PhD thesis, Chalmers University of Technology, Department of Product and Production Development, SE-412 96 Gteborg, 2012.

[12] Durward K Sobek, Allen CWard, and Jeffrey K Liker. Toyotas principles of set-based concurrent engineering. Sloan management review, 40(2):67, 1999.

[13] William L Oberkampf, Sharon M DeLand, Brian M Rutherford, Kathleen V Diegert, and Kenneth F Alvin. Error and uncertainty in modeling and simulation. Reliability Engineering & System Safety, 75(3):333357, 2002.

[14] Raymond Brach and Matthew Brach. The tire-force ellipse (friction ellipse) and tire characteristics. Technical report, SAE Technical Paper, 2011.

[15] Marco Cavazzuti. Design of experiments. In Optimization Methods, pages 1342. Springer, 2013.

B

State of the Art Patents on Wheel Sorters

In this Chapter the patents found by the classifications B65G13/10 and B65G47/52 are discussed. Only the patents from these classifications that have a significant different mechanism than the IQ-Grid will be described. These different insights can be useful to develop new concepts during the research, in which the patents can serve as an inspiration. In the following sections each patent is individually discussed.

B.1. Electromagnetically Actuated Sorter

This patent describes two designs for diverters using magnetic field. The first design has fixed diverter wheels which are positioned in between conveyor rollers. These wheels are driven by an electromagnectic field induced by a linear stator consisting of a series of poles that are energised by coil windings [33]. This configuration is shown in Figure B.1.

The second design has the same electromagnetic drive induced by a linear stator but the wheels have an adjustable divert angle. This divert angle can be set by the direction of the stator's magnetic flux wave. The position of the wheel is ensured to remain stable using a plunger (68) and a spring [33]. This configuration is shown in Figure B.2.

B.2. Steerable Diverter System

This patent looks similar to the IQ-Grid but uses a different transmission to adjust the divert angle. The angle is set using a gear plate driven by a pivotal or rotational movement. The gear plate can serve multiple wheels [10], which is shown in Figure B.3.

The wheels are driven by a motorised roller connected to the wheels via belts or o-rings similar to the mechanism used in the IQ-Grid. This transmission is shown in Figure B.4.

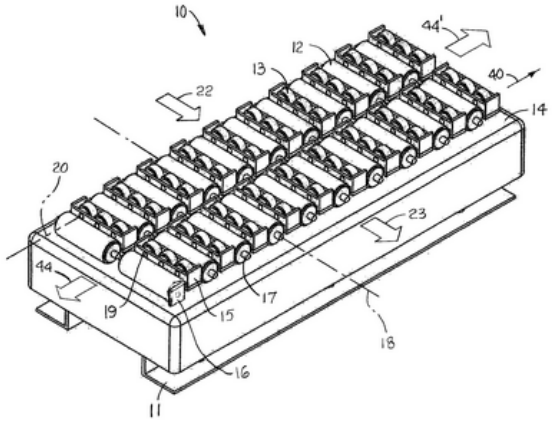

Figure B.1: First design in the patent using fixed divert angles [33].

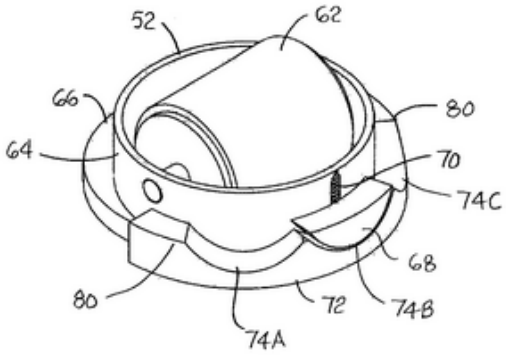

Figure B.2: Second design with an adjustable divert angle using the magnetic flux wave [33].

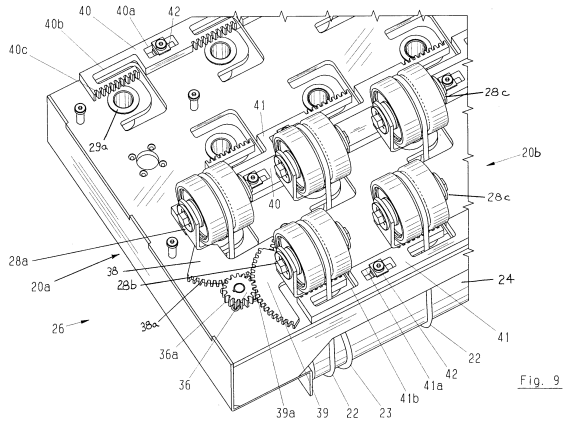

Figure B.3: Divert angle adjusted using a gear plate connected to multiple wheels [10].

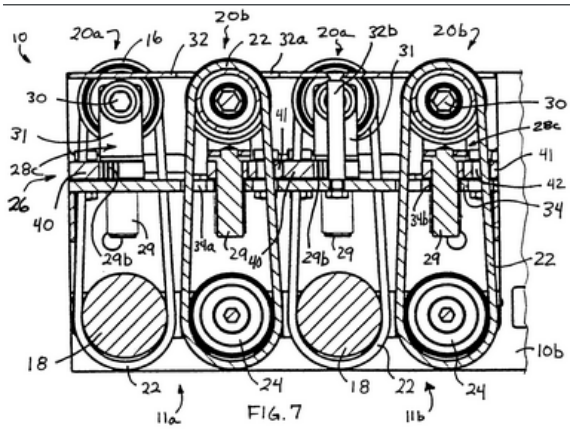

Figure B.4: Drive transmission between the roller and wheels using o-rings [10].

B.3. Bidirectional Transfer Mechanism

This design can be used to divert packages 90°. The transfer mechanism is capable of sorting packages into two directions and can also operate in reversed direction (bidirectional). The divert system is usually placed in between roller conveyors. When a package needs to be diverted the system is moved upward by a pneumatic cylinder and transfers the package [13]. This cylinder is shown by (60) in Figure B.5.

The wheels are driven by an endless elastomeric belt which runs along the width of the conveyor. The belt is in direct contact with the package and ensures the transfer to a different conveyor. This configuration is shown in Figure B.6.

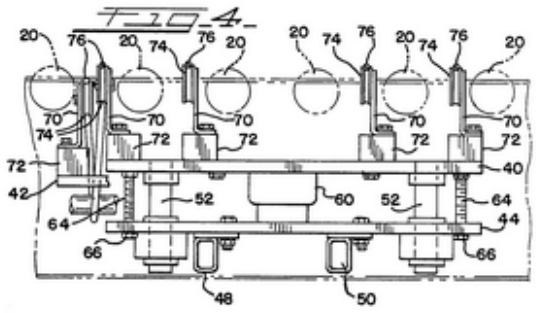

Figure B.5: Lifting mechanism with a pneumatic cylinder (60) used for the bidirectional transfer [13].

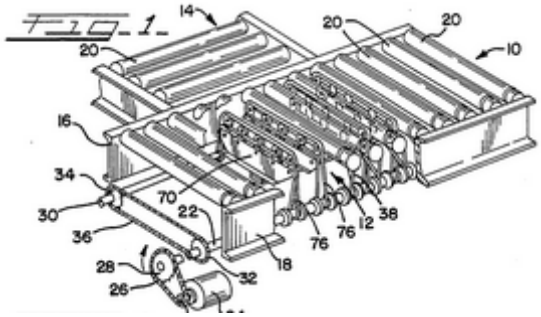

Figure B.6: Drive belts used to move the package onto another conveyor [13].

B.4. Activated Roller Belt (ARB) Conveyor

This patent consists of a special conveyor belt equipped with longitudinal lanes of small rotatable wheels. These wheels are arranged to rotate oriented in a different direction than the conveyor belt movement. These wheels can be rotated using an belt underlying the conveyor. Activating this belt will propel conveyed articles in one direction or another [6]. The mechanism is shown in Figure B.7. The patent is also used in the product described in Section C.6.

A different version of this mechanism is shown in Figure B.8. This mechanism uses rollers instead of a belt to move the wheels mounted on the conveyor. However, the functionality of the product is similar to the first design [15].

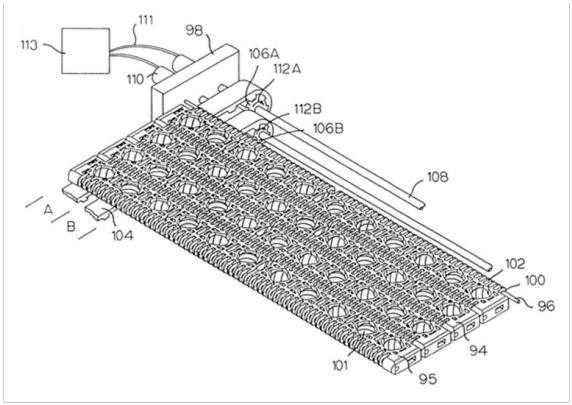

Figure B.7: ARB system consisting of wheels rotated by an underlying belt [6].

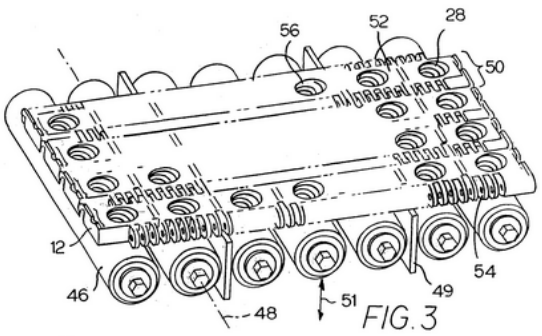

Figure B.8: ARB system consisting of wheels rotated by an underlying rollers [15].

B.5. High Speed Take-Off

This mechanism has a similar layout as the product discussed in Section C.2. The divert angle is fixed, the mechanism is positioned lower than the conveyor and is elevated when a package needs to be diverted. The track is elevated using a electrical solenoid [7] which is shown in Figure B.9.

Despite the similar layout the drive mechanism is different. In this configuration the package is

transported by wheels mounted on a chain or belt which is driven by an electric motor [7]. This principle is shown in Figure B.10.

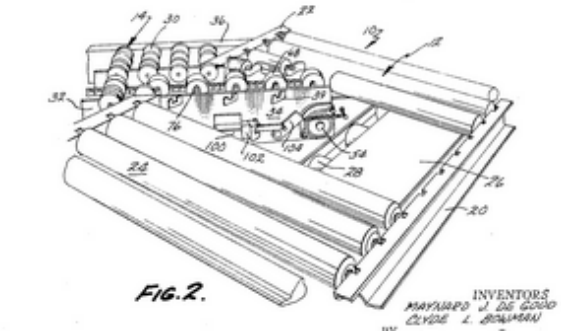

Figure B.9: Diverter mechanism including the pneumatic cylinder (102) for elevation [7].

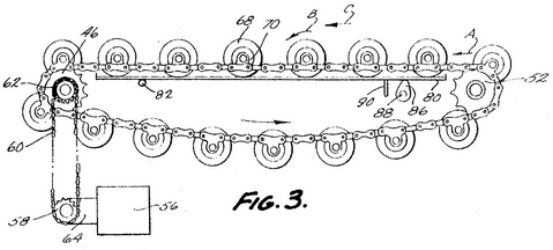

Figure B.10: The driver mechanism consisting of wheels mounted on a chain [7].

B.6. Conveying Apparatus and Article Diverter

This diverter hold several modules which consist of two small flat powered diverter belts. These are powered by a common driver roller which are connected using o-rings. The common driver is connected to the main conveyor [30].

The carriages are pivoted using a draw bar which is driven by a rotary actuator. The carriages are vertically and angular adjustable in incline which enables them to connect to a large variety of product. The mechanism is shown in Figure B.11 & B.12.

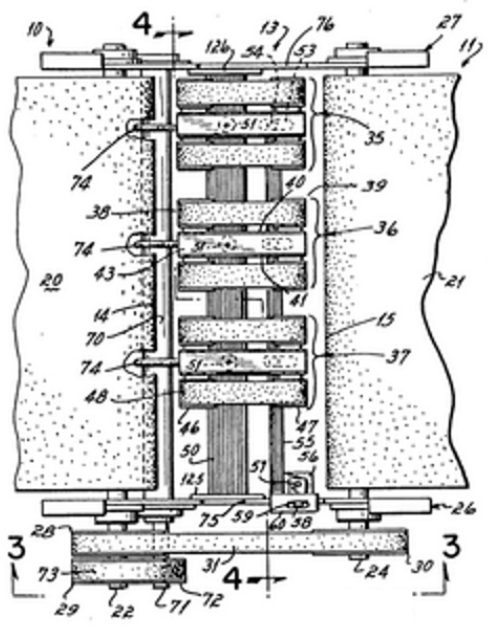

Figure B.11: Diverter mechanism while stationary [30].

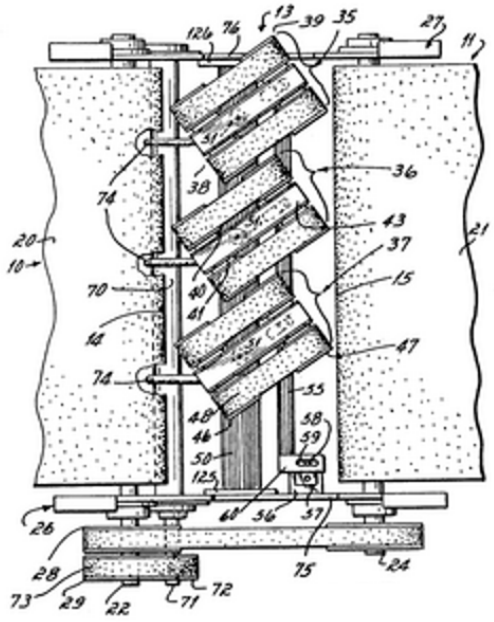

Figure B.12: Diverter mechanism while sorting packages [30].

B.7. Transmission Having Variable Output Orientation

This patent results in a similar product as the IQ-Grid but uses a different transmission to divert and rotate the wheels. The wheels are rotated using a underlying belt conveyor which rotates the wheels on the bottom of the transmission. This rotation is transmitted to the upper wheels via several gears [45]. This mechanism is shown in Figure B.13.

An advantage of this configuration is the decoupling of the rotation and divert angle. The wheels can be freely turned at variable angles using the side gear. The different modules can be coupled using gears to ensure block control [45]. This is shown in Figure B.14.

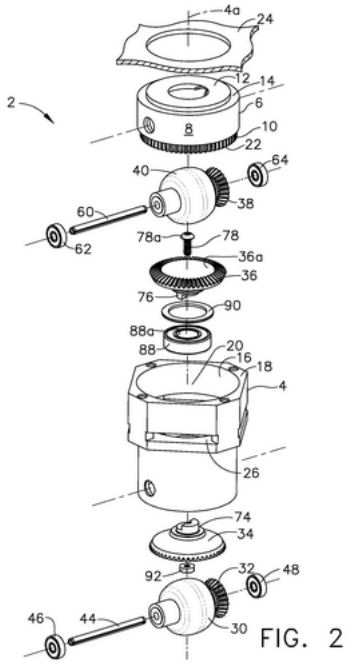

Figure B.13: Transmission used in the diverter [45].

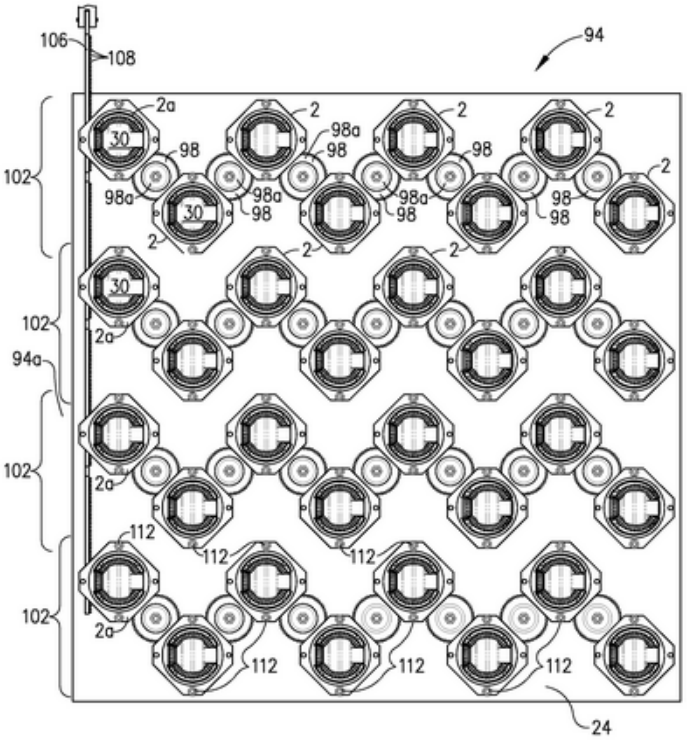

Figure B.14: Configuration with coupled transmissions to enable block control [45].

C

State of the Art Wheel Sorters

In this Chapter products will be described which are available in the market. In contrast to the patents discussed in Chapter B these designs are actually available. Each product will be individually discussed, in contrast with Chapter B this chapter will also discuss products which have a similar configuration as the IQ-Grid. This can be useful to see what functions competitor's products feature or miss compared to the IQ-Grid.

C.1. High Speed Wave Sorter, Gubunki

This wheel sorter is an all electric solution using a DC motor for diverting and a three phase motor for the wheels. The sorter can divert between 30 and 90° and has four sortation directions (double outputs). It can handle up to 6.000 packages per hour. The configuration has a fixed height but variable divert angles [17]. The wheels are driven via o-rings belts. The complete product is shown in Figure C.1.

C.2. NBS Wave 200, TGW

This product operates in combination with a narrow belt conveyor. The divert wheels pop up between the belt conveyors and pick up the packages after which it is send to the fixed sorting direction. The wheels are driven by the main conveyor and the divert angle is fixed. It can handle 12.000 packages per hour [41]. The product is shown in Figure C.2.

Figure C.1: Wheel sorter by Gubunki.

Figure C.2: NBS Wave 200 by TGW.

C.3. Wave Sorter, Garam

This wave sorter can sort into 5 directions using wave controls (controlling rows of the sorter individually). Both actuators (divert and wheel rotation) are electric. The sorter can adjust its divert angle from 30 to 40°. It is capable of handling 10.000 packages per hour [16]. The product is shown in Figure C.3.

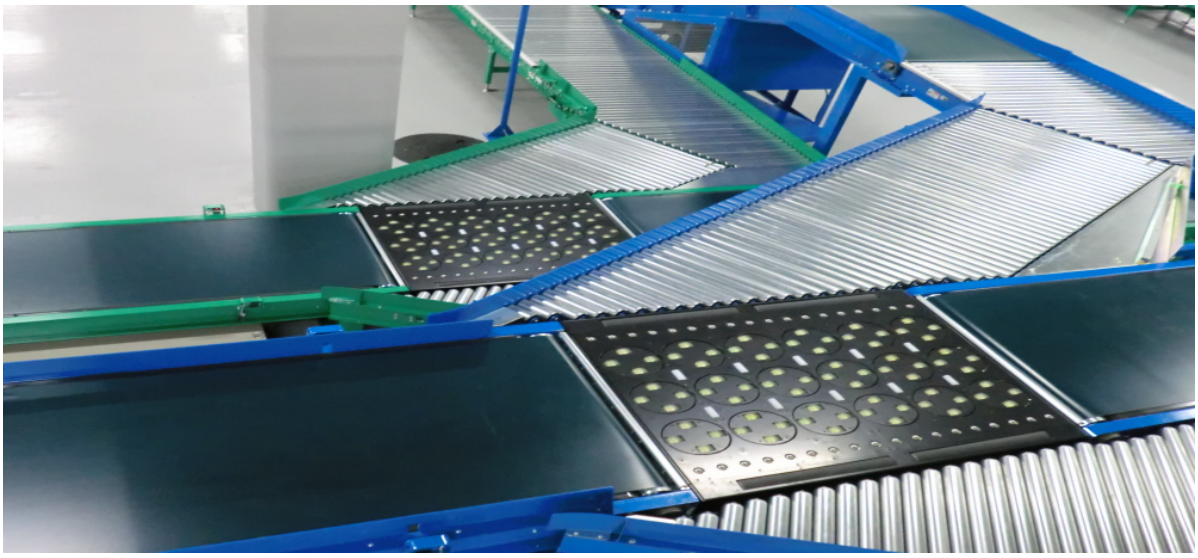

Figure C.3: Wave sorter by Garam.

C.4. PWDSorter, ZiPline

This product uses servo motors for the divert angle and can therefore vary its angle from 0 to 30°. The height of the wheels is fixed and driven by o-ring belts. It has a maximum of 4 rows and is capable of handling 4.500 packages per hour [40]. The product is shown in Figure C.4.

Figure C.4: PWDSorter by ZiPline

C.5. ProSort, Hytrol

This product is diverted by two pneumatic cylinders (two-sided diverter). Therefore, the angles are fixed positions. The wheels and belt are driven by the main conveyor and the diverter consists of 2

rows. It is capable of handling 4.800 packages per hour [19]. The product is shown in Figure C.5.

Figure C.5: ProSort SC by Hytrol

C.6. Activated Roller Belt Sorters, Intralox

This product (also described in Section B.4) is noticeably different than the other products since the diverter is integrated into the conveyor, consisting of small wheels that can be driven by underlying belts. When activating these belts, the package will move following the direction of the wheels. The Activated Roller Belt (ARB) is shown in Figure C.6.

These small wheels are assembled into the conveyor and therefore the divert angles are predetermined and fixed. The ARB sorting solution can handle 6.000 packages per hour and operates fully electric [22].

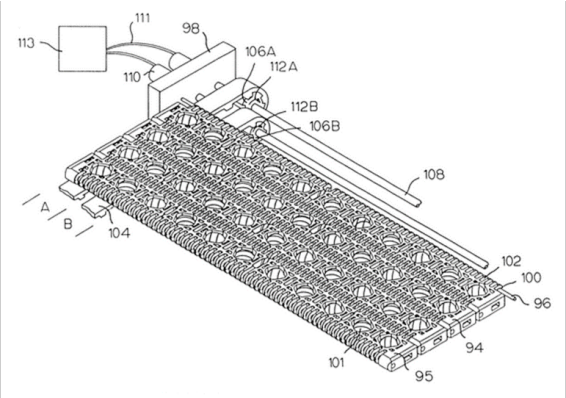

Figure C.6: ARB system obtained from a patent [6].

Figure C.7: Sorting solution by Intralox [21].

C.7. Swivel Belt Sorter

This product stands out with its drive mechanism which consists of small belt conveyors instead of wheels as usually. The belts are driven by electric motors and the divert angle is set with pneumatic cylinders. Unfortunately no further information or specifications are available. The product is shown in Figure C.8.

Figure C.8: Diverter using belts instead of wheels.

C.8. Wheel Sorter, OCM

This product is similar to the IQ-Grid and shares some design aspects such as the O-rings, modular system and pneumatic actuators. The system can also operate bidirectional and 2-3 sorting ways. There is also a full electric version available. It can handle 10.000 packages per hour [32]. The product is shown in Figure C.9.

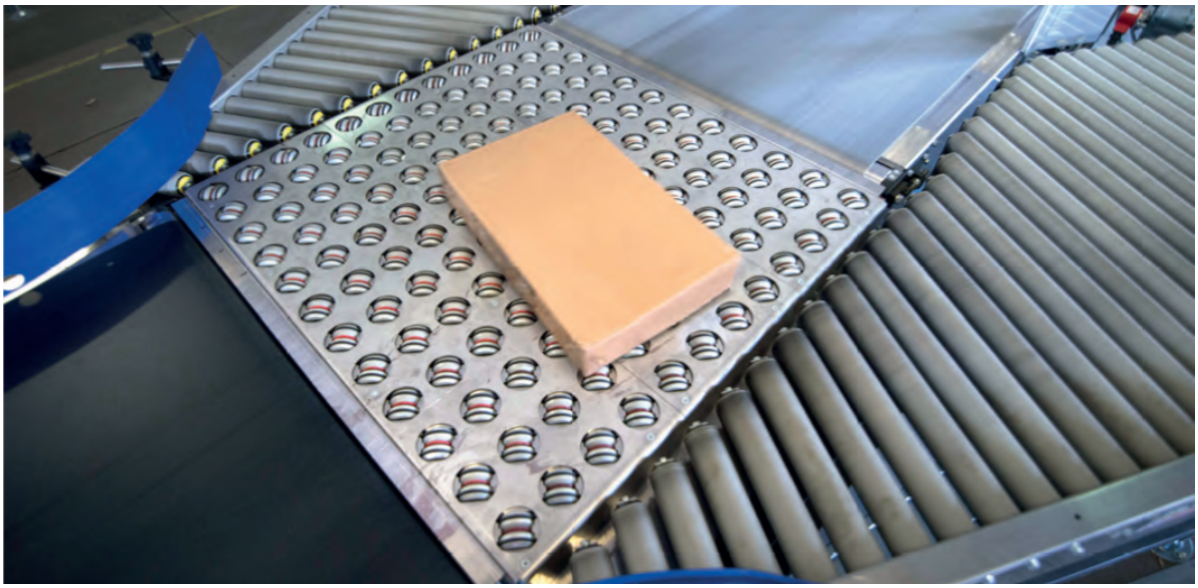

Figure C.9: Wheel Sorter by OCM

C.9. Steerable Wheel Divert, Dematic

This product uses pneumatic cylinders to set the divert angle and electric wheel drivers. The design is similar to the in section C.8 described wheel sorter and the IQ-Grid. However, this product can only divert at an angle of 30° with a pneumatic actuator [9]. The product is shown in Figure C.10.

Figure C.10: Steerable Wheel Divert by Dimatic.

C.10. OneSorter, FBA Italy

This product is also similar to the previously described products. But an advantage of this product are the double cylinders which enable separate control of the left and right side of the grid which can help to centre or split packages. The Onesorter is capable of handling 3.000 packages per hour [24]. The product is shown in Figure C.11.

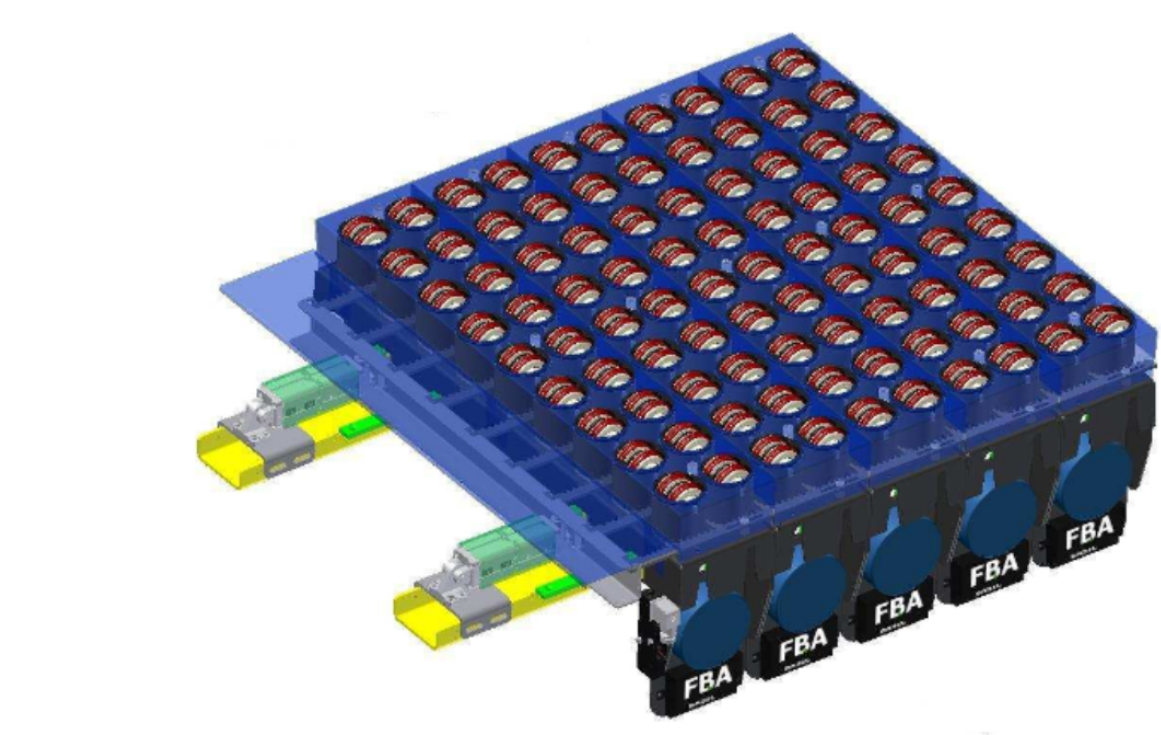

Figure C.11: Onesorter by FBA

C.11. Truxorter, Vanderlande

This product sorts packages using a pop-up system. The wheels move upwards and turn 45° to the desired side simultaneously. This function lifts the package off the belt conveyor and sends it into the right lane. During rest the Truxorter wheels are inline with the belt conveyor. The Truxorter is capable of handling 5.000 packages per hour [44]. The product is shown in Figure C.12.

Figure C.12: Truxorter by Vanderlande.

C.12. Swivel Wheel Sorter, Damon

This product has no pop-up functionality despite similar looks as the Truxorter. The wheels are turned to a divert angle of 30°. Because of the lack of a pop up function this product can operate bidirectional. It can handle 4.200 packages per hour [5]. The product is shown in Figure C.13.

Figure C.13: Swivel Wheel Sorter by Damon

C.13. Smart-Sort, Transnorm

This product diverts packages at a fixed angle of 45°, it has no pop-up functionality but can operate bidirectional. The wheels are diverted using pneumatic cylinders and can be driven using the main conveyor. The Smart-Sort can handle 2000 packages per hour [42]. The product is shown in

Figure C.14.

Figure C.14: Smart-Sort by Transnorm.

C.14. Intellisort WD, Intelligrated

This product uses a pneumatic pop up mechanism, the wheels have a fixed divert angle which limits them to one side sorting. Travelling straight over the sorter is made possible by roller conveyors connected with belts. The Intellisort WD is able of handling 6.000 packages per hour [20]. The product is shown in Figure C.15.

Figure C.15: Intellisort WD by Intelligrated

C.15. Siemens Varioroute

This product is an all-electric solution, the divert angles are set per row and can vary between ±45°. The speed can be regulated per individual roller. This is possible since each roller has it's own integrated motor. The product has the same cassette layout as the IQ-Grid but the rollers are shifted by 0.5· pitch per row. The Varioroute is able of handling 13.000 parcels per hour [38]. The product is shown in Figure C.16.

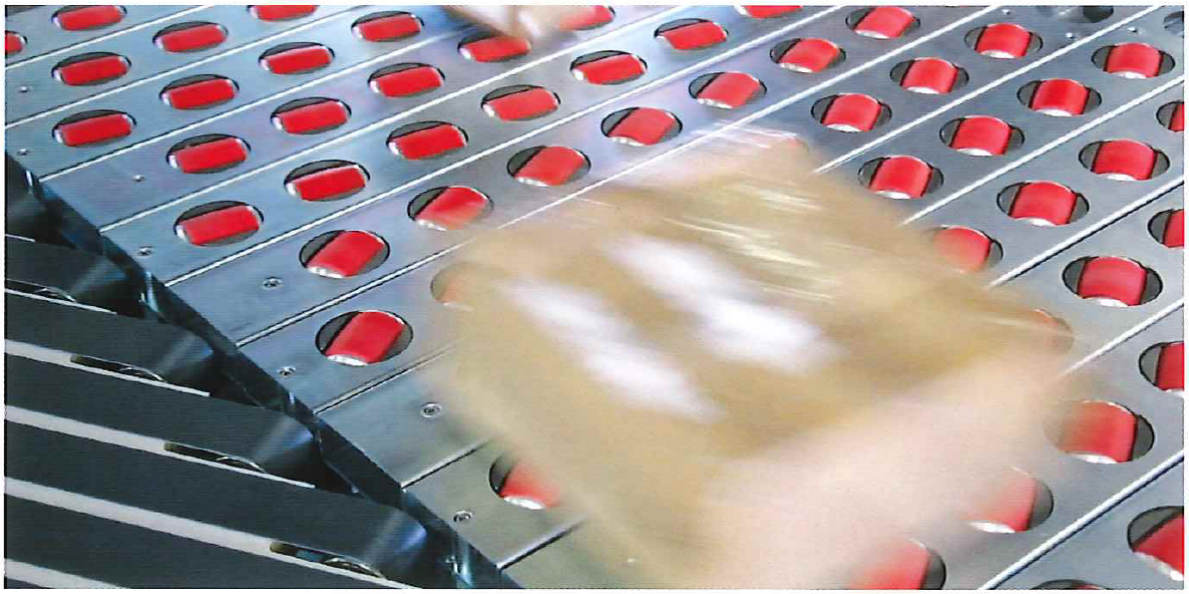

Figure C.16: Varioroute by Siemens

D

Patent Overview

Patent number:	Member					Divert Coupling			Transmission				Driven Coupling				Transmission			
	Wheel	Omni	Ball	Belt	Mecanum	Gear	Bar	None	Belt	Spindel	Direct	Gear	Motor	Rack	Belt	Axis	:iction whe	Gear	Chain	None	Direct	Gear	Chain	Motor	Belt
US20140116841A1	X					X				X					X						X				
US5117961A				X			X				X				X						X				
US3679043A			X													X						X			
US4730718A				X											X								X		
US9248981B1	X					X						X			X									X	
DE102010044239A1		X														X									X
EP0563824A2		X														X					X				
EP1323647A1	X							X					X		X										X
US5113993A	X						X				X				X						X				
EP1277675A1			X													X									X
US3552541A		X														X									X
US6073747A	X						X				X						X								X
US4598815A	X						X				X				X										X
EP1375389A1	X					X						X						X			X				X
US4981209A					X											X									
US20080169171A1	X					X														X				X	
US5921374A	X						X				X						X								X
US3828917A			X														X								X
US5000305A			X						X		X				X						X				
US5636086581					X											X			X				X		
US4913277A	X						X				X				X						X				
US8474596B2	X						X				X				X										X
US3874491A		X																		X				X	
US6340083B1					X											X			X						
US8567587B2		X														X							X		
US5335780A		X																	X		X				
US1460539A	X					X					X							X				X			
US6619465B1	X						X				X				X									X	
US3058567A	X						X				X				X						X				
US5890582A			X													X									X
US20130192954A1		X				X								X	X						X				
US3174613A	X						X				X				X							X			
KR101725337B1	X						X				X				X										X

Figure D.1: Patent overview of bidirectional sorters having a member which is in contact with the parcel, a divert mechanism which sets the divert angle for the member and a drive mechanism which drives the member such that it is able to transport the parcel.

E

Experimental Plan

Table E.1: Experimental plan for the model validation, including high and low settings for each independent variable resulting in a Resolution IV setting. Furthermore, a base measurement is repeated three times during the experiments to indicate the variance and systematic error.

Experiment:	α	h_w	$\frac{V_g}{V_c}$	S_m	S	$\frac{I}{L_p^2 m_p}$	$\frac{W_p}{L_p}$
1	-1	-1	-1	-1	-1	-1	-1
2	-1	-1	-1	-1	-1	-1	1
3	-1	-1	-1	-1	-1	1	-1
4	-1	-1	-1	-1	-1	1	1
5	-1	-1	-1	-1	1	-1	-1
6	-1	-1	-1	-1	1	-1	1
7	-1	-1	-1	-1	1	1	-1
8	-1	-1	-1	1	-1	-1	-1
9	-1	-1	-1	1	-1	-1	1
10	-1	-1	-1	1	-1	1	-1
11	-1	-1	-1	1	1	-1	-1
12	-1	-1	1	-1	-1	-1	-1
13	-1	-1	1	-1	-1	-1	1
14	-1	-1	1	-1	-1	1	-1
15	-1	-1	1	-1	1	-1	-1
16	-1	-1	1	1	-1	-1	-1
17	-1	-1	-1	-1	-1	-1	-1
18	-1	1	-1	-1	-1	-1	-1
19	-1	1	-1	-1	-1	-1	1
20	-1	1	-1	-1	-1	1	-1
21	-1	1	-1	-1	1	-1	-1
22	-1	1	-1	1	-1	-1	-1
23	-1	1	1	-1	-1	-1	-1
24	1	-1	-1	-1	-1	-1	-1
25	1	-1	-1	-1	-1	-1	1
26	1	-1	-1	-1	-1	1	-1
27	1	-1	-1	-1	1	-1	-1
28	1	-1	-1	1	-1	-1	-1
29	1	-1	1	-1	-1	-1	-1
30	1	1	-1	-1	-1	-1	-1
31	-1	-1	-1	-1	-1	-1	-1